SPRINGER BRIEFS IN CLIMATE STUDIES

Mauri Pelto

Climate Driven Retreat of Mount Baker Glaciers and Changing Water Resources

Springer

SpringerBriefs in Climate Studies

More information about this series at http://www.springer.com/series/11581

Mauri Pelto

Climate Driven Retreat of Mount Baker Glaciers and Changing Water Resources

Springer

Mauri Pelto
Environmental Science
Nichols College
Dudley, MA, USA

ISSN 2213-784X ISSN 2213-7858 (electronic)
SpringerBriefs in Climate Studies
ISBN 978-3-319-22604-0 ISBN 978-3-319-22605-7 (eBook)
DOI 10.1007/978-3-319-22605-7

Library of Congress Control Number: 2015946562

Springer Cham Heidelberg New York Dordrecht London

Printed on acid-free paper

Springer International Publishing AG Switzerland is part of Springer Science+Business Media (www.springer.com)

Preface

This volume examines the impact of climate change on a specific group of glaciers and the watersheds they support to emphasize the details in their response that are both unique to location and shared. The data is derived from our 31-year field study the North Cascade Glacier Climate Project (NCGCP), streamflow and temperature data from the US Geological Survey (USGS), snow measurements from the US Department of Agriculture (USDA) SNOTEL system, and weather data from the National Weather Service Coop Stations. The images come from our own field work, the USGS/NASA Landsat Satellite database, and pictures donated by Austin Post, William Long, and Tom Hammond.

Contents

Chapter 1
Introduction to Mount Baker and the Nooksack River Watershed

1.1 Mount Baker Glaciers and the Nooksack River Watershed

A stratovolcano, Mount Baker is the highest mountain in the North Cascade Range subrange at 3286 m. Mount Baker has the largest contiguous network of glaciers in the range with 12 significant glaciers covering 38.6 km^2 and ranging in elevation from 1320 to 3250 m (Figs. 1.1 and 1.2). The Nooksack tribe refers to the mountains as Komo Kulshan, the great white (smoking) watcher. Kulshan watches over the Nooksack River Watershed, and its flanks are principal water sources for all three branches of this river as well as the Baker River.

The Nooksack River consists of the North, South, and Middle Fork which combine near Deming to create the main stem Nooksack River. The Nooksack River empties into Birch Bay near Bellingham, Washington. The Baker River drains into the Skagit River at Concrete, WA. The glaciers of Mount Baker are a key water resource to the aquatic life and the local communities, and globally have proven to be some of the most sensitive to climate, responding quickly to changes. This is what prompted initiation of a long term glacier study in 1984, that continues today, examining the response of Mount Baker glaciers and their resultant runoff to climate change.

In 2013, The Nooksack River watershed had glaciers with a combined area of 17.4 km^2, and the Baker River watershed had glaciers with a combined area of 29.6 km^2. In a typical summer (June–September) our measurements indicate that there is 3.2 m water equivalent (w.e.) of ablation from glaciers in these watersheds (Pelto 2008; Pelto and Brown, 2012). This is equivalent to, 150.4 million m^3 w.e., an average discharge of 4.0 m^3/s all summer in the Nooksack River, and 6.7 m^3/s for Baker River. In this region dominated by a temperate maritime climate, summer is the driest season, with limited precipitation from July 1 to October 1. This is the season when glaciers are especially important to regional water supplies (Fountain and Tangborn 1985). The dependable supply of water in part due to the glaciers has led to

M. Pelto, *Climate Driven Retreat of Mount Baker Glaciers and Changing Water Resources*, SpringerBriefs in Climate Studies,
DOI 10.1007/978-3-319-22605-7_1

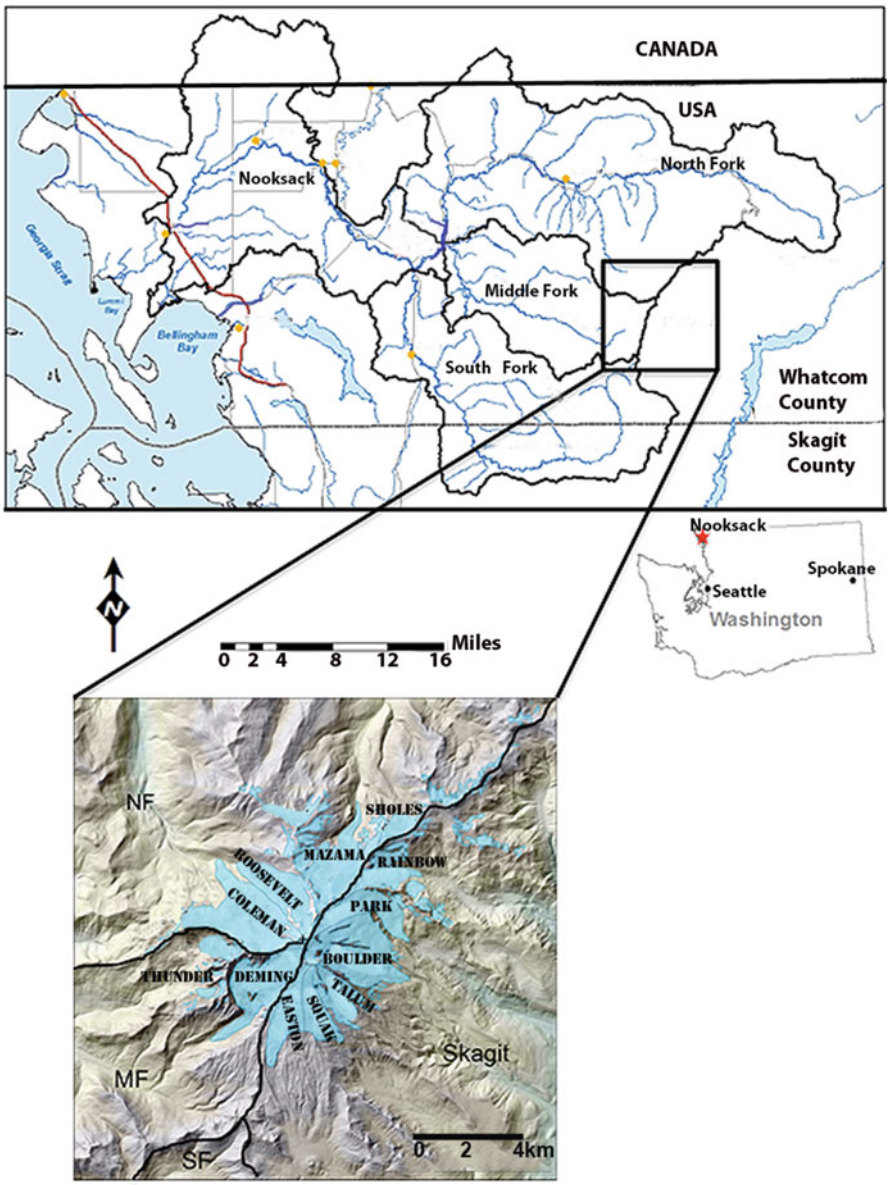

Fig. 1.1 Map of Mount Baker glaciers and the Nooksack River watershed

the development of economies that rely on this water resource, from farming to sport and commercial fisheries to recreational activities and hydropower generation.

The Nooksack River system is home to five species of Pacific salmon, chinook, coho, pink, chum and sockeye as well as, steelhead and bull trout. Three different fish species in the Nooksack River system have been listed as Threatened under the

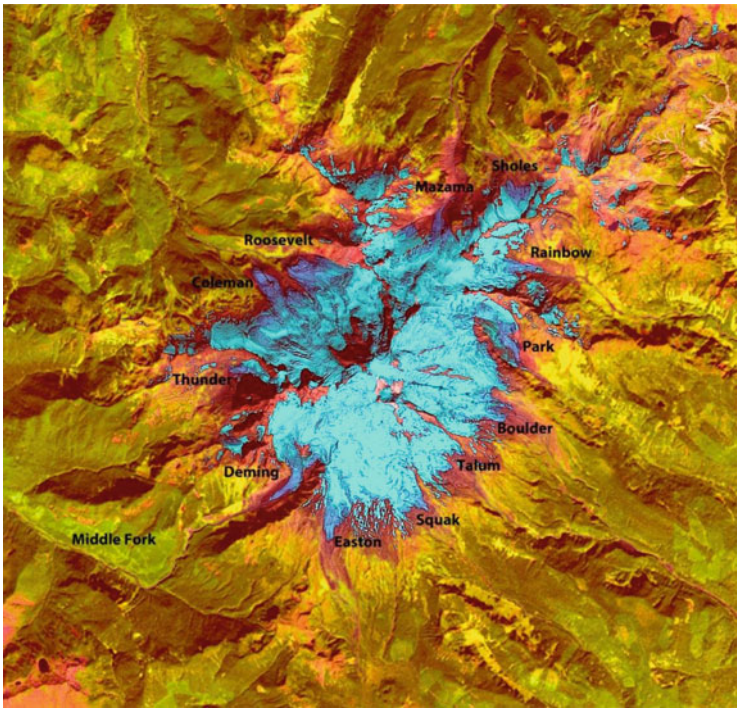

Fig. 1.2 Landsat 8 satellite image of Mount Baker, *light blue* is snow, *purple* is bare glacier ice, *darker green* is evergreen forests, *pink* is a mixture of rock and alpine vegetation, *lighter green* is areas dominated by deciduous shrubs

Endangered Species Act (ESA). These include: chinook salmon, steelhead and bull trout (Grah and Beaulieu 2013).

Salmon runs begin in summer with Chinook (king) and continue in fall with chinook, coho (sliver), chum and pink salmon on odd numbered years. The coho and king salmon runs move upstream into the Nooksack and Deming areas in October. The South Fork coho run is strongest in October through November. Generally, there is a strong run of chum salmon starting in October and running through December in the Main and North Fork (Washington Department of Fish and Wildlife 2014).

Agricultural production, supported by Nooksack River water, has an approximate $290 million market value (Whatcom Farm Friends 2013). Whatcom County's berry industry is world-class, raising the largest per capita crop of red raspberries in the world with a harvested area of over 29 km^2, supplying more than 65 % of all the raspberries in the U.S. (Whatcom Farm Friends 2013).

The City of Bellingham obtains 10 % of its drinking water from the Middle Fork Nooksack River which is fed by Deming and Thunder Glacier on Mount Baker.

At Nooksack Falls there is a hydropower plant constructed in 1906, on the North Fork Nooksack River that is rated at a production of 3.5 MW, though its operation

has been sporadic since 1997. On the Baker River there are two large hydropower projects that can generate 215 MW of electricity at the Upper and Lower Baker Dams. The Lower Baker Dam is located on the Baker River in Concrete, Washington. It is 87 m tall and the reservoir capacity of Lake Shannon is 199,000,000 m^3. Lake Shannon is 11 km long, covers 8.9 km^2 at its full pool, and has an elevation of 134 m. The Upper Baker Dam is 95 m high and impounds Baker Lake. The lake has a normal full lake elevation of 221 m, an area of 19 km^2 and a volume of 352,000,000 m^3.

The widespread use of the water resource provided by melting Mount Baker glaciers is evident. Alpine glaciers in many areas of the world are important for water resources melting in the summer when precipitation is lowest and water demand from society is largest. Glaciers melt more during hot dry summers helping to reduce streamflow variability. The loss of glaciers does not necessarily reduce annual streamflow, but it does change the timing, leading to more runoff in winter, spring and early summer and less in the late summer, when it is most needed.

1.2 Glaciers and Climate

Glaciers have been studied as sensitive indicators of climate for more than a century. Observations of alpine glaciers most commonly focus on changes in terminus behavior, to identify glacier response to climate changes (Forel 1895; Oerlemans 1994; IPCC, 1995). The glaciers of Mount Baker have proven particularly quick to respond to climate change with terminus advance commencing within 5–15 years of a cooler wetter climate as occurred in 1944 (Hubley, 1956); and terminus retreat within 3–12 years of a change to a warmer drier climate, as occurred in 1977 (Harper, 1993; Pelto and Hedlund 2001). Annual mass balance measurements are the most accurate indicator of short-term glacier response to climate change (Haeberli et al. 2000). A glacier with a sustained negative mass balance is out of equilibrium and will retreat, while one with a sustained positive mass balance is out of equilibrium and will advance. In either case the response is an attempt to reach a new point of equilibrium. If a glacier cannot retreat to a point of equilibrium during a warmer and drier climate regime, it experiences a disequilibrium response (Pelto 2006), ultimately resulting in the disappearance of the glacier entirely.

Annual mass balance is the change in mass of a glacier during a year resulting from the difference between net accumulation and net ablation of snow. The importance of monitoring glacier mass balance was recognized during the International Geophysical Year (IGY) in 1957 (WGMS 2008). For the IGY a number of benchmark glaciers around the world were chosen where mass balance would be monitored. This network continued by the World Glacier Monitoring Service (WGMS 2011) has proven valuable, but in many areas the number of glacier is limited, for example, there is just one benchmark glacier in the North Cascades and in the conterminous United States-South Cascade Glacier (Fountain et al. 1991). Glacier mass balance varies due to geographic characteristics such as aspect,

elevation and location with respect to prevailing winds. Since no single glacier is representative of all others, to understand the causes and nature of changes in glacier mass balance throughout a mountain range, it is necessary to monitor a significant number of glaciers (Fountain et al. 1991). In 1983 the National Academy of Sciences called for monitoring the response of glaciers to climate change across an ice clad mountain range. In response to this the NCGCP began monitoring the mass balance, terminus response and glacier runoff from ten North Cascades glaciers, including three on Mount Baker. The NCGCP continues after 31 consecutive summers of research, actively monitoring the mass balance of ten glaciers, more glaciers than any other program in North America.

1.3 Area Climate

The North Cascade region has a temperate maritime climate. Approximately 80 % of the region's precipitation occurs during the accumulation season (October–April) when the North Cascades are on the receiving end of the storm track crossing the Pacific Ocean. The mean annual precipitation for the basin is 3.3 m (Rasmussen and Tangborn 1976). Lower elevations of the basin receive an average precipitation of 1.8 m, while the slopes of Mt. Baker receive greater than 3.8 m total precipitation per year, most of that as snow in the winter (PRISM 2010).

Snowfall is the principal precipitation type above 800 m elevation from November to April. This combination of mountains and high precipitation leads to an unusually large average annual snowfall that is crucial to glacier formation and maintenance in the region. Mt. Baker received a world record annual snowfall of 28.55 m in 1999 and averages 13.5 m of snowfall per winter with a typical maximum snow depth of 4.5 m at the 1,340 m Mount Baker measurement site. In the transition zone (500–1000 m), rain-on-snow events occur from late-October through February, often resulting in rapid snowmelt. These events are characterized by accumulation of wet loosely packed snow that is subject to large, warm, and windy rainstorms that melt snow and cumulatively combine with rainfall, generating high runoff over a short period of time. Most peak flows occur during these late-fall/early-winter months atmospheric river events, known locally as "pineapple express" and sometimes result in severe flooding (Kresch and Dincola 1996). From late spring to early fall, high pressure to the west keeps the Pacific Northwest comparatively dry. These seasonal variations are related to changes in large-scale atmospheric circulation occurring over the Pacific Ocean, including the Gulf of Alaska.

Climate observations in the Pacific Northwest, United States show an accelerated warming for the 1970–2012 time periods of approximately 0.2 °C per decade (Abatzoglou et al. 2014). North Cascade temperatures have increased during the twentieth century. On average, the region warmed about 0.6 °C (Fig. 1.3); warming was largest during winter (Abatzoglou et al. 2014). From 1980 to 2012 the warming was strongest in winter and summer, with no trend in spring. During the 1980–2012 period spring precipitation increased, with 2009–2012 having the highest spring

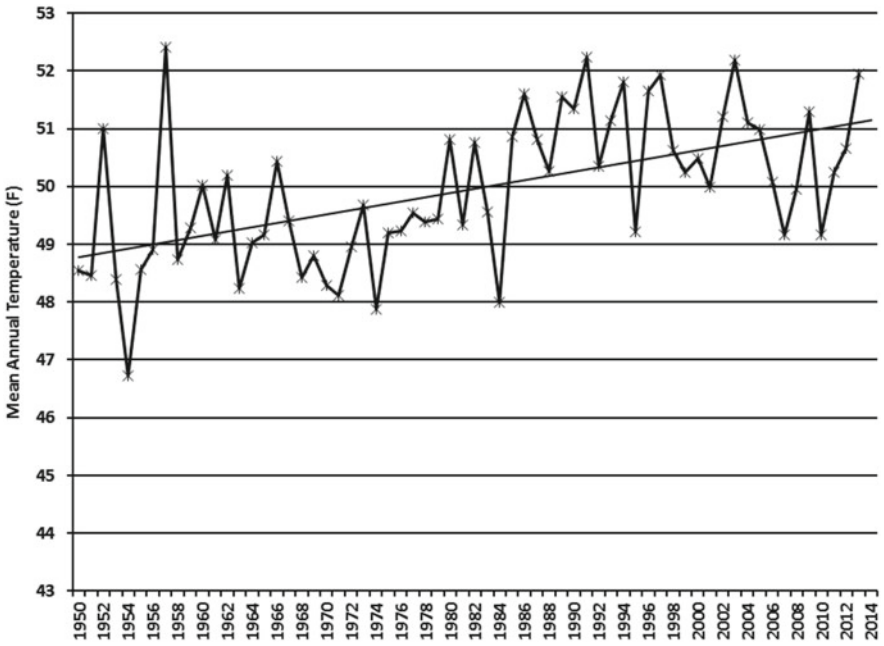

Fig. 1.3 Rise in annual temperature observed in the Pacific Northwest 1890–2012 (Grah and Beaulieu 2013)

precipitation in the observational record (2009–2012), more than 30 % above twentieth century normal. The Pacific Northwest region's annual mean temperature indicates long term warming modulated by interdecadal variability with cool periods 1910–1925, 1945–1960 and warm periods around 1940 and since the mid-1980s. The warmest 10-year period was 1998–2007 (Abatzoglou et al. 2014).

In the Nooksack Watershed the Clearbrook weather station has the longest record dating back to 1895, and is located approximately 42 km west northwest of Mount Baker at an elevation of 20 m. This station is useful for temperature trends, but is not necessarily representative of the precipitation conditions affecting the glaciers. Mean annual temperature at Clearbrook has increased 1.4 °C from 1895 to 2010, a rate of 0.12 °C per decade.

1.4 Accumulation Snowpack

The North Cascades region experienced a substantial climate change in 1976, to generally warmer-drier conditions (Ebbesmeyer et al. 1991). This transition led to the definition of the Pacific Decadal Oscillation (PDO) (Mantua et al. 1997). The key climate variables that in particular affect glaciers are the mean ablation season temperature (June–September) and winter season snowfall (November–April).

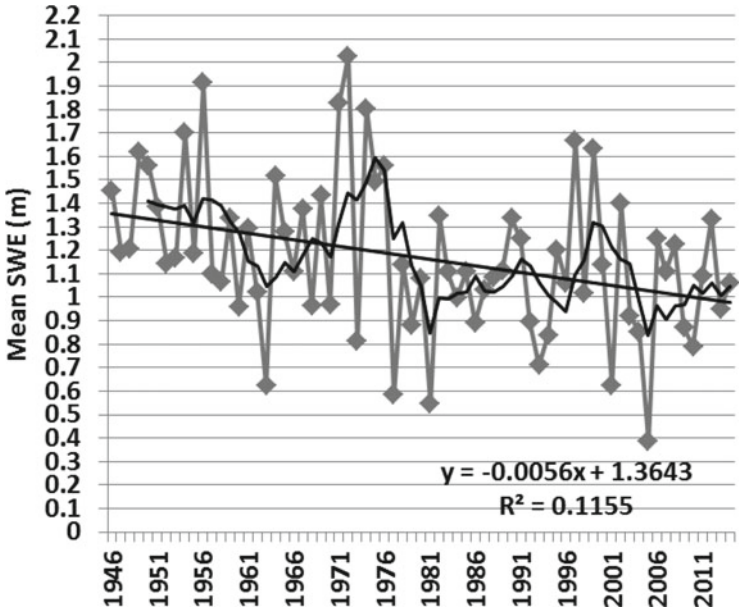

Fig. 1.4 Mean April 1 SWE at six North Cascade SNOTEL stations from 1946 to 2014

Winter season snowfall is directly measured by the USDA at a series of USDA SNOTEL sites, and the April 1 snow water equivalent (SWE) provides an excellent measure of winter season snowfall. The April 1 SWE from six long terms SNOTEL stations (Fish Lake, Lyman Lake, Park Creek, Rainy Pass, Stampede Pass, Stevens Pass) in Fig. 1.4 declined by 23 % from the 1946–1976 period to the 1977–2014 period. Winter season precipitation has declined only slightly 3 % at the Snotel stations and at Diablo Dam. Thus, most of the loss reflects increased melting of the snowpack or rain events during the winter season.

Mote et al. (2008) referred to the ratio of 1 April SWE to November–March precipitation, as the storage efficiency. This ratio declined by 28 % for the 1944–2006 period (Mote et al. 2008), which indicates less of total precipitation is being retained as snowpack. Pelto (2008) noted a similar change specifically for the six long term North Cascade SNOTEL stations, for the 1946–2014 period indicate a 22 % decline in this ratio (Fig. 1.5).

This decline in snowpack has been noted throughout the Pacific Northwest. Mote et al. (2008) examined observed and simulated SWE in the Washington Cascade and Olympic Mountains. The SWE trend is quite variable depending on the time period analyzed ranging from 30 to 35 % declines between the 1940s and 2003, to an upward trend for periods beginning in 1976. Casola et al. (2009) examined and 16 U. S. Historical Climate Network stations, seven Hydro-Climate Data Network streamflow records and SNOTEL stations in the Cascade Mountains of Washington and Oregon. They found the trend in April 1 SWE for the full period of record

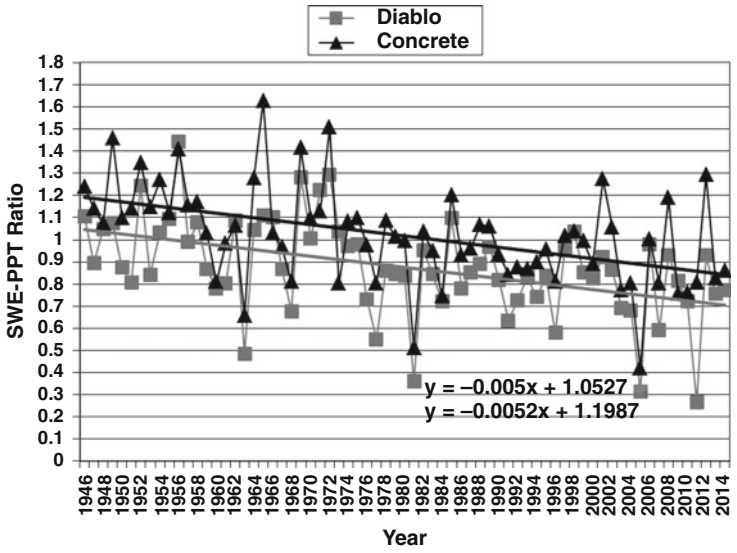

Fig. 1.5 Ratio of April 1 SWE six North Cascade SNOTEL stations to winter season precipitation at Diablo Dam and Concrete from 1946 to 2014

(1930–2007) is a 23 % decline. The period of maximum change is 1950–1997 showing a large, decline of 48 % in April 1 SWE associated with the cool-to-warm Pacific Decadal Oscillation (PDO) shift in 1976. They also noted the lack of a clear trend in April 1 SWE since 1976.

1.5 Ablation Season Temperature

The other key factor in glacier behavior is the amount of ablation, which is primarily controlled by air temperature. That air temperature is the key is indicated by the success of degree day functions for assessing glacier ablation on glaciers (Hock 2005; Rasmussen 2009). The majority of ablation takes place during the June–September period, and nearly all ablation during the May–September period. The most reliable long term weather station in the region is Diablo Dam. An examination of trends in summer temperature at this station indicates a nearly identical pattern, for May–September and June–September (Fig. 1.6). Six of the ten warmest summers during the 1946–2014 have occurred since 2003. The long term summer temperature trend is 0.6 °C for the region (Abatzoglou et al. 2014), and 0.7˚C at Diablo Dam. The average June–September temperature from 2003 to 2014 is 0.6 °C above the mean for the 1946–2002 period.

Several climate models agree that the Pacific Northwest will likely experience a 1.7–2.8 °C temperature increase and a small increase in winter precipitation during

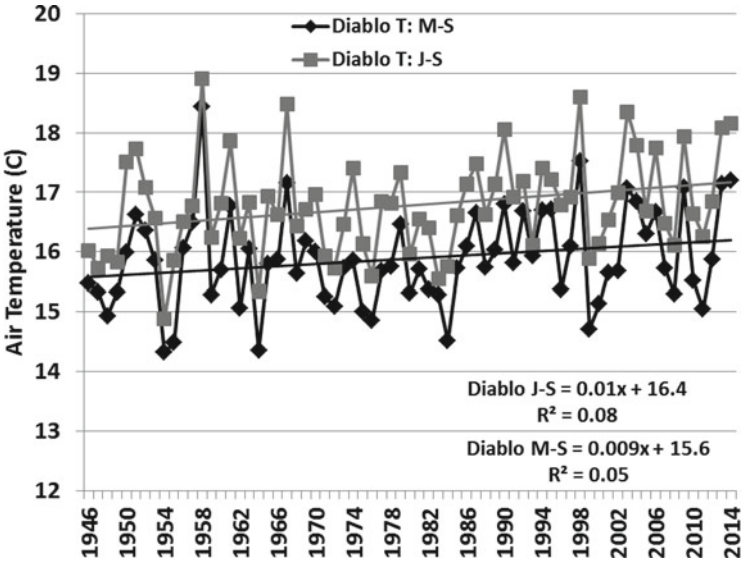

Fig. 1.6 Mean melt season temperature at Diablo Dam for June–September and May–September for the 1946–2014 period

early twenty-first century (Dalton et al. 2013). A portion of this warming has already placed glaciers in jeopardy.

The 2014 winter accumulation season featured 101 % of mean (1984–2013) winter snow accumulation at the long term USDA SNOTEL stations in the North Cascades (Fig. 1.7). The melt season has been exceptional by several measures. The mean summer temperature from June–September and July–September at Lyman Lake is tied for the warmest melt season for the 1989–2014 period (Fig. 1.8). We have used Lyman Lake as an initial comparison, which is 200 km from the Nooksack watershed, but is the most reliable high elevation long term temperature record in the North Cascades, and SNOTEL stations have more immediate data availability. At the Middle Fork Nooksack station, 2014 is tied for highest summer temperature, but this station has a more limited record.

1.6 Key Climate Indices

The PDO Index is the leading principal component of North Pacific monthly sea surface temperature variability, poleward of 20N (Mantua et al. 1997). During the positive PDO phase warm weather is favored in the Pacific along the northwest coast and over the Pacific Northwest. During the negative phase cool ocean water is found off the northwest coast and cooler temperatures across the Pacific Northwest (Mantua et al. 1997). In the past century: negative PDO regimes prevailed from

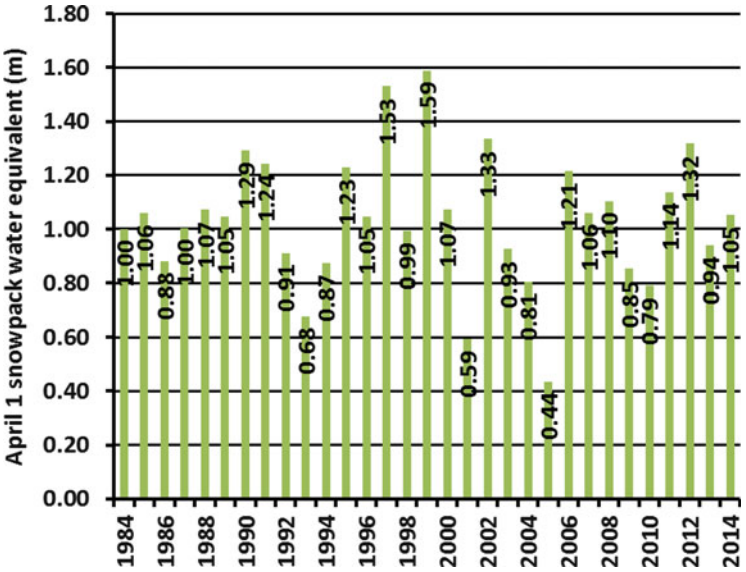

Fig. 1.7 Mean annual accumulation season snowpack on April 1st at USDS Snotel stations in the North Cascade 1984–2014, this is the period of glacier observations

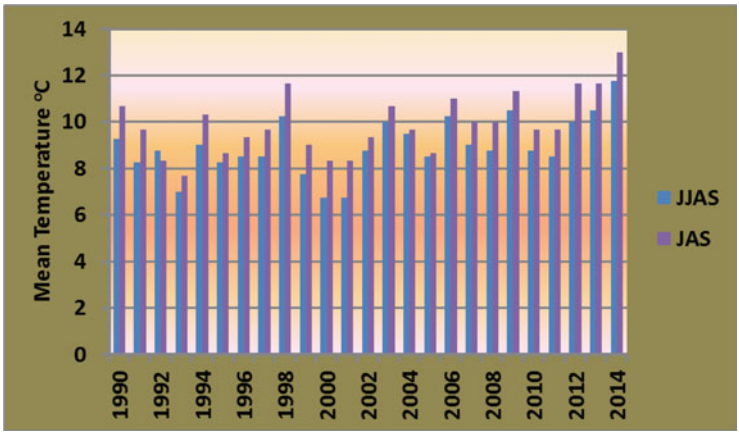

Fig. 1.8 Average mean summer temperatures at Lyman Lake, WA 1990–2014

1890 to 1924 and again from 1947 to 1976, while positive PDO regimes dominated from 1925 to 1946 and from 1977 to 2007 (Mantua et al. 1997, 2010). The positive phase of the PDO features warm sea surface temperatures (SST) near North America and cool SST in the central Pacific. Negative phase of the PDO is the reverse. During periods of positive PDO values the North Cascade Range experiences warmer and drier conditions such as in 1925–1944 and 1977–1998. During negative phases the

region has a cooler wetter climate such as in 1944–1976. From 2008 to 2013 negative PDO values dominated and the climate was wet. In 2014 there was a transition to positive PDO values and the region is now entering a period of drought.

The El Niño/Southern Oscillation (ENSO) phenomenon is the most observable of the atmospheric circulation indices that lead to year-to-year climate variability. ENSO positive events (El Nino) herald abnormally warm sea surface temperatures (SST) over the eastern half of the equatorial Pacific. The ENSO negative phase (La Niña) is the opposite phenomenon, indicative of abnormally cold SST in the eastern half of the equatorial Pacific. ENSO is an east-west atmospheric pressure see-saw that directly affects tropical weather around the globe and indirectly impacts a much larger area (Wolter and Timlin 1998). There are also ENSO Neutral periods where there is no statistically significant deviation from average conditions at the equator. The duration of the ENSO phases tends to be 1–2 years.

The positive phase spatial patterns are very similar for both indices and it is postulated that they reinforce each other substantially when in phase (Gershunov et al. 1999). The same is true of a negative phase of PDO and ENSO. When the indices are opposed their impact is likely weakened. In early 2015 a positive PDO and ENSO have developed leading to exceptionally warm dry conditions in the Pacific Northwest.

References

Abatzoglou JT, Rupp D, Mote PW (2014) Seasonal climate variability and change in the pacific northwest of the United States. J Climate 27:2125–2142, doi:http://dx.doi.org/10.1175/JCLI-D-13-00218.1

California Dept. of Water Resources. Interagency Ecological Studies Program Technical Report 26, 115–126

Casola J, Cuo L, Livneh B, Lettenmaier D, Stoelinga M, Mote P, Wallace J (2009) Assessing the impacts of global warming on snowpack in the Washington Cascades. J Climate 22:2758–2772

Dalton MM, Mote PW, Snover AK (2013) Climate change in the Northwest: implications for our landscapes, waters, and communities. Island Press, Washington, DC

Ebbesmeyer CC, Cayan DR, McLain FH, Nichols DH, Peterson DH, Redmond KT (1991) 1976 step in the pacific climate: forty environmental changes between 1968–1975 and 1976–1984. In: Betancourt JL, Tharp VL (eds) Proceedings on the 7th annual Pacific climate workshop, California Department of water resources. Interagency Ecological Studies Program Technical Report 26, 115–126.

Forel F (1895) Les variations périodiques des glaciers. Arch Sci Phys Nat XXXIV:209–229

Fountain A, Tangborn W (1985) The effect of glaciers on streamflow variations. Water Resour Res 21:579–586

Fountain A, Trabant D, Bruggman M, Ommaney C, Monroe D (1991) Glacier mass balance standards. EOS 72(46):511–514

Gershunov A, Barnett T, Cayan D (1999) North Pacific interdecadal oscillation seen as factor in ENSO-related north American climate anomalies. EOS 80:25–30

Grah O, Beaulieu J (2013) The effect of climate change on glacier ablation and baseflow support in the Nooksack River basin and implications on pacific salmonid species protection and recovery. Clim Change 120:657–670. doi:10.1007/s10584-013-0747-y

Haeberli W, Cihlar J, Barry R (2000) Glacier monitoring within the global climate observing system. Ann Glaciol 31:241–246
Harper JT (1993) Glacier terminus fluctuations on Mt. Baker, Washington, USA, 1940–1980, and climate variations. Arct Alp Res 25:332–340
Hock R (2005) Glacier melt: a review of processes and their modelling. Prog Phys Geogr 29:362–391
Hubley RC (1956) Glaciers of Washington's Cascades and Olympic mountains: their present activity and its relation to local climatic trends. J Glaciol 2(19):669–674
IPCC: Climate Change (1995) Contributions of working group I to the second assessment of the Intergovernmental Panel on Climate Change. Cambridge University Press, Cambridge, pp 241–265, 1996
Kresch D, Dincola K (1996) What causes floods in Washington State. USGS Fact Sheet, pp 228–296
Mantua NJ, Tohver I, Hamlet A (2010) Climate change impacts on streamflow extremes and summertime stream temperature and their possible consequences for freshwater salmon habitat in Washington State. Clim Change 102(1–2):187–223
Mantua NJ, Hare SR, Zhang Y, Wallace SM, Francis RC (1997) A Pacific interdecadal climate oscillation with impacts on salmon production. Bull Am Meteorol Soc 78:1069–1079
Mote P, Hamlet A, Salathe E (2008) Has spring snowpack decline in the Washington Cascades? Hydrol Earth Syst Sci 12:193–206
Oerlemans J (1994) Quantifying global warming from the retreat of glaciers. Science 264:243–245
Pelto MS (2006) The current disequilibrium of North Cascade glaciers. Hydrol Process 20:769–779. doi:10.1002/hyp.6132
Pelto MS (2008) Impact of climate change on North Cascade alpine glaciers and alpine runoff. Northwest Sci 82(1):65–75
Pelto MS, Brown C (2012) Mass balance loss of Mount Baker, Washington glaciers 1990–2010. Hydrol Process 26(17):2601–2607
Pelto MS, Hedlund C (2001) Terminus behavior and response time of North Cascade glaciers, Washington USA. J Glaciol 47:497–506
PRISM Climate Group, Oregon State University, http://prism.oregonstate.edu, created 4 Feb 2004.
Rasmussen LA (2009) South Cascade Glacier mass balance, 1935–2006. Ann Glaciol 50:215–220
Rasmussen LA, Tangborn WV (1976) Hydrology of the North Cascade region, Washington 1. Runoff, precipitation, and storage characteristics. Water Resour Res 12(2):187–202
Washington Department of Fish and Wildlife (2014) SalmonScape. http://apps.wdfw.wa.gov/salmonscape/map.html. Accessed Feb 2014
WGMS (2008) Global glacier changes: facts and figs. In: Zemp M, Roer I, Kääb A, Hoelzle M, Paul F, Haeberli W (eds). UNEP, World Glacier Monitoring Service, Zurich
WGMS (2011) Glacier mass balance bulletin no. 11. In: Zemp M, Nussbaumer SU, GärtnerRoer I, Hoelzle M, Paul F, Haeberli W (eds) (2008–2009). ICSU(WDS)/IUGG(IACS)/UNEP/UNESCO/WMO, WGMS, Zurich
Whatcom Farm Friends (2013) Whatcom Farm facts. http://www.wcfarmfriends.com/#!farm-facts/citg. Accessed Feb 2015
Wolter K, Timlin M (1998) Measuring the strength of ENSO how does 1997/98 rank? Weather 53:315–324

Chapter 2
Terminus Response to Climate Change

2.1 Terminus Observations

Terminus observations have long been the hallmark of glaciologic observations, due to the ease and frequency with which the terminus can be mapped, painted or photographed (Oerlemans 1994). These observations identify the response of the glacier to recent climate changes and are considered a key indicator of climate change (IPCC 1995). However, the response of the terminus does not address the ability of a glacier to survive. A glacier can retreat rapidly, while maintaining a significant accumulation zone, which will allow the glacier to survive. Or a glacier could retreat slowly, but thin considerably along its entire length and then melt away, a disequilibrium response. Only glaciers lacking a significant accumulation zone will not survive the climate conditions causing the retreat.

2.2 Equilibrium Response

Typically glacier terminus retreat results in the loss of the lowest elevation region of the glacier. Since higher elevations are cooler than lower ones, the disappearance of the lowest portion of the glacier reduces overall ablation, thereby increasing mass balance and potentially reestablishing equilibrium (Pelto 2006). Typically a glacier's thinning is greatest at the terminus, and at some distance above the terminus, usually in the accumulation zone, the glacier is no longer thinning appreciably even during retreat (Schwitter and Raymond 1993). This behavior of greatest thinning at the terminus and limited thinning in the accumulation zone suggests a glacier that will retreat to a new stable position (Schwitter and Raymond 1993).

M. Pelto, *Climate Driven Retreat of Mount Baker Glaciers and Changing Water Resources*, SpringerBriefs in Climate Studies,
DOI 10.1007/978-3-319-22605-7_2

2.3 Disequilibrium Response

For alpine glaciers typically 50–70 % of the glacier must retain snowcover even at the conclusion of the melt season to be in equilibrium, this is referred to as the Accumulation Area Ratio (AAR). Without a substantial consistent accumulation area a glacier cannot survive. If a non-surging alpine glacier is experiencing extensive thinning and marginal retreat in the accumulation zone of the glacier it lacks a persistent accumulation (Pelto 2011). The result is a more unstable form of retreat with substantial thinning throughout the length and breadth of the glacier. A glacier in this condition is unlikely to be able to survive in anything like its present extent given the current climate. This is evident in satellite or aerial photographs of glaciers. The emergence of bedrock outcrops or the recession of the upper margins of a glacier are the key symptoms to observe (Fig. 2.1) (Kääb et al. 2002; Pelto 2010; Carturan et al. 2013).

2.4 Survival Forecast

Meier and Post (1962) used oblique aerial photography to assess glacier activity using the appearance of the terminus, focusing on the extent of crevassing, convexity of the terminus, extent of recent glaciated terrain and moraine cover on terminus in the Pacific Northwest. Paul et al. (2004) utilized satellite imagery to identify non-uniform changes in glacier geometry, emerging rock outcrops, disintegration and tributary separation to determine collapse versus a dynamic (equilibrium) response to climate change. It has become practical to examine the terminus and areal extent change of all glaciers in the region and more recently surface elevation changes (Key et al. 2002; Paul et al. 2004; Andreassen et al. 2008; Huss 2012). This does quantify the extent of the retreat, but not the nature of the equilibrium or disequilibrium response. To identify disequilibrium requires identification of significant thinning in the accumulation zone, which will occur if a persistent accumulation zone is lacking (Paul et al. 2004; Pelto 2010).

It is now possible using Digital Globe, Landsat and SPOT satellite imagery and USGS maps based on aerial photography from the 1950s to 1960s to distinguish glacier activity in terms of equilibrium or disequilibrium response. To identify disequilibrium three parameters are observed:

1. Greater than 35 % areal extent change.
2. Changes in the glacier margin in the accumulation zone averaging greater than 50 m.
3. Thinning in the accumulation zone results in retreat of the margin at the head of the glacier and emergence of significant rock outcrops (Fig. 2.1).

A glacier in disequilibrium with present climate cannot achieve equilibrium by retreating and disappears. Glacier loss has been noticed in mountain ranges around

Fig. 2.1 Lynch Glacier, North Cascades in 1979 and 2009. Bedrock outcrops have emerged in the *upper* portion of the glacier at Point *B*. This thinning of the *upper* portion of this glacier is a sign of disequilibrium

the world including the North Cascades (Pelto 2010), Wind River Range (Maloof et al. 2014) and Glacier National Park (Key et al. 2002). Terminus change is the typical focus for glacier changes this does identify the current state of the glacier with respect to climate. Observing the changes in the upper portion of the glacier are key to determining future survival.

2.5 Mount Baker Terminus Response

Schwitter and Raymond (1993) noted the ease of identification and utility of the well-preserved Little Ice Age maximum moraines (LIAM) formed from 1700 to 1850, for reconstructing former glacier profiles in the North Cascades and elsewhere. Post (1975) in a special map produced for Mount Baker during a period of volcanic unrest in the 1970s indicates the location of the LIAM for Mount Baker glaciers. The distance from the typically well preserved, fresh LIAM moraines and trimlines to the current glacier front has been measured in each case using a laser ranging device with an accuracy of ±1 m. Additionally on each of the 12 Mount Baker glaciers field measurements from the same LIAM moraines to the current glacier front was completed on at least three occasions between 1984 and 2014. The goal being to verify both the LIAM and the actual terminus position changes from 1984 to 2014.

Terminus change from 1850 to 1950 is the distance from the aforementioned LIAM and the position of the glacier terminus in 1950 noted by Hubley (1956) in aerial photographs. Terminus change from 1950 to 1979 is the change between the position noted by Hubley (1956) and the USGS aerial observations in 1979. Neither 1950 nor 1979 perfectly match the timing of climate changes noted in the following section; however, they are closest to the climate shifts, beginning in 1944 and 1976 respectively, for which adequate aerial photographic observations were made. Terminus change from 1979 to the present is based on comparison of the USGS aerial observations and repeated field measurements of the NCGCP from 1984 to 2014 (Pelto and Hedlund 2001; Pelto 2010).

Since the LIAM there have been three climate changes in the North Cascades sufficient to substantially alter glacier terminus behavior. During the LIA mean annual temperatures were 1.0–1.5 °C cooler than at present (Burbank 1981; Porter 1986; Kunkel et al. 2013). The lower temperatures in the North Cascades led to a snowline lowering of 100–150 m during the LIA (Porter 1986; Burbank 1981). Depending on the glacier, the maximum advance occurred in the sixteenth, eighteenth, or nineteenth century (Miller 1971; Long 1956). North Cascade glaciers maintained advanced terminal positions from 1650 to 1890, emplacing one or several Little Ice Age terminal moraines (Heikkinen 1984).

The first substantial climate change was a progressive temperature rise from the 1880s to the 1940s. The warming led to ubiquitous rapid retreat of Pacific Northwest alpine glaciers from 1890 to 1944 (Meier and Post 1962; Hubley 1956; Long 1956). Retreat from the LIAM was modest prior to a still stand in the 1880s (Burbank 1981; Long 1956). On Mt. Rainier mapping of terminus changes by (Burbank 1981) indicate that rapid and continuous retreat of Mt. Rainier glaciers from their LIAM began after the 1880–1885 still stand. Long (1953) noted that retreat on Lyman Glacier and Easton Glacier became substantial only after 1890 (Fig. 2.2). The primary retreat on Mount Baker glaciers occurred after 1910 (Heikkinen 1984; Long 1955).

Fig. 2.2 Easton Glacier in 1952 (NCGCP Archives, William Long)

Each Mount Baker glacier retreated significantly from its LIAM. It must be emphasized that the entire retreat noted from the LIAM to 1944 did not occur in the 1890–1944 interval, as observations do not exist on most glaciers to distinguish the exact timing of the initial post LIAM retreat, though retreat was minor before 1890 on glaciers where observations exist. Average retreat of glaciers on Mt. Baker was 1440 m from LIAM to 1950 (Pelto 1993).

From 1944 to 1976 conditions became cooler and precipitation increased (Hubley 1956; Tangborn 1980; Ebbesmeyer 1991). Approximately half the North Cascade glaciers advanced during the 1950–1979 period, while the remaining glaciers continued to retreat at varying rates (Pelto and Hedlund 2001). Harper (1993) examined six Mt. Baker glaciers and found all retreated a significant distance after 1940, and all six were advancing by 1960. On Mount Baker all 12 glaciers advanced during this period, again indicating their sensitivity in responding to climate (Harper 1993; Pelto and Hedlund 2001). Advances of Mount Baker glaciers ranged from 60 to 750 m, an average of 480 m, and ended in 1978 (Heikkinen 1984; Harper 1993; Pelto 1993). The first glaciers to advance were the glaciers with a steeper slope profile such as Coleman, Deming and Roosevelt, which had all begun to advance by 1950 (Bengston 1956; Long 1956). The last glacier to advance was the lower slope profile Easton Glacier, which was still in retreat in 1952 (Long 1956). This is an indication of the slower response time to a climate change of a glacier with a lower slope and slower velocity. In each case the initial response of the glacier to climate change occurred within a decade. In the Wind River Range no

advances were reported, though the rate of retreat decreased (Pochop et al. 1989). In Glacier National Park the retreat of Sperry Glacier diminished from 1960 to 1979, but advances did not occur (Key et al. 2002). On Mount Rainer, WA a general glacier advance was noted from 1955 to 1975.

The third change to warmer and drier conditions began in 1977 (Ebbesmeyer 1991; Hodge et al. 1998). Recent climate change has caused ubiquitous retreat of Pacific Northwest glaciers (Pelto and Hedlund 2001; Key et al. 2002; Granshaw and Fountain 2006). The retreat and negative mass balances from 1977 to 2014 have been noted by Bidlake et al. (2007) and Pelto and Brown (2012). Between 1979 and 1984, 35 of the 47 North Cascade glaciers observed annually had begun retreating (Pelto and Hedlund 2001). By 1984, all the Mount Baker glaciers, which were advancing in 1975, were again retreating (Harper 1993; Pelto 1993). By 1992 all 47 glaciers termini observed by NCGCP were retreating (Pelto 1993). By 2006, four had disappeared entirely: Lewis Glacier, David Glacier, Spider Glacier and Milk Lake Glacier (Pelto 2010). The retreat on each Mount Baker glacier was measured in the field from benchmarks established in 1984 or 1985 at their recent maximum position (late 1970s–early 1980s). In each case a maximum advance moraine had been emplaced. The advance moraines were quite prominent in the 1980s as each was ice cored increasing its topographic prominence. By 1997–1998, the average retreat had been −197 m (Pelto and Hedlund 2001). The retreat has continued to 2014 with the average retreat of 430 m for the nine principal Mt. Baker glaciers in this interval. In Table 2.1 each Mt. Baker glacier is described specifically, going counterclockwise from Deming Glacier.

Table 2.1 Characteristics and terminus change of Mount Baker glaciers

Name	Area km^2	Terminus (m)	Top (m)	Slope	Orientation	Terminus change LIAM-1947	Terminus change 1947–1979	Terminus change 1979–2014
Deming	4.79	1270	3270	0.39	215	−2700	+600	−615
Easton	2.87	1680	2900	0.35	195	−2420	610	−320
Squak	1.55	1700	3000	0.45	155	−2550	310	−300
Talum	2.15	1800	3000	0.55	140	−1975	280	−240
Boulder	3.46	1530	3270	0.50	110	−2560	740	−520
Park	5.17	1385	3270	0.41	110			−360
Rainbow	2.03	1340	2200	0.37	90	−1370	510	−480
Sholes	0.94	1610	2110	0.30	330	−1170	−60	−95
Mazama	4.96	1480	2980	0.44	10	−2500	−450	−410
Coleman-		1350	3270	0.47	320	−2600	+400	−480
Roosevelt		1560	3270	0.45	320	−3200	+375	−400

2.6 Initial Response Time

Mount Baker glaciers provide a unique opportunity to examine alpine glacier response time to climate change. The glaciers all experience the same climate change and yet have different geographic characteristics, such as aspect, slope angle and altitude that will affect response time. The time between the onset of a mass balance change and the onset of a significant change in terminus behavior is called the initial terminus response time or reaction time (*Ts*) (Johannesson et al. 1989). *Ts* is a descriptive quantity that quantifies the time lag between climate forcing and terminus response for a particular climate event, rather than a physical property of a glacier. *Ts* in this study is based solely on the first observed terminus change from retreat to advance after 1944, and from advance to retreat after 1976. *Ts* has been identified from the response of North Cascade glaciers to the relative cooler and wetter weather beginning in 1944 (Hubley 1956; Long 1955, 1956; Tangborn 1980), and to the subsequent warmer and drier conditions beginning in 1977 (Ebbesmeyer and others 1991; Pelto 1988, 1993; Krimmel 1994; Harper 1993).

From 1890 to 1946 a retreat of at least 1000 m occurred on each of the significant glaciers (over 1.5 km^2) on Mt. Baker: Rainbow, Mazama, Roosevelt, Coleman, Deming, Easton, Squak, Talum, Boulder and Park Glacier. Each glacier was still retreating appreciably in 1940 but had approached close enough to equilibrium that the climate shift beginning in 1944 brought about a rapid change from retreating to advancing conditions (Hubley 1956). By 1960 all of the glaciers were advancing.

Similarly by 1976 advance had brought these glaciers close enough to equilibrium, as evidenced by the slow rate of terminus change (Harper 1993), that the modest (10 %) recent decline in winter precipitation and rise in summer temperature (1.1 °C) resulted in glacier retreat (Pelto 1993, 1996; Harper 1993). By 1979 the advance had ended and by 1989 each glacier had begun to retreat (Pelto and Hedlund 2001).

Focusing on the ten largest Mount Baker glaciers that responded to these two climate shifts, all having an area over 1.5 km^2, the initial terminus response invariably is less than 16 years (Pelto 1993; Hubley 1956; Harper 1993). Table 2.2 is a list of 12 Mount Baker glaciers where *Ts* was noted for both advance and retreat for the post-1944 period by Hubley (1956), or Long (1955, 1956). In each case the glaciers were observed to be in retreat during the 1940s, and subsequently each advanced within 16 years of the climate change. Table 2.2 also notes the response of the same glaciers from a period of advance by each glacier in the early 1970s to retreat by 1988, 12 years after the climate change (Pelto 1988, 1993; Harper 1993). The observed *Ts* is not significantly different on individual glaciers for initiation of advance, versus initiation of retreat.

Many North Cascade glaciers did not respond (advance) during the 1950–1980 period. This may be the result of longer *Ts*, or that the climate change was insufficient to substantially alter mass balance on these glaciers.

Table 2.2 Date of first observed advance following the 1944 climate change

Glacier	Advance observed	Retreat observed
Rainbow	1955	1985
Mazama	1955	1987
Roosevelt	1950	1979
Coleman	1950	1979
Deming	1955	1986
Easton	1960	1989
Squak	1955	1985
Boulder	1953	1985
Park	1955	1985

Date of the first observed retreat following the climate change in 1976–1977

2.7 Complete Response Time

The period it takes a glacier to complete two thirds of its adjustment to a step change in climate is considered the response time (*Tm*) (Johannesson and others 1989). A primary difficulty in the identification of *Tm* is that after a climate change climate conditions do not reach a new steady state for periods comparable to the *Tm* of glaciers. Each glacier is then adjusting to the continually changing climate conditions and never achieves a steady state, due to the non-steady state climate (Schwitter and Raymond 1993). Schwitter and Raymond (1993) noted that these difficulties are minimized with regard to changes from the LIAM to the present, since the basic climate change since the late 1800s has been from a LIA climate favorable to glaciers and a post LIA climate unfavorable for glaciers. Changes in North Cascade terminus behavior and glacier thickness from the LIAM to the present are large compared to changes in response to more recent climate changes (Schwitter and Raymond 1993).

Pelto and Hedlund (2001) observed that North Cascade glaciers where the terminus history has been determined for the 1890–1998 period exhibit three distinct response types (1) Retreat from 1890 to 1950 then a period of advance from 1950 to 1976, followed by retreat since 1976. (2) Rapid retreat from 1890 to approximately 1950, slow retreat or equilibrium from 1950 to 1976 and moderate to rapid retreat since 1976. (3) Continuous retreat from the 1890 to the present. Distinction of a glacier's Type is based solely on its terminus behavior in this analysis.

The observed terminus record of North Cascade glaciers indicates a range of *Tm* from 20 to 30 years on Type 1 glaciers, approximately 40–60 years on Type 2 glaciers, and a minimum of 60–100 years on Type 3 glaciers. All the glaciers on Mount Baker except for Thunder and Sholes are Type 1 glaciers. The glacier types are distinguished by varied terminus behavior since the LIAM, but also exhibit different physical characteristics.

Johannesson and others (1989) compared two means of calculating *Tm*:

$$\mathrm{Tm} = \mathrm{f\,L} / \mathrm{u(t)} \tag{2.1}$$

and

$$\mathrm{Tm} = \mathrm{h} / -\mathrm{b(t)} \tag{2.2}$$

Tm in these equations is potentially dependent on four variables: *L* the glacier length, *u*(*t*) velocity of the glacier at the terminus, *h* the thickness of the glacier, and *b*(*t*) the net annual balance at the terminus. The former equation, which was proposed by Nye (1960), produces longer full response times of 100–1000 years, the latter full response times of 10–100 years (Johannesson and others 1989). The variable *f* is a shape factor that is the ratio between the changes in thickness at the terminus to the changes in the thickness at the glacier head (Schwitter and Raymond 1993). Similar changes in ice thickness will yield a value of $f = 1$, $f = 0.5$ corresponds to a linear decrease of thickness change from a maximum at the terminus to zero at the head. The mean value of *f* has been determined as 0.3 (Schwitter and Raymond 1993), and this value of *f* is applied. This equation is quite sensitive to terminus velocity, which is often spatially inconsistent.

Table 2.3 identifies the mean slope, mean altitude and area of each glacier of the 12 Mount Baker glaciers. Type 1 glaciers have the highest mean elevations (2200 m), largest mean slope (0.42, ±0.07), highest measured mean accumulation (Pelto 1988, 1996), most extensive crevassing and highest measured terminus region velocity (>10 m/a). Type 3 glaciers have the lowest slopes (0.23, ±0.06), least crevassing, and lowest mean terminus velocity (<5 m/a) of any of the glacier types. Type 2 glaciers have on average, a lower slope (0.35, ±0.08), a lower terminus region velocity (5–10 m/a), less crevassing, and a lower mean accumulation rate than Type 1 glaciers.

It is evident that Eq. (2.2) yields values that are lower than the observations of *Tm* but match *Ts* for Mount Baker for Type 1 glaciers. Equation (2.1) overestimates *Tm* and because of the wide spatial variability of *u*(*t*), it is not expected to yield a consistently accurate result on alpine glaciers

Table 2.3 Displays the variables used in determining *Tm* for Mount Baker glaciers, the calculated *Tm*1 from Eq. (2.1), and *Tm*2 from Eq. (2.2)

Glacier	Type	L	U(t)	h	b(t)	^l	Tm1	Tm2
Easton	1	4000	12	75	−6.5	−2420	55	11
Rainbow	1	2700	18	75	−5	−1370	60	20
Deming	1	5150	15	85	−8	−2700	125	11
Coleman	1	4050	20	85	−7.5	−2600	60	12
Boulder	1	3400	20	85	−7	−2560	50	12

Each variable, except *h* has been observed by NCGCP, *h* is derived from field measurements of Harper (1993) and Finn et al. (2012).

References

Andreassen LM, Paul F, Kääb A, Hausberg JE (2008) The new Landsat-derived glacier inventory for Jotunheimen, Norway, and deduced glacier changes since the 1930s. Cryosphere Discuss 2:299–339

Bengston K (1956) Activity of the Coleman Glacier, Mt. Baker, Washington, USA., 1949–1955. J Glaciol 2:708–713

Bidlake WR, Josberger EG, Savoca ME (2007) Water, ice, and meteorological measurements at South Cascade Glacier, Washington, Balance Years 2004 and 2005: U.S. Geological Survey scientific investigations report 2007–5055

Burbank DW (1981) A chronology of late Holocene glacier fluctuations on Mt. Rainier. Arct Alp Res 13:369–386

Carturan L, Baroni C, Becker M, Bellin A, Cainelli O, Carton A, Casarotto C, Dalla Fontana G, Godio A, Martinelli T, Salvatore MC, Seppi R (2013) Decay of a long-term monitored glacier: Careser Glacier (Ortles-Cevedale, European Alps). Cryosphere 7:1819–1838. doi:10.5194/tc-7-1819-2013

Ebbesmeyer CC, Cayan DR, McLain FH, Nichols DH, Peterson DH, Redmond KT (1991) 1976 step in the Pacific climate: forty environmental changes between 1968–1975 and 1976–1984. In: Betancourt JL, Tharp VL (eds) Proceeding on the 7th annual pacific climate workshop, Sacramento, CA pp 129–141

Finn CA, Deszcz-Pan M, Bedrosian PA (2012) Helicopter electromagnetic data map ice thickness at Mount Adams and Mount Baker, Washington, USA. J Glaciol 58(212):1133–1143. http://dx.doi.org/10.3189/2012JoG11J098

Harper JT (1993) Glacier terminus fluctuations on Mt. Baker, Washington, USA, 1940–1980, and climate variations. Arct Alp Res 25:332–340

Heikkinen A (1984) Dendrochronological evidence of variation of Coleman Glacier, Mt. Baker, Washington. Arct Alp Res 16:53–54

Hodge SM, Trabant DC, Krimmel RM, Heinrichs TA, March RS, Josberger EG (1998) Climate variations and changes in mass of three glaciers in western North America. J Clim 11:2161–2179

Hubley RC (1956) Glaciers of Washington's Cascades and Olympic Mountains: their present activity and its relation to local climatic trends. J Glaciol 2(19):669–674

Huss M (2012) Extrapolating glacier mass balance to the mountain-range scale: the European Alps 1900–2100. Cryosphere 6:713–727. doi:10.5194/tc-6-713-2012

IPCC: Climate Change (1995) Contributions of working group I to the second assessment of the intergovernmental panel on climate change. Cambridge University Press, Cambridge, pp 241–265

Johannesson T, Raymond C, Waddington E (1989) Time-scale for adjustment of glacier to changes in mass balance. J Glaciol 35(121):355–369

Kääb A, Paul F, Maisch M, Hoelzle M, Haeberli W (2002) The new remote-sensing-derived Swiss glacier inventory: II. First results. Ann Glaciol 34:362–366

Key CH, Fagre DB, Menicke RK (2002) Glacier retreat in glacier National Park, Montana. In: Williams RS Jr, Ferrigno JG (eds) Satellite image atlas of glaciers of the world, glaciers of North America – glaciers of the Western United States. U.S. Geological Survey professional paper 1386-J. United States Government Printing Office, Washington, DC, pp J365–J381

Krimmel RM (1994) Water, ice and meteorological measurements at South Cascade Glacier, Washington, 1993 balance year. USGS WRI-94-4139

Kunkel KE, Karl TR, Easterling DR, Redmond K, Young J, Yin X, Hennon P (2013) Probable maximum precipitation (PMP) and climate change. Geophys Res Lett 40:1402–1408

Long WA (1953) Recession of Easton and Deming Glacier. Sci Mon 76:241–247

Long WA (1955) What's happening to our glaciers. Sci Mon 81:57–64

Long WA (1956) Present growth and advance of Boulder Glacier, Mt. Baker. Sci Mon 83:1–2

Maloof A, Piburn J, Tootle G, Kerr G (2014) Recent alpine glacier variability: wind river range, Wyoming, USA. Geosciences 4:191–201

Meier MF, Post A (1962) Recent variations in mass net budgets of glaciers in western North America. IAHS 58:63–77
Miller CD (1971) Chronology of neoglacial moraines in the Dome Peak Area, North Cascade Range, Washington. Arct Alp Res 1:49–66
Nye JF (1960) The response of glaciers and ice-sheets to seasonal and climate changes. Proc R Soc Lond A 256(1287):559–584
Oerlemans J (1994) Quantifying global warming from the retreat of glaciers. Science 264:243–245
Paul F, Kääb A, Maisch M, Kellenberger TW, Haeberli W (2004) Rapid disintegration of alpine glaciers observed with satellite data. Geophys Res Lett 31:L21402
Pelto MS (1988) The annual balance of North Cascade, Washington Glaciers measured and predicted using an activity index method. J Glaciol 34:194–200
Pelto MS (1993) Current behavior of glaciers in the North Cascades and effect on regional water supplies. Wash Geol 21(2):3–10
Pelto MS (1996) Annual net balance of north cascade glaciers, 1984–1994. J Glaciol 42(140):3–9
Pelto MS (2006) The current disequilibrium of North Cascade glaciers. Hydrol Process 20:769–779. doi:10.1002/hyp.6132
Pelto MS (2010) Forecasting temperate alpine glacier survival from accumulation zone observations. Cryosphere 3:323–350
Pelto MS (2011) Skykomish river, Washington: impact of ongoing glacier retreat on streamflow. Hydrol Process 25(21):3267–3371
Pelto MS, Brown C (2012) Mass balance loss of Mount Baker, Washington glaciers 1990–2010. Hydrol Process 26(17):2601–2607
Pelto MS, Hedlund C (2001) Terminus behavior and response time of North Cascade glaciers, Washington U.S.A. J Glaciol 47:497–506
Pochop L, Marston R, Kerr G, Varuska M (1989) Long-term trends in glacier and snowmelt runoff Wind River Range, Wyoming. Wyoming Water Research Council 89-05
Porter SC (1986) Pattern and forcing of Northern Hemisphere glacier variations during the last millennium. Quat Res 26:27–48
Post A (1975) Interim topographic map of Mount Baker, Washington. USGS-Map: 1975-0-689-909/61, Washington DC
Schwitter MP, Raymond C (1993) Changes in the longitudinal profile of glaciers during advance and retreat. J Glaciol 39(133):582–590
Tangborn WV (1980) Two models for estimating climate-glacier relationships in the North Cascades, Washington, USA. J Glaciol 25:3–21

Chapter 3
Glacier Mass Balance

3.1 Glacier Mass Balance Measurement

Annual mass balance (Ba) is the sum of accumulation and ablation over the balance year (Cogley et al. 2011). Mass balance of Mount Baker glaciers has been assessed in four ways. (1) Direct field measurements of mass balance on three glaciers as part of the World Glacier Monitoring Service (WGMS) system. (2) From the regression of mass balance and AAR (Kulkarni 1992). (3) Calculated from the summation of the products of the mean mass balance for each elevation band and the glacier area in that elevation band. (4) A median elevation approach adjusting the balance gradient based on glacier median elevation Kuhn et al. (2009).

3.2 Field Methods

NCGCP essentially measures conditions on a glacier near the time of minimal mass balance at the end of the hydrologic year, using a fixed date method. Measurements are made at the same time each year from late July to mid-August and again in late September near the end of the ablation season. Any additional ablation that occurs after the last visit to a glacier is measured during the subsequent hydrologic year. NCGCP methods emphasize surface mass balance measurements with a relatively high density of sites on each glacier (>100 sites/km^2) (Fig. 3.1), consistent measurement methods, measurements on fixed dates, and at fixed measurement locations (Pelto 1996, 1988; Pelto and Riedel 2001; Pelto and Brown 2012). The use of a high measurement density and consistent methods generates errors resulting from an imperfectly representative measurement network that are largely consistent and correctable, the error range has been observed at $\pm$0.10–0.15 ma^{-1} for using a less dense measurement network (Pelto 2000). The three Mount Baker glaciers examined;

M. Pelto, *Climate Driven Retreat of Mount Baker Glaciers and Changing Water Resources*, SpringerBriefs in Climate Studies,
DOI 10.1007/978-3-319-22605-7_3

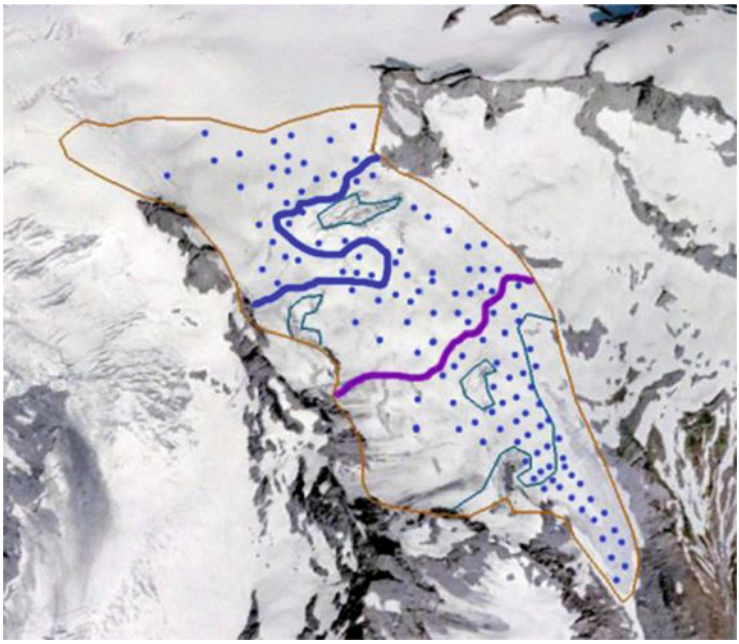

Fig. 3.1 Mass balance measurement map for Rainbow Glacier

Rainbow, Sholes and Easton do not lose significant mass by calving or avalanching, thus changes observed are primarily a function of winter accumulation and summer ablation on the glacier's surface.

Measurement of accumulation thickness is accomplished using probing and crevasse stratigraphy. Probing has been proven as a successful method on most temperate glaciers and is a point measurement of retained snowpack depth (Østrem and Brugman 1991). LaChapelle (1954) noted that repeated thawing and freezing during the ablation season creates a dense layer on the surface of the snowpack. The result is a marked increase in probe ram resistance, which allows for determination of the thickness of the previous winter's snow-pack. Ice lenses are rare in the North Cascades and these layers within the most recent annual layer are easily penetrated by a probe, since the snow below the layer is weak. Crevasses provide a two dimensional view of accumulation layer thickness. In the North Cascades the annual layers are evident in crevasse walls as thick continuous dirty ice layers. Distinguishing annual layers in ice cores or snowpits in the region rely on the same distinguishing techniques. Crevasses provide a two dimensional view of the annual layer, instead of just a point measure. Only vertically walled crevasses can be used. In extensive tests, NCGCP found crevasse measurements had a lower standard error in duplicate measurements than probing (Pelto 1996, 1997).

In the North Cascades at the end of summer, the density of the previous winter's snow-pack that remains on a glacier is remarkably consistent (Pelto 1996). NCGCP dug approximately 100 snow pits in late summer to measure bulk density between

1984 and 1987, and found a range from 0.59 to 0.63 Mg/m^3. This consistent density is also observed on South Cascade Glacier (Krimmel 1999). Due to this consistency, snow pits are no longer used, and bulk density at the end of the ablation season is assumed to be 0.60 Mg/m^3.

Conventional mass balance assessment typically utilizes ablation stakes to measure glacier surface ablation. The increased height of the top of the ablation stake above the glacier surface provides a direct measure of surface ablation (Østrem and Brugman 1991). Ablation on Mount Baker glaciers is measured using ablation stakes that can be checked both daily and periodically. Daily ablation observations have been made on 192 different days on Mount Baker, which has identified the relationship between temperature and ablation referred to as the degree day function (DDF). Ablation is also assessed from mapping of the transient snow line (TSL). Østrem (1975) identified the TSL as a useful parameter to measure in the course of mass balance assessment. The TSL is the location of the transition from bare glacier ice to snow cover at a particular time during the ablation season (Østrem 1975), whereas the equilibrium line altitude (ELA) is the altitude of the snow line at the end of the ablation season. On temperate alpine glaciers that lack superimposed ice the TSL coincides with the ELA at the end of the melt season (Østrem 1975; Williams et al. 1991; Miller and Pelto 1999). The TSL can be identified near the end of the ablation season using satellite imagery (Østrem 1975; Hall et al. 1989).

Point measurement data are then used to construct balance maps for each glacier, data are integrated across the entire surface of the glacier within each 50 m elevation contour.

On Easton Glacier the measurement network consists of 240 measurement locations ranging from 1650 to 2750 m. On Rainbow Glacier there are 120 sites from 1400 to 2200 m. On Sholes Glacier the network extends from 1600 to 2000 m with 120 sites. In individual years depending on snowpack depth the number of measurements can vary. This provides approximately 480 point measurements of mass balance each year from 1400 to 2900 m.

3.3 Crevasse Stratigraphy

Crevasses have typically been avoided in mass balance measurements because of the dangers they present, despite the ease with which the annual layer can be measured. Meier and others (1997) questioned the accuracy of crevasse stratigraphic measurements. However, all of these measurements rely on distinguishing the same harder/dirtier annual layer within the snowpack. Crevasse stratigraphic measurements provide a means to efficiently measure snowpack thickness using a natural incision in the glacier, versus an artificial incision such as snowpits, probing or ice cores. Measurements are conducted only in vertically walled crevasses with distinguishable annual layer dirt bands where the annual layer is not distorted by a slump.

Most of the vertically walled crevasses also tend to be narrow less than 2 m across. In the North Cascades the ablation surface of the previous year is always marked by to 5 cm thick band of dirty-firn or glacier ice (Figs. 3.2, 3.3, and 3.4).

It is possible that the annual layer is difficult to distinguish in a crevasse because of a poorly developed summer icy-dirty layer. This difficulty is even more apparent in snowpits and cores, where the view of the previous summer surface is much more limited. The lack of dirt layers in crevasses is rare in the North Cascades and many other regions. This is expected given the two dimensional view of crevasse stratigraphy versus a single dimension in snowpits and probing. In ice sheet areas distant from a dust source this is difficult, but on alpine glaciers mountaineers and glaciologists have long noticed the ubiquitous nature of these layers (Post and LaChapelle 1971; Pelto 1997).

Fig. 3.2 Measuring snow pack layer thickness in a crevasse

Fig. 3.3 Crevasse layer thickness in a crevasse in 2013

Fig. 3.4 Crevasse layer for 2008 on Easton Glacier

The accuracy of crevasse stratigraphy and probing measurements are cross-checked on at least 25 % of the accumulation area of each glacier where probing is used between crevasses. This cross-checking identifies measurement points that either represents an ice lens and not the previous summer surface in the case of probing, or areas where crevasses do not yield representative accumulation depth in the case of crevasse stratigraphy.

The standard deviation in snow depth obtained in cross checking and duplicate measurements are smallest for crevasse stratigraphy, $\pm$0.02 m, and $\pm$0.03 m for probing. The narrow range of deviation in vertically walled crevasses indicates that they do yield consistent and representative accumulation depths late in the summer.

3.4 Ablation Assessment Using Transient Snow Line Observations

At the TSL the glacier balance is zero. At a specific time if the depth of snowpack above the TSL is known, then as the TSL migrates upglacier intersecting these locations, the ablation rate at each location for the specific time period from depth measurement to TSL intersection is identified (Pelto 2011; Hulth et al. 2013; Mernild et al. 2013). On Sholes Glacier there is limited avalanche accumulation which results in an accumulation pattern that does not vary abruptly. Extensive snowpack depth assessment is conducted between August 6th and 11th each summer identifying the distribution of snowpack depth on the glacier. Subsequent probing and transient snowline mapping is completed on 1–3 occasions by the end of the melt season. As the TSL migrates through location of measured snow depth the total ablation from the date of probing to the date of exposure identifies the ablation rate.

The TSL provides a map of both the zero balance line for the date of observation, which can be used to determine the transient AAR, which Hulth et al. (2013) indicated is useful for transient mass balance determination. The ablation can also be determined at specific points where the TSL intersects previous accumulation measurement sites. Because of this ease of observation of the TSL, repeat imaging during a single season has been used on Abramov Glacier, Kyrgyzstan Storglaciaren, Sweden and Vernagtferner, Austria to aid in mass balance assessment (Hock et al. 2007).

3.5 Record Snowfall Accumulation

During the 1998/1999 winter season, Mount Baker, Washington, set a verified single season world snowfall record of 28.70 m, at the 1300-m Mount Baker Ski Area weather station. Measurements at higher elevation on two Mount Baker glaciers have been completed each year since 1990. In early June 1999 snowpack depths were too large for safe measurement of depth. A series of 6-m-long stakes were

driven into the snowpack from 1950 to 2300 m. By late August the stakes from 2100 to 2300 m had each recorded 3.85 m of ablation. Measurement of snowpack thickness in numerous crevasses on Easton Glacier in late August 1999 indicated that 9.45 m of snowpack remained at 2150 m and 10.65 m at 2450 m. This is in sharp contrast to 1998 when snowpack was 1.55 m at 2150 m and 3.35 m at 2450 m.

The snowpack in late August had a density of 0.60 g/cm^3; this is 400 % the normal new-fallen snow density. The average density of new snowfall at Paradise, Mt. Rainier is Washington at 1650 m is 0.13–0.15 g/cm^3. Reconstructing snowpack is completed by summing the water equivalent from ablation loss and retained in crevasses assessment and converting to the likely density of new snowfall. The 8.2 m sum of the observed August snowpack SWE (6.0 m w.e.) and ablated snowpack June–August (2.2 m w.e.), combined with a density of 0.15 g/cm^3 yields an expected snowfall of 54.5 m at 2150–2450 m on Easton Glacier.

On Easton Glacier at each altitude the 1998/1999 snowpack depth was more than 25 % greater than any year from 1990 to 1998. On Rainbow Glacier, 1999 stands out as exceptional with an August snowpack depth of 8.0 m, 24 % greater than any other year from 1984 to 1999.

3.6 Glacier Mass Balance 2013

The Ba of three glaciers was assessed on Mount Baker: Sholes Glacier, Rainbow Glacier and Easton Glacier. On the three glaciers a total of 320 snow depth measurements were made (Fig. 3.5). Snow covered area was mapped in early August on each glacier, in mid-September and at the end of September. The weekend of Sept. 27–28th, 2013 featured heavy rain in the mountains but also new snow on the glaciers, marking the end of the melt season. The Ba loss exceeded 1 m w.e. on all of the Mount Baker glaciers. Details of the observations are described below. This provides an example of the analysis that is completed each year.

3.6.1 Sholes Glacier 2013

Sholes Glacier is at the headwaters of Wells Creek the standard measurement sites for mass balance are indicated by blue dots and the standard site for streamflow observations at the purple arrow (Fig. 3.6).

Snow depth was measured at 120 locations on the Sholes Glacier on August 6th, 2013. Snow depth was measured at a 30–50 m spacing across the entire glacier on August 6th, yielding a map of snow depth across the glacier (Fig. 3.6). The position of the snowline indicates the location where snow depth is zero. The glacier was 97 % snow covered at the time a blue ice area of 12,500 m^2 was mapped.

The launch of the Landsat 8 satellite in March of 2013 has provided usable imagery of the Mount Baker area with sufficient resolution for the first time in over a

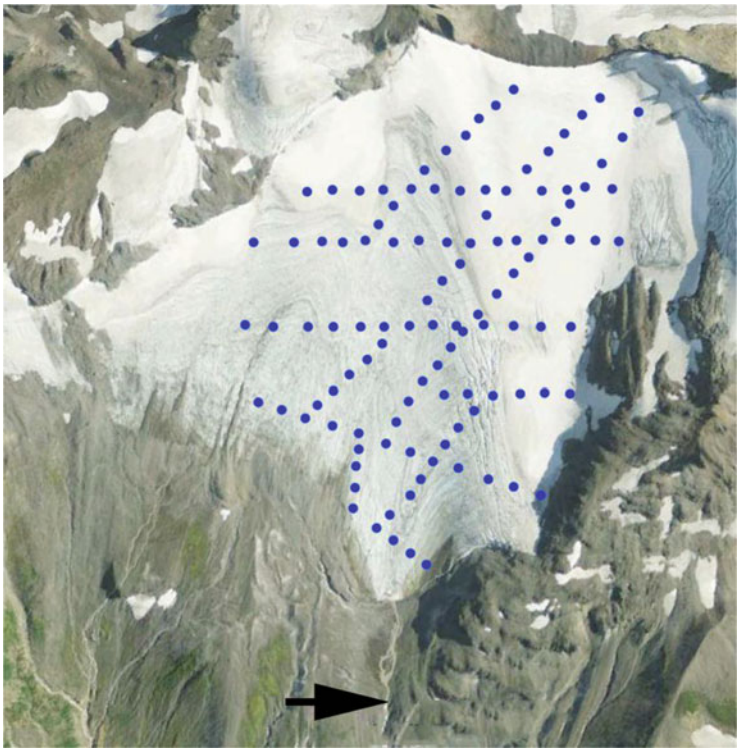

Fig. 3.5 Sholes Glacier measurement network and potential stream gaging locations. *Blue dots* are accumulation measurement sites, and in some instances ablation stake locations

decade. On July 11, 2013 the Mount Baker glaciers were 100 % snowcovered. On July 19th a Landsat image indicated 100 % snowcover for Sholes Glacier (Fig. 3.7). On Aug. 4th the mapped snow covered area is confirmed by a Landsat image indicating a single small blue ice area (Fig. 3.8). By Aug. 20th a satellite image indicates that the blue ice area had expanded to an area of 220,000 m^2. Field observations on Sept. 1 indicate the snowcovered area had expanded to 320,000 m^2 (Fig. 3.9) Satellite imagery from September 12, indicates a further expansion of the blue ice and firn from winters before 2013 to 400,000 m^2 (Fig. 3.10).

The location of the snowline where snow depth is zero is currently measured using GPS and with Landsat imagery. On Sholes Glacier the snowline was mapped again on August 20th, Sept. 12th and Sept. 29th. Additional probing was completed on these dates and ablation stakes were monitored, but here we focus simply on the ablation after August 6th at the TSL. On Aug 20th the TSL intersected ten probing lines, the depth of snowpack on August 6th had ranged from 1.15 to 1.3 m at the intersection points, a mean of 1.2 m or 5.1 cm w.e. d^{-1}. On Sept 12th the TSL intersected seven probing lines that had a depth of 2.75–2.95 m on August 6th, a mean of 2.8 m or 4.5 cm w.e. d^{-1} (Table 3.1).

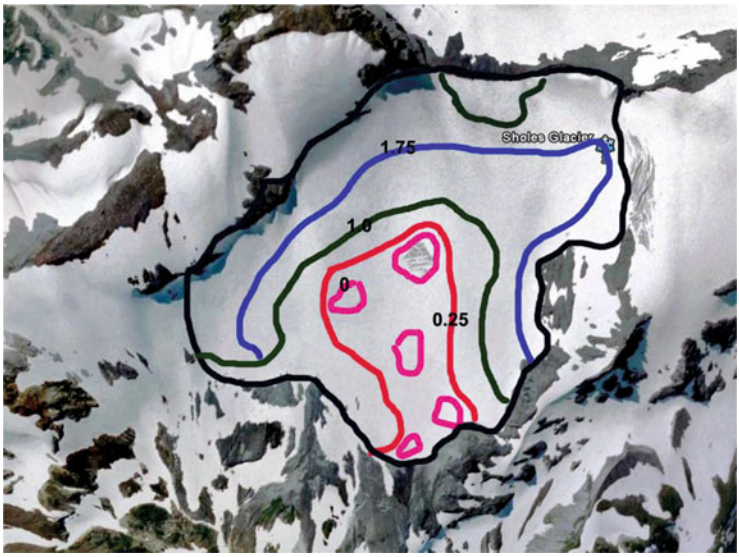

Fig. 3.6 Snow depth distribution in snow water equivalent on Sholes Glacier on Aug. 8th, 2013

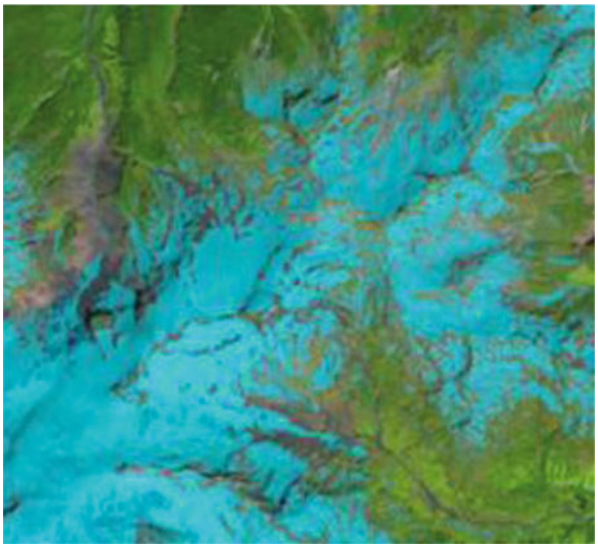

Fig. 3.7 July 19th, 2013 Landsat satellite image indicating 100 % snowcover on Sholes Glacier

We measured ablation daily during the August 3–9 period at a series of 12 stakes on the Sholes Glacier. Average ablation during the week was 8.8 cm/day of snowpack or 5.3 cm/day of water equivalent. Subsequent assessment of the same stakes on Aug. 20th indicates mean ablation during the period of 7.8 cm/day. Assessment of ablation from remapping of the snowline on Sept. 1, which intersected locations

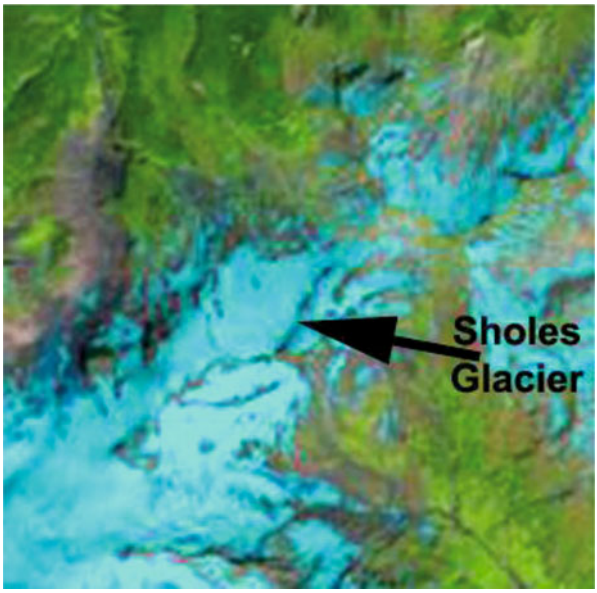

Fig. 3.8 Landsat image indicating snowcover on August 4th, 2013 a few small bare ice patches are apparent

Fig. 3.9 Comparison of snowpack on Sholes Glacier on August 4th and September 1st, 2013

of know snow depth on August 6th indicates mean ablation of 7.5 cm/day during the Augurs 6th–Sept. 1st period. The snow depth at a particular location of the snowline on Sept. 12th indicates the snow ablation between since August 6th. Observations of the snowline margin on Aug. 20, Sept. 1 and Sept. 12 indicated mean ablation of 7.4 cm per day from Aug. 4th to Sept. 12th. The snowline location indicated 2.9 m of snow melt after 8/4. The ice melt was the same rate in thickness, but because of the greater density the water equivalent loss is higher. By Sept. 12th the glacier was 30 % snowcovered. Final assessment occurred on September 29th, and indicated that the glacier had a Ba of −1700 mm w.e (Table 3.2).

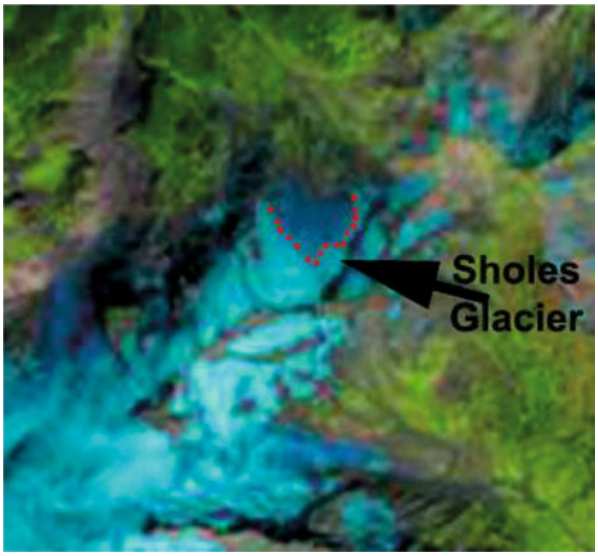

Fig. 3.10 Sept 12th Landsat image indicating snowline position on Sholes Glacier

Table 3.1 Satellite observations of accumulation area ratio from Landsat 8 images

	AAR-Sholes	AAR-Rainbow	AAR-Easton
7/11/2013	100	100	100
7/19/2013	100	100	100
8/4/2013	98	87	90
8/20/2013	53	N/A	N/A
9/12/2013	41	50	62
9/29/2013	30	38	40

Table 3.2 Ablation rate measurements on Sholes Glacier in 2013 from ablation stakes and transient snowline migration

Start	End		Ablation rate cm/day
8/3/2013	8/9/2013	Stakes	5.3
8/9/2013	8/20/2013	Stakes	4.7
8/20/2013	9/1/2013	Stakes	4.4
8/6/2013	9/1/2013	TSL	4.5
8/6/2013	8/20/2013	TSL	5.1
8/4/2013	9/12/2013	TSL	4.4
8/6/2013	9/12/2013	TSL	4.5

Fig. 3.11 Easton Glacier snowpack assessment in August at 2000 m

3.6.2 Easton Glacier 2013

On August 10–11th probing and crevasse observations identified the snowpack on Easton Glacier. Peak snow depth observed was in crevasses at 2500 m, at 5.5 m. There was limited snowpack on the lowest bench of the glacier below 1800 m. On the bench, below the main icefall at 2000 m, a transect of 35 measurements yielded an average depth of 2.9 m on Aug. 10th (Fig. 3.11). The bench was completely snowcovered on Aug. 10th. Below this bench 75 measurements of snow depth indicated a mean depth of 1.4 m. By Sept. 15th the TSL was on this bench. GPS measurements of the TSL on Sept. 15th indicate ablation of 2.75 m since Aug. 10th. This is an ablation rate of 7.6 cm d^{-1}. This is 0.2 cm d^{-1} higher than Sholes Glacier over a similar but not identical period. The southern aspect of Easton Glacier typically leads to higher ablation rates at specific elevations than on Sholes Glacier. Satellite observations of the change in snowline position compared to snow depth observations from Aug. 4th to Sept 12th indicate mean ablation of 7.2–8.0 cm d^{-1}. By the end of the melt season on Sept. 29 the TSL was at 2100 m.

3.6.3 Rainbow Glacier 2013

Mass balance was assessed on Rainbow Glacier with 140 measurements of probing and crevasse stratigraphy on Aug. 7th and 8th. Snowpack depth below the main icefall at 1725–1800 m was consistent between 2.9 and 3.3 m. Above the icefall at

Fig. 3.12 Rainbow Glacier at the end of September (Tom Hammond)

1925–2000 m snowpack ranged from 3.5 to 4.25 m. On Aug. 7th the glacier had snowcover on 83 % of the glacier with the TSL at 1600 m. Snow depth below 1725 m averaged less than 1.5 m. By Sept. 30th the snowcover extent was 38 % and the TSL had risen to 1775 m. Given the TSL snowpack was unusually limited at the 2000 m level of Rainbow Glacier. This fit the pattern of limited maximum snowfall on Easton Glacier. Ablation on Rainbow Glacier averaged 3.1 m from August 7th to Sept. 30th. The retained snowpack area was mainly limited to regions above 1800 m (Fig. 3.12).

3.7 Glacier Mass Balance 2014

The mass balance of three glaciers was assessed on Mount Baker in 2014 Sholes Glacier, Rainbow Glacier and Easton Glacier. On the three glaciers a total of 340 snow depth measurements were made. Snow covered area was mapped in early August on each glacier and again in mid to late September. The Ba loss exceeded 1.0 m w.e. on all of the glaciers; Easton Glacier −1.30 m, Rainbow Glacier −1.94 m and Sholes Glacier −1.65 m. A map of Sholes Glacier mass balance for Aug. 11 is seen below (Fig. 3.13). The contours are in meters of water equivalent, which is the amount of water thickness that would be generated if the snow or ice was melted. Note the similarity of the 1.75 m contour and the Sept. 12th snowline. A final map of the snow depth thickness at the time of the last September that is completed for the mass balance assessment for the World Glacier Monitoring Service is in Fig. 3.14.

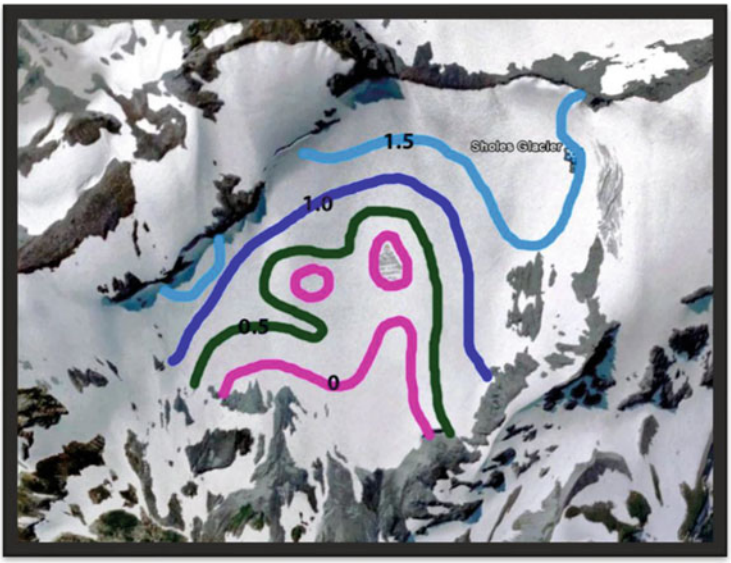

Fig. 3.13 Snow depth distribution in m w.e. on Sholes Glacier on Aug. 11th, 2014

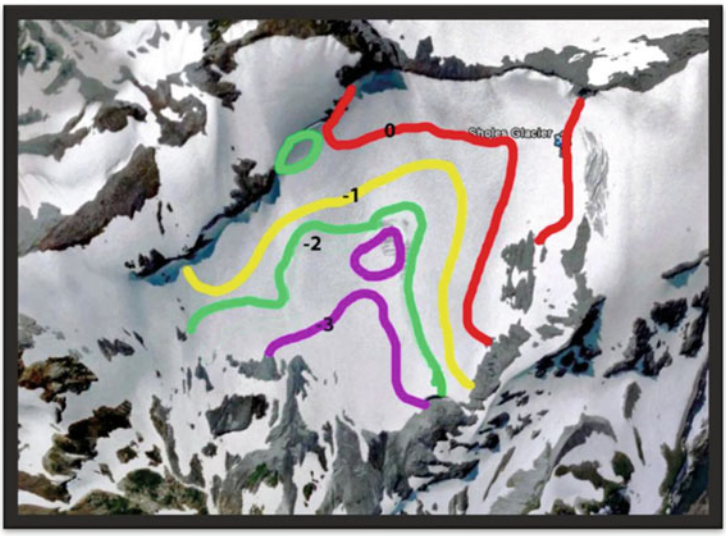

Fig. 3.14 Annual mass balance map of Sholes Glacier in 2014

3.7.1 Sholes Glacier

The extent of snowcover is measured directly on the glacier in early August and again in late September. On July 13, 2014 the Mount Baker glaciers were 100 % snowcovered (Fig. 3.15). On August 7th Landsat 8 satellite imagery indicates the

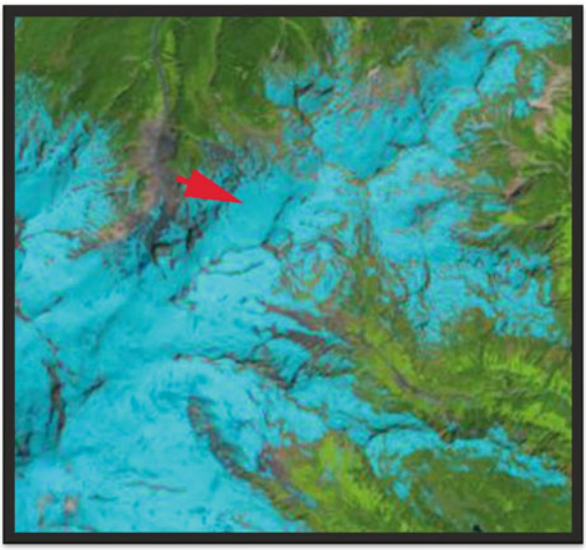

Fig. 3.15 July 13th, 2014 Landsat satellite image indicating 100 % snowcover on Sholes Glacier

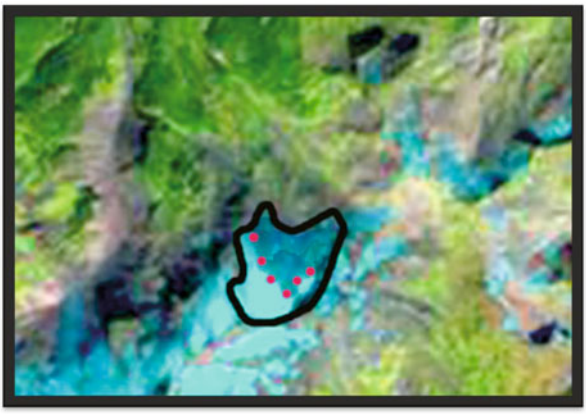

Fig. 3.16 Sholes Glacier snowpack extent on Sept. 15, 2014. The glacier boundary is in *yellow, red dots* are the snowline

Sholes Glacier is still 87 % snowcovered. On Aug. 11th our surface measurements indicated a blue ice area of 125,000 m^2. Mapping of the snowline in the field on Aug. 11th indicated that 78 % of the glacier was snowcovered. On Aug. 23rd, 55 % of the Sholes Glacier retained snowcover before declining to 35 % snowcover by Sept. 15th (Fig. 3.16).

Fig. 3.17 Sholes Glacier terminus and outlet stream on Aug. 11th, 2014

We measured ablation during the August 5–11 period at a series of stakes on the Sholes Glacier. Average ablation during the week was 8.0 cm d^{-1} of snowpack or 4.6 cm w.e.d^{-1}. Subsequent assessment of the same stakes on Aug. 24th indicates mean ablation during the period of 4.3 cm w.e. d^{-1}.

The best measure of ablation over the period from August 11th to Sept. 15th is the shift in the snowline. Snow depth was measured with 30 m spacing across the entire glacier on August 11th (Fig. 3.17). The position of the snowline indicates the location where snow depth is zero. The previously measured snow depth at a particular location intersected by the snowline on Sept. 15th indicates the snow ablation since August 11th. Assessment of ablation from remapping of the snowline on Sept. 15th indicates mean ablation of 3.5 cm w.e.d^{-1} during the Aug. 11th–Sept. 15th period. The August 23rd snowline coincided with snow depths of 1.7 m measured on Aug. 11th. By Sept. 15th the snowline on the glacier coincided with locations that had 2.7 m of snowpack on Aug. 11th. The water equivalent of 2.7 m of snowpack is 1.7 m w.e. of snowpack (Fig. 3.18).

3.8 Field Observations of Annual Mass Balance

The cumulative Ba trend for North Cascade glaciers indicates an increasing trend of negative mass balance. The mean annual balance from 1984 to 2014 on North Cascade glaciers is reported in water equivalence –0.47 m.w.ea^{-1}. The cumulative Ba is –14.5 m, equal to an ice thickness loss of nearly 16 m. The mean annual balance of Rainbow, Sholes and Easton Glacier has been –0.48, –0.53 and –0.44 ma^{-1} from 1990 to 2014. This is comparable to the mean Ba on South Cascade Glacier of –0.78 ma^{-1} from 1990 to 2009 (Bidlake et al. 2007, 2010). Given a mean thickness of 50–75 m the mass loss is a 19–29 % loss in total glacier volume (Post et al. 1971; Harper 1993; Finn et al. 2012). The increase in negative mass balance during a

Fig. 3.18 Sholes Glacier on Sept. 15th, limited remaining snowpack (Oliver Grah, Photograph)

period of substantial retreat, suggests that the current retreat is insufficient for the glaciers to approach equilibrium.

3.9 AAR-Annual Mass Balance Relationship

That there are three glaciers on this single mountain with long term mass balance records of at least 25 years is unique globally. A combination of AAR observations and annual balance measurements on Mount Baker glaciers provides an opportunity to assess the mass balance of the entire glacier complex from 1990 to 2014 using several methods both for comparison and validation. The validation can identify the best regional method for mass balance assessment that can be widely applied to glaciers without detailed mass balance records (Khalsa et al. 2004).

At regional scales and on specific glaciers there are two common proxies for assessing mass balance without detailed observations. They are the AAR and ELA that can be derived from satellite imagery (Østrem 1975; Racoviteanu et al. 2008). The ELA is the elevation at which ablation equals accumulation, on temperate alpine glaciers this is coincident with the TSL at the end of the melt season. The ELA is often not an easily discernible line or elevation on Mount Baker glaciers, due to variability of snow accumulation from impacts of wind and avalanche redistribution. AAR is a more accurately determined parameter and a better proxy in this case. Rabatel et al. (2008) and Dyurgerov (1996) developed methods to derive mass balance from long term AAR observations. The AAR-Ba method has proven

reliable (Hock et al. 2007; Racoviteanu et al. 2008; Pelto and Brown 2012). The WGMS has adopted the reporting of AAR with all mass balance values (WGMS 2007, 2008) and plotting the relationship for each glacier. AAR is a parameter that can be evaluated using satellite imagery, providing an efficient mechanism for utilization of AAR based mass balance determination on numerous glaciers (Kulkarni 1992).

A comparison of annual AAR and Ba observations in WGMS (2007, 2009) indicate correlation coefficients ranging from 0.70 to 0.92 for 15 glaciers with at least 10 years of records. The AAR0 value is the AAR for a glacier with an equilibrium mass balance (Meier and Post 1962). Braithwaite and Muller (1980) noted that the AAR0 for an alpine glacier with an equilibrium balance was 0.67. The mean AAR0 reported for 89 glaciers temperate alpine glaciers is 0.57 (WGMS 2007, 2009).

AAR observations are completed each year on Rainbow, Sholes and Easton Glacier. The TSL is delineated using photographs and GPS measurement on the glacier surface. In addition AAR observations have been made on all Mount Baker glaciers during selected years from photographs and satellite imagery 1993, 1999, 2003, 2005, 2006, 2009, 2010, and 2013 (Fig. 3.19). The error in AAR assessment from aerial photography is 1–3 % (Racoviteanu et al. 2008).

The regression line from the plot of the AAR and Ba for Rainbow, Sholes and Easton Glacier indicates an AAR0 of 0.64 of and a correlation coefficient of 0.89 with Ba (Fig. 3.20). A comparison of the observed AAR in 2009 of these three glaciers 0.34 versus that for the entire mountain 0.39 indicates the slightly higher AAR of Mount Baker glaciers overall than the three index glaciers. In years where the AAR is 0.50 or less for the index glaciers the AAR of all Mount Baker glacier is greater on average by 0.03. During years when the AAR on the index glaciers is greater than the ELA0 of 0.67 there is not a significant difference in the AAR between the two groups. This suggests a slightly different slope to the Ba-AAR relationship, but too few data points to construct with confidence. In this study we assume the same mass balance-AAR relationship for the entire mountain as for the three index glaciers, but adjust the AAR by 0.03 for years when the AAR is below 0.50. The mean Ba derived from the AAR relationship for the index glaciers from 1990 to 2010 is 0.55 ma^{-1}, and Ba for the entire mountain of 0.57 ma^{-1}.

3.10 Balance Gradient Based Mass Balance Assessment

A third approach to assessing the mass balance of Mount Baker is to sum the product of mass balance and glacier area at each 100 m elevation interval. The balance gradient is constructed from the 11,000 point measurements of mass balance on Easton, Rainbow and Sholes Glacier. The area elevation distributions for each glacier were obtained by combining mapped glacier limits from the analysis of the 2009 NAIP orthoimage with elevation data from the 10 m DEM. Glacier polygons were then separated into 100-m elevations bands, such that each subdivision contains the total glacier area that falls within that elevation range (Fig. 3.21). The area

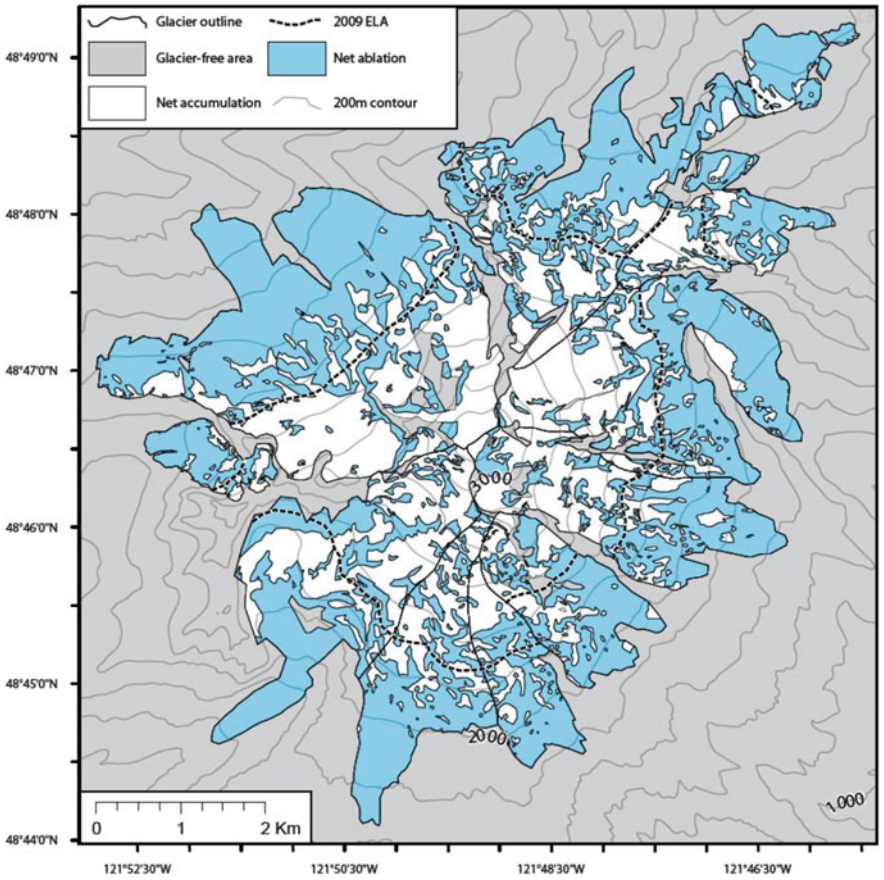

Fig. 3.19 Map of the accumulation area of Mount Baker glaciers in 1990 (Completed by Courtenay Brown, SFU

covered by glaciers and the elevation distribution were determined from the 2009 NAIP (National Agriculture Imagery Program) 1-m resolution, 1:40,000-scale orthoimage, acquired in late August, combined with the National Elevation Dataset 10 m DEM of the Mount Baker area (vertical resolution ±7 m), based on 2006 imagery. The mean Ba derived from this balance gradient method is –0.50 ma^{-1} for the 1990–2010 period. The area will be reassessed in 2015 given the low snowpack that will allow good resolution of glacier area.

3.11 Median Elevation Mass Balance Assessment

Kuhn et al. (2009) developed a means to transfer the balance gradient from a measured to an unmeasured glacier to determine Ba. The method is based on the change in median elevation of the glacier. The balance gradient is transferred along the axis

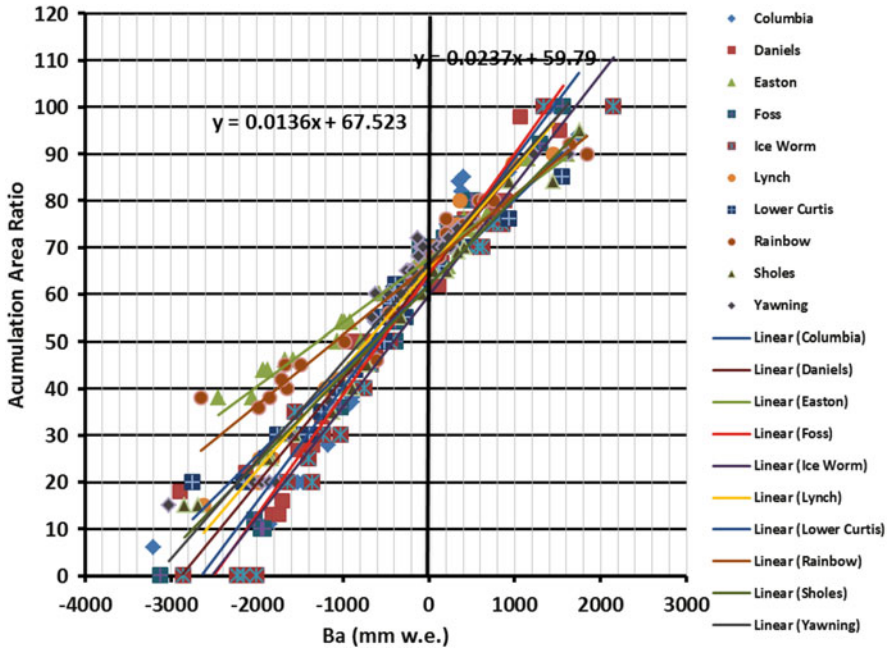

Fig. 3.20 Annual mass balance-Accumulation area ratio relationship for North Cascade glaciers

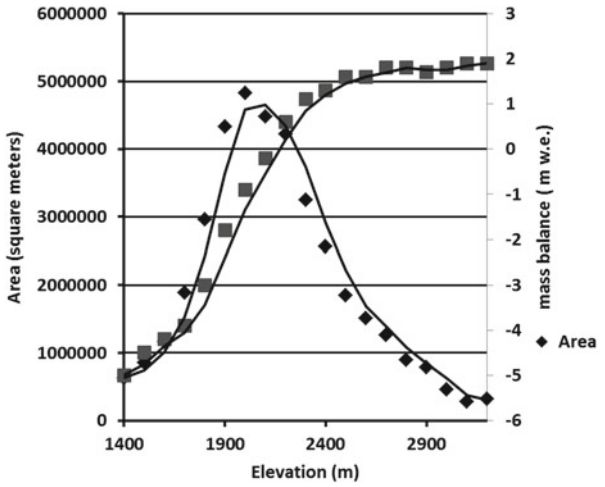

Fig. 3.21 Balance gradient and hypsometry on Mount Baker glaciers 1990–2010

of elevation with the median elevations having equivalent mass balances at that point. The median elevation for the index glaciers is 1950 m and for all Mount Baker glaciers is 2000 m. This difference leads to an elevation shift of the balance gradient of 50 m. With the adjusted values of mass balance than the mean Ba from

1990 to 2010 is –0.77 ma^{-1}. This Ba value is significantly more negative than that determined from the other methods. The small change in the median elevation from the index glaciers to all Mount Baker glaciers, and the steep balance gradient suggests that this balance gradient transfer should yield reasonable results. The result is not as accurate as the direct measurement based methods due to the extrapolation required.

3.12 Conclusion

Mass balance assessment of the mass balance of all glaciers has been made using several methods for the 1990–2010 period (Fig. 3.22): (1) direct observations of the annual balance on three glaciers, –0.51 ma^{-1}. (2) from the observed Ba-AAR relationship on the three index glaciers –0.55 ma^{-1}, 0.57 ma^{-1} from the Ba-AAR relationship for the entire mountain. (3) calculated from the observed balance gradient on three glaciers and the observed glacier covered area –0.50 ma^{-1}, (4) adjusting the balance gradient for the different median elevation of all Mount Baker glaciers compared to the three index glaciers, –0.77 ma^{-1}. The first three methods all yield mean Ba of –0.50 $ma^{-1}$to –0.55 ma^{-1}, indicating each provides a reasonable assessment. The fourth method yielded a mean Ba of –0.77 ma^{-1}, significantly more negative, suggesting this is not the best approach.

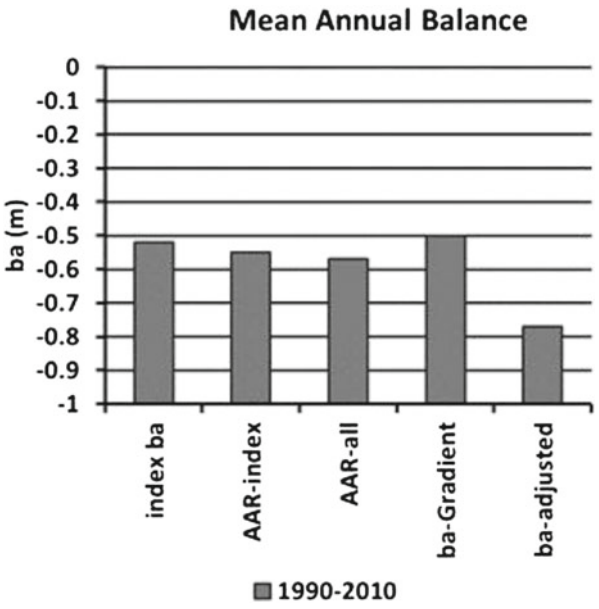

Fig. 3.22 Comparison of mass balance calculation for Mount Baker glaciers using different methods

Deriving Ba from AAR observation or from balance gradient information provided a reasonable assessment of Ba compared to detailed field observations. The balance gradient method is dependent on detailed mass balance records from a glacier in the specific region limiting its applicability. The AAR method allows for calculation of mass balance of North Cascade glaciers from end of the year observations of the snowline position, which is the only observation needed to determine AAR along with a recent glacier DEM.

References

Bidlake WR, Josberger EG, Savoca ME (2007) Water, ice, and meteorological measurements at South Cascade glacier, Washington, Balance Years 2004 and 2005: U.S. Geological Survey Scientific Investigations Report 2007–5055

Bidlake W, Josberger E, Savoca M (2010) Modeled and measured glacier change and related glaciological, hydrological, and meteorological conditions at South Cascade Glacier, Washington, balance and water years 2006 and 2007. U.S. Geological Survey scientific investigations report 2010–5143

Braithwaite RJ, Muller F (1980) On the parameterization of glacier equilibrium line altitude. IAHS Publ 126:263–271

Cogley JG et al (2011) Glossary of glacier mass balance and related terms. UNESCO–International Hydrological Programme. IACS. (IHP-VII technical documents in hydrology no. 86

Dyurgerov M (1996) Substitution of long term mass balance data by measurements of one summer. Gletscherkd Glazialgeol 32:177–184

Finn C, Deszcz-Pan M, Bedrosian P (2012) Helicopter electromagnetic data map ice thickness at Mount Adams and Mount Baker, Washington, USA. J Glaciol 58(212):1133–1143. http://dx.doi.org/10.3189/2012JoG11J098. doi:10.3189/2012JoG11J098#doilink

Hall DK, Chang ATC, Foster JL, Benson CS, Kovalick WM (1989) Comparison of in situ and Landsat derived reflectance of Alaskan glaciers. Remote Sens Environ 28:23–31

Harper JT (1993) Glacier terminus fluctuations on Mt. Baker, Washington, USA, 1940–1980, and climate variations. Arct Alp Res 25:332–340

Hock R, Koostra D, Reijmeer C (2007) Deriving glacier mass balance from accumulation area ratio on Storglaciären, Sweden. In: Glacier mass balance changes and meltwater discharge, vol 318. IAHS, pp 163–170

Hulth J, Rolstad Denby C, Hock R (2013) Estimating glacier snow accumulation from backward calculation of melt and snowline tracking. Ann Glaciol 54(62):111–119. doi:10.3189/2012AoG62A083

Khalsa S, Dyurgerov M, Khromova T, Raup B, Barry R (2004) Space-based mapping of glacier changes using ASTER and GIS tools. IEEE Trans Geosci Remote Sens 42(10):2177–2183

Krimmel R (1999) Analysis of difference between direct and geodetic mass balance measurements at South Cascade glacier. Wash Geogr Ann 81A(4):653–658

Kuhn M, Abermann J, Bacher M, Olefs M (2009) The transfer of mass-balance profiles to unmeasured glaciers. Ann Glaciol 50:185–190 50(50): 185–190, 2009

Kulkarni A (1992) Mass balance of Himalayan glaciers using AAR and ELA methods. J Glaciol 38(128):101–104

LaChapelle E (1954) Snow studies on the Juneau Icefield', JIRP report no. 9. American Geographical Society, New York

Meier MF, Post A (1962) Recent variations in mass net budgets of glaciers in western North America. IAHS 58:63–77

Meier M, Armstrong R, Dyugerov M (1997) Comments on "Annual net balance of North Cascade glaciers 1984–1994" by M S. Pelto. J Glaciol 43(143):192–193
Mernild S, Pelto M, Malmros J, Yde J, Knudsen N, Hanna E (2013) Identification of snow ablation rate, ELA, AAR and net mass balance using transient snowline variations on two Arctic glaciers. J Glaciol 59:649–659. doi:10.3189/2013JoG12J221
Miller MM, Pelto MS (1999) Mass balance measurements on the Lemon Creek glacier, Juneau Icefield, AK 1953–1998. Geogr Ann 81A:671–681
Østrem G (1975) ERTS data in glaciology—an effort to monitor glacier mass balance from satellite imagery. J Glaciol 16:403–415
Østrem G, Brugman M (1991) Glacier mass-balance measurements: a manual for field and office work, NHRI science report, 224 pp
Pelto MS (1988) The annual balance of North Cascade, Washington glaciers measured and predicted using an activity index method. J Glaciol 34:194–200
Pelto MS (1996) Annual net balance of north cascade glaciers, 1984–1994. J Glaciol 42(140):3–9
Pelto MS (1997) Reply to comments of Meier and others on "Annual net balance of North Cascade glaciers 1984–1994" by M. S. Pelto. J Glaciol 43(143):193–196
Pelto MS (2000) The impact of sampling density on glacier mass balance determination. Proc Hydrol 14:3215–3225
Pelto MS (2011) Skykomish River, Washington: impact of ongoing glacier retreat on stream flow. Hydrol Process 25(21):3267–3371
Pelto MS, Brown C (2012) Mass balance loss of Mount Baker, Washington glaciers 1990–2010. Hydrol Process 26(17):2601–2607
Pelto M, Riedel J (2001) Spatial and temporal variations in annual balance of North Cascade glaciers, Washington 1984–2000. Hydrol Process 15:3461–3472
Post A, LaChapelle E (1971) Glacier ice. University of Washington Press, Seattle
Post A, Richardson D, Tangborn WV, Rosselot FL (1971) Inventory of glaciers in The North Cascades, Washington. US Geological Survey professional paper, 705-A
Rabatel A, Dedieu J, Thibert E, Letreguilly A, Vincent C (2008) Twenty-five years of equilibrium-line altitude and mass balance reconstruction on the Glacier Blanc, French Alps (1981–2005), using remote-sensing method and meteorological data. J Glaciol 54:307–314
Racoviteanu A, Williams M, Barry R (2008) Optical remote sensing of glacier characteristics: a review with focus on the Himalaya. Sensors 8(5):3355–3383. doi:10.3390/s8053355
WGMS (2007) Glacier mass balance bulletin no. 9 (2004–2005). ICSU (FAGS)/IUGG (IACS)/UNEP/UNESCO/WMO/World Glacier Monitoring Service, Zurich, 100 pp
WGMS (2008) Global glacier changes: facts and figs. In: Zemp M, Roer I, Kääb A, Hoelzle M, Paul F, Haeberli W (eds) Glacier mass balance bulletin no. 10. UNEP, World Glacier Monitoring Service, Zurich
WGMS (2009) Glacier mass balance bulletin no. 10 (2006–2007) (Haeberli W, Gartner-Roer I, Hoelzle M, Paul F, Zemp M, eds). CSU(FAGS)/IUGG(IACS)/UNEP/UNESCO/WMO, WGMS, University of Zurich, Zurich
Williams R, Hall D, Benson C (1991) Analysis of glacier facies using satellite techniques. J Glaciol 37(125):120–128
World Meteorological Organization (n.d.) World Glacier Monitoring Service, Zurich

Chapter 4
Alpine and Glacier Runoff

4.1 Timing

Watersheds in the Pacific Northwest are comprised of rainfall dominated (pluvial), snowmelt dominated (nival) and glacier melt dominated segments. The pluvial segments have peak mean flows in the winter due to winter storm events (Dery et al. 2009). Nival streams experience peak flow in May and June due to high snowmelt (Fig. 4.1). Glacially fed streams peak in July and August during peak glacier melt (Fountain and Tangborn 1985; Dery et al. 2009). Contributions from groundwater, precipitation and snowmelt from non-glacier areas are at a minimum after July 1 (Isaak et al. 2012). The loss of glaciers from a watershed would result in reduced streamflow primarily during late summer minimum flow periods (Nolin et al. 2010; Stahl and Moore 2006). Annual glacier runoff is highest in warm, dry summers and lowest during wet, cool summers helping offset reduced flow from nival and pluvial segments (Rasmussen and Tangborn 1976).

Analysis of key components of the alpine North Cascade hydrologic system indicate significant changes in glacier mass balance, terminus behavior, alpine snowpack and alpine streamflow from 1950 to 2005 (Pelto 2008), that has continued up to 2014. Glacier runoff is of particular importance to streamflow and stream temperature, and consequently aquatic life late in the summer when other water sources are at a minimum. Without consideration of changing glacier runoff, impacts of climate change on the Nooksack River cannot be assessed.

The amount of glacier runoff is the product of surface area and ablation rate (Pelto 2008). Glacier volume loss can contribute to changes in streamflow, leading to an increase in overall streamflow if the rate of volume loss is sufficiently large (Stahl and Moore 2006), or a decline in streamflow if the area of glacier cover declines sufficiently to offset any increase in ablation rate.

Stewart et al. (2005) and Fritze et al. (2011) noted a coherent shift toward earlier runoff in snow fed basins across the western US. They noted for the Pacific

M. Pelto, *Climate Driven Retreat of Mount Baker Glaciers and Changing Water Resources*, SpringerBriefs in Climate Studies,
DOI 10.1007/978-3-319-22605-7_4

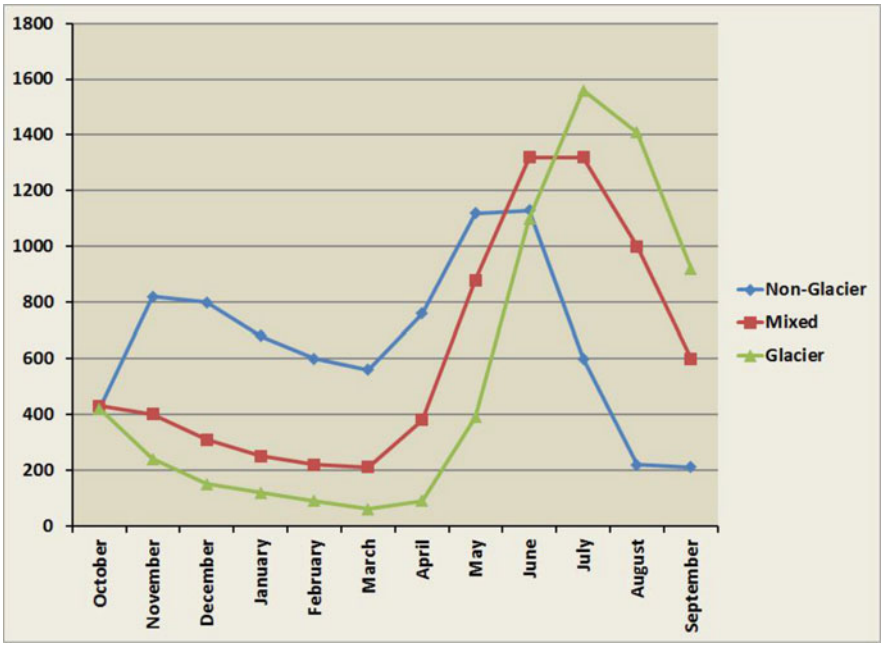

Fig. 4.1 Comparison of hydrographs for non-glacier and glacier fed watersheds

Northwest that many of higher-elevation, snowmelt dominated streams peak flow period (CT) has shifted earlier by 6–12 days in 2008 as compared to 1948, with a significant number experiencing an earlier CT of 12–18 days. Pelto (2008) identified a reduction in summer streamflow in six North Cascade basins from 1956 to 2006. In the North Cascades in general the glacier volume loss has contributed up to 6 % of the total August–September stream-flow (Granshaw and Fountain 2006). The overall loss in area in the North Cascades and British Columbia is greater than the increase in rate of ablation, resulting in the dominant change in glacier runoff being a decline in overall summer streamflow due to continued glacier area reductions (Stahl and Moore 2006; Pelto 2008). This relationship is not true of every watershed.

The reduction of the glacial melt component augmenting summer low flows is already resulting in more low-flow days in the North Cascade region (Luce and Holden 2009). In the Skykomish River watershed from 1958 to 2009 glacier area declined from 3.8 to 2.1 km^2, a 40 % decline (Pelto 2011). A key threshold of in-stream flow levels considered insufficient to maintain short term survival of fish stocks is below 10 % of the mean annual flow (Tennant 1976). For the Skykomish River 10 % of mean annual flow is 14 m^3s^{-1}. In the Skykomish River from 1950 to 2013 there have been 230 melt season days with discharge below 14 m^3s^{-1}. Of these 228 or 99 % of the low flow days have occurred since 1985. The loss of 40 % of the glacier runoff is a key reason for the onset of critical low flow days.

Of more concern for aquatic life is the occurrence of extended periods of low flow (Tennant 1976). From 1929 to 2009 in the Skykomish River basin there have been 8 years where streamflow dropped below 14 m^3s^{-1} for ten consecutive days during the melt season, 1986, 1987, 1992, 1998, 2003, 2005, 2006 and 2007. Precipitation has not declined substantially during this interval, hence earlier snowmelt, reduced glacier runoff and greater evapotranspiration must be causing the increase in late summer low flow periods.

4.2 Glacier Runoff Stream Thermal Response

Climate change combined with the resultant glacier retreat is altering late summer streamflow in the North Cascades. Isaak et al. (2012) has found significant and ubiquitous warming of streams in the Pacific Northwest during the summer in unregulated rivers from 1980 to 2009 of 0.12 °C/decade. Rates of warming in the Pacific Northwest's rivers have been highest during the summer (Issak et al. 2012). Thermal regimes are determined by numerous physical processes, with air temperature noted as the dominant factor in both long term and inter-annual variability (Issak et al. 2012; Luce et al. 2014). As discharge rates decrease, streams become more susceptible to thermal warming. Consequently, lower discharges in August typically result in lower thermal capacity (Cassie 2006). Cassie (2006) noted that discharge and air temperature are additive and the seasonal variation in stream warming rates is determined by how the two operate in concert or opposition over a period of time. The streams with the largest warming trend during the summer were in regions with the largest air temperature increases combined with the largest discharge decrease. This is further supported by Luce et al. (2014) who identified a pattern where water temperature in cold streams did not show high sensitivities to air temperature, while warm streams had a tendency for higher sensitivity. In the North Cascades cold streams are typically more nival or glacial in origin. In the Nooksack River basin the South Fork is currently the warmer stream with no glacier inputs and limited nival inputs.

A particular issue in the Nooksack River is the stress of warming stream temperatures on salmon (Grah and Beaulieu 2013). The Nooksack Basin is an ideal location to examine the role of glaciers in mitigating thermal stress, since there is discharge and temperature data for all three forks of the Nooksack River and each has a different glacial contribution (Table 4.1). There are no significant reservoirs or flow diversions upstream of the gaging locations (Table 4.1). The mean monthly stream temperatures for the 2008–2013 period from the USGS gage locations for the Nooksack River watershed indicates a significant positive temperature divergence of the South Fork from July to September (Fig. 4.2). The stream temperature is 5–6 °C above that of the Middle Fork and North Fork in late summer. This is indicative of a watershed that is dominantly pluvial. The discharge record for the 2008–2013 period is variable due to the short time period, yet it is clear that peak runoff is delayed a month in the North Fork Nooksack River (Fig. 4.3)

Table 4.1 USGS stations characteristics and data records utilized

	USGS station ID	Mean elevation m	Basin area km^2	Glacier cover %	Discharge records	Stream temperature records
Nooksack	12213100		2036	1.0	1970–2013	None
SF Nooksack	12210000	914	334	0	2008–2013	2008–2013
MF Nooksack	12208000	1141	190	2.1	2007–2013	2008–2013
NF Nooksack	12205000	1311	272	6.1	1950–2013	2008–2013

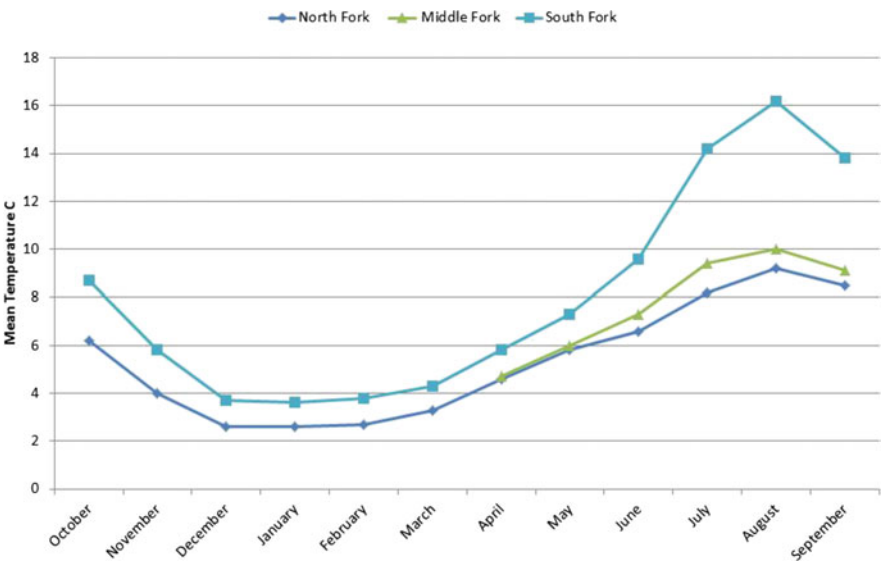

Fig. 4.2 Mean monthly stream temperature in the Nooksack River basin 2008–2013

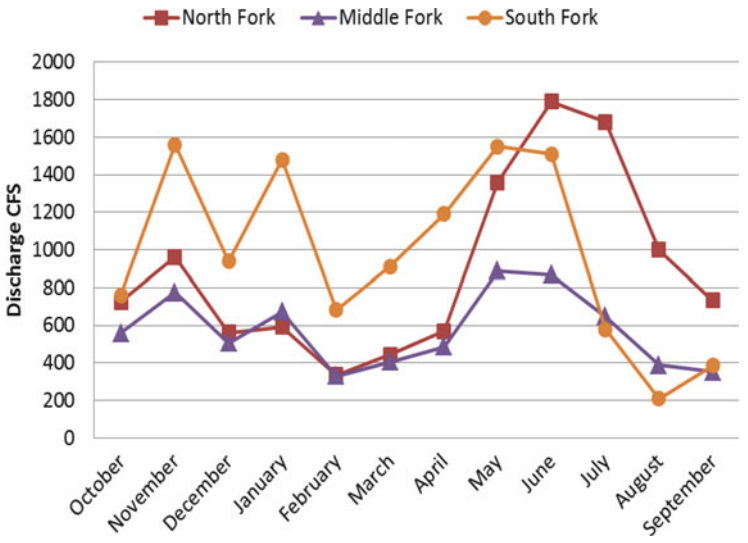

Fig. 4.3 Mean monthly discharge in the Nooksack River basin 2008–2013

4.3 Nooksack Watershed Study Area

Glaciers comprise the headwaters of the Middle Fork and North Fork Nooksack River (Fig. 1.1). In the Nooksack River basin, glacier runoff supplies 10–20 % of summer streamflow (Bach 2002). Nine species of salmon migrate up the Nooksack River from the sea that the Nooksack Indian Tribe is dependent upon (Grah and Beaulieu 2013). In the last two centuries the numbers of fish that return to spawn have greatly diminished because of substantial loss of habitat, primarily due to human-caused alteration of the watershed. Climate change is an additional threat that has caused and will continue to cause an increase in winter flow, earlier snowmelt, decreased summer baseflow, and increased water temperature (Grah and Beaulieu 2013). Without mitigating steps, climate change combined with habitat alteration will increase the frequency of conditions that exceed the tolerance levels of salmon. Here we focus only on the changing impact of glaciers and the resultant evolving water temperature threat. This is accomplished by examining the discharge and stream temperature in the three principal forks of the Nooksack River, that have varying amounts of glacier cover, and monitoring melting and runoff directly from glaciers.

The Nooksack River as a whole is a hybrid basin with the various segments reaching maximum discharge at different times, reducing the magnitude and duration of the summer minimum flow period. The period from October-March is a storage period with precipitation exceeding discharge, whereas April-August is a period of excess runoff release (Bach 2002; Dery et al. 2009). The percent of glaciated area is 6.0 % in the North Fork, 3.3 % in the Middle Fork and 0 % in the South Fork; with 1.1 % in the overall basin as measured at Ferndale, Washington (Table 4.1). Thirty years of mass balance work in the basin indicate a mean contribution of 11–12 m^3/s from July to September. This is 10–20 % of the total summer flow at Ferndale, depending on the specific year. This difference allows assessment of the impact of glaciers on both discharge and stream temperature. From 1950 to 1980 the areal extent of glaciers in the basin increased, with all Mount Baker glaciers advancing (Harper 1993; Pelto and Hedlund 2001). Since 1980 all of the glaciers in the basin have retreated significantly (Pelto and Hedlund 2001; Pelto and Brown 2012). Areal extent loss in the Nooksack Basin has been 10–15 %, since 1980 (Granshaw and Fountain 2006; Pelto and Brown 2012).

4.4 Glacier Runoff Assessment Methods

In this study we utilize streamflow records from the USGS stations at: Glacier, Washington for the North Fork of the Nooksack; Deming, Washington for the Middle Fork; Saxon Bridge for the South Fork; and the composite of the Nooksack River at Ferdale and Cedarville, Washington. Table 4.1 indicates the data type and periods utilized. Both daily and monthly records were utilized.

The United States Department of Agriculture-SNOTEL program has three stations in the Nooksack Basin that are utilized, Elbow Lake, Wells Creek and Middle Fork Nooksack. The principal annual SNOTEL snow water equivalent (SWE) measurement used for hydroclimatological analysis is the April 1 SWE. Air temperature is recorded at these stations as well. The Middle Fork Nooksack SNOTEL station provides a consistent measure of hourly temperature at an elevation 300 m below the glacier elevation.

Direct measurement of ablation using ablation stakes, changes in snow depth from repeat probing measurements and from snowline migration as part of the mass balance program directly measures snow and ice ablation and resultant glacier runoff (Pelto 2008). These data, including the specific glacier area is reported annually to the World Glacier Monitoring Service (WGMS). The change in glacier area has also been assessed with repeat mapping and reported by Pelto (2011) and Pelto and Brown (2012).

In the stream that discharges from Sholes Glacier at the headwaters of the North Fork Nooksack River we have measured daily runoff for comparison with daily ablation measurements on the glacier during the 1990–2013 period, the duration is limited to 3–5 days per year. In 2013 we installed a stream gage that measured discharge, and air temperature at this site from August 6th to Sept. 19th. In 2014 this gage was again installed from August 4th to Sept. 12th, the gage is removed during the winter as it would be unlikely to survive intact.

4.5 Nooksack River Discharge and Stream Temperature

Trends in discharge for summer, from 1971 to 2013, in the North Fork Nooksack and Nooksack River indicate no change and a 16 % decline respectively (Fig. 4.4). This indicates the role that glaciers have played in limiting the decline in summer runoff to date, which was also observed by Fleming and Clarke (2003) in British Columbia. The South Fork Nooksack and Middle Fork Nooksack lack a long term consistent discharge record.

Stream temperature and discharge records are continuous in the three basins only after the summer of 2008. Thus, we focus only on the 2009–2013 summer seasons for examining the specific relationships between discharge, water temperature, air temperature and glacier runoff. Table 4.2 contains the correlation coefficient for each basin between water temperature, air temperature and discharge. For the North Fork there is a strong direct relationship between air temperature and discharge, indicative of the contribution of glacier melt. There is a negative relationship in the North Fork between precipitation and discharge during the late summer indicating that the reduction in glacier melt that accompanies cooler-wet events offsets the contribution of precipitation. In the South Fork there is a negative correlation between air temperature and discharge, and a positive correlation with late summer precipitation events. All three branches of the river exhibit a positive correlation between stream temperature and air temperature. At present the stream temperature record is too short to generate a robust model of stream temperature from discharge, air temperature, glacier ablation and precipitation.

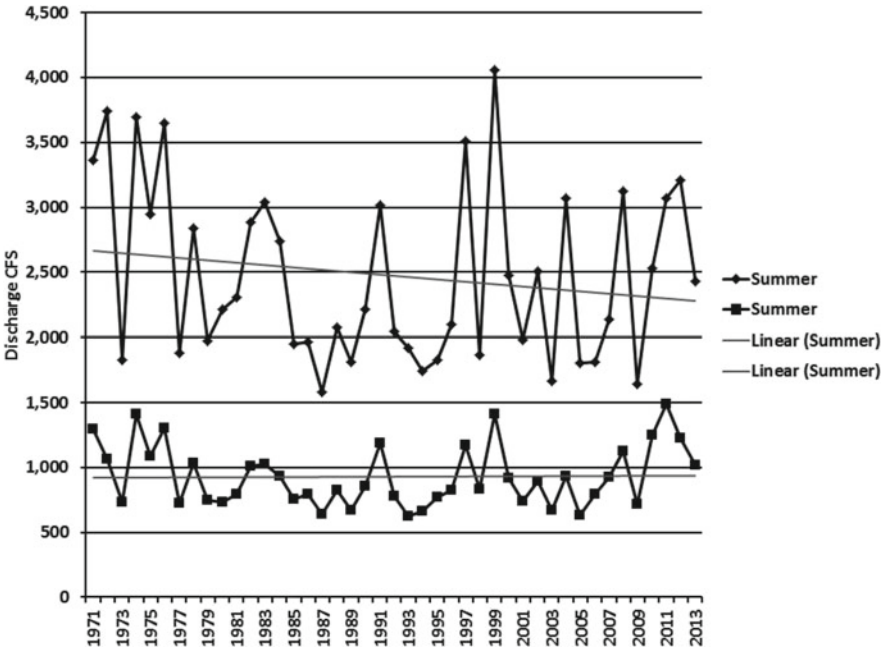

Fig. 4.4 Long term runoff changes in the North Fork Nooksack River and Nooksack River for the July-September period

Table 4.2 Correlation coefficients for each basin between hydrologic and climatic variables during late summer

Basin	Air temperature-discharge	Precipitation-discharge	Air temperature-stream temperature	Stream temperature-discharge
SFK	–0.25	0.44	0.67	–0.28
NFK	0.43	0.13	0.56	–0.07
MFK	–0.35	0.41	0.56	0.00

4.6 Warm Weather Thermal Response

To distinguish the different thermal response we focused on the most stressful period, late summer warm weather events. Warm weather events were defined as at least 3 days with mean daily air temperature above 16 °C at the Middle Fork Nooksack Snotel station. For the 2009–2013 period 12 warm weather events were identified. The mean increase in air temperature during the warm weather events from prior to their beginning was 7 °C. Such warm weather events are the key periods that lead to high stream temperatures and lower discharge in streams not fed by glaciers. For water temperature an increase of 2 °C is the threshold of significance used for response to warm weather events. This value was chosen as this is a deviation that is seldom achieved without a warm weather event in the South Fork. For

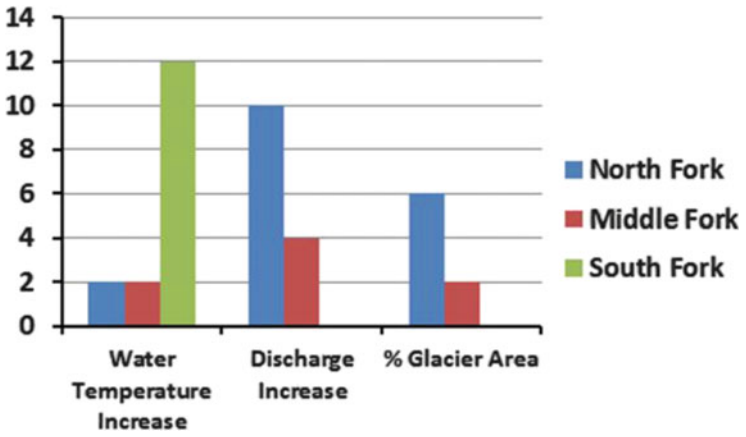

Fig. 4.5 Of the 12 warm weather events 2009–2013, the number where discharge increased by 15 % or temperature increased by 2 °C

Table 4.3 Mean response of Nooksack River watershed to the 14 warm weather events from 2009 to 2013. The change in air temperature is assessed at the rise in the mean daily temperature at the Middle Fork Nooksack SNOTEL site

Basin	Air temperature change C	Stream temperature change C	Stream discharge change (%)
SFK	+8	+3.4	−15
NFK	+8	+1.1	+23
MFK	+8	+1.0	+16

the North Fork and Middle Fork of 12 events exceeded this threshold, and for the South Fork 12 of 12 events exceeded this threshold (Fig. 4.5). Warm weather events consistently generate a significant increase in stream water temperature only in the non-glaciated South Fork Basin, the mean increase was 3.2 °C (Table 4.3). The different response of the three basins is evident in the graphs from 2009 to 2010, indicating the temperature response of each stream to warm weather events, orange ellipses (Figs. 4.6 and 4.7).

Increased glacier discharge largely offset the impact of increased air temperature on stream water temperature during the warm weather events leading to a mean change of 1.1 °C in the North Fork and 1.0 °C in the Middle Fork, effectively one third of the temperature increase seen in the South Fork. The thermal response for specific events during the summer of 2009, and 2010 are illustrated below, each event is indicated by an orange ellipse. The South Fork is responsive and the North Fork and Middle Fork are largely unresponsive. In the Nooksack River basin during late summer the correlation between air temperature and water temperature is strong during warm weather events.

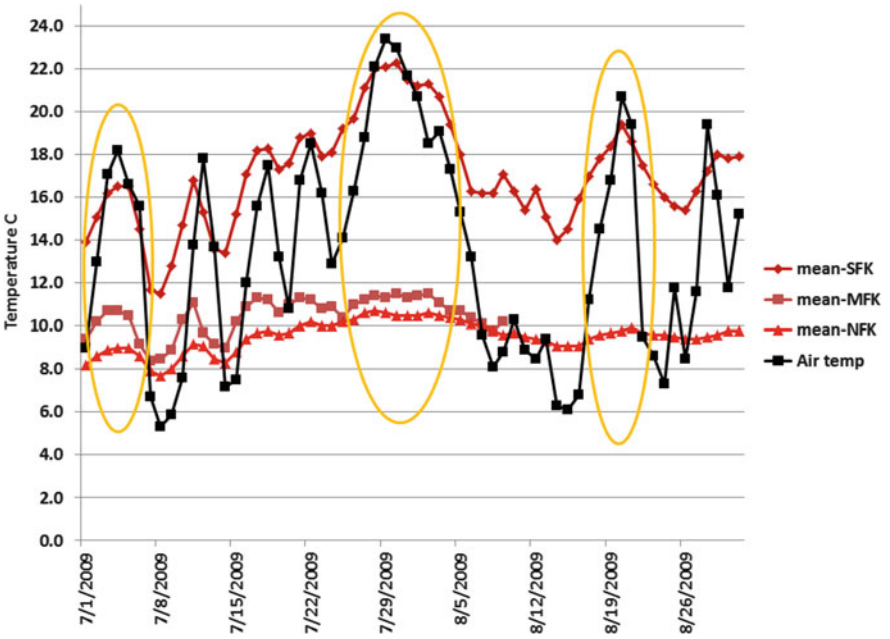

Fig. 4.6 Water temperature summer 2009 at the USGS gages in the Middle Fork, North Fork and South Fork Nooksack River compared to daily air temperature at the Middle Fork Nooksack SNOTEL site

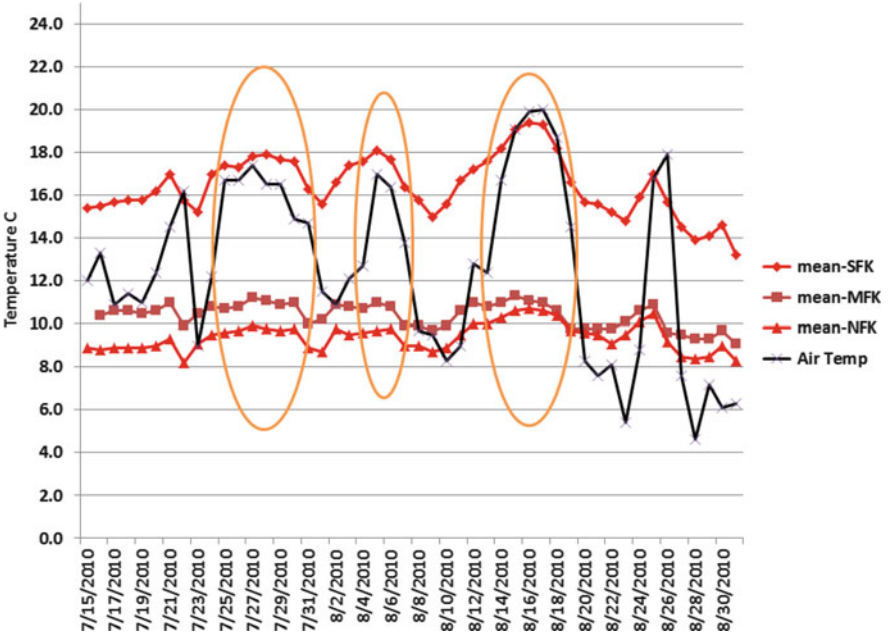

Fig. 4.7 Water temperature summer 2010 at the USGS gages in the Middle Fork, North Fork and South Fork Nooksack River compared to daily air temperature at the Middle Fork Nooksack SNOTEL site

4.7 Discharge Response to Warm Weather Events

For discharge during the same warm weather events a 15 % increase is set as the key threshold for a significant response to each warm weather event. This threshold was chosen as only significant rain or melt events generate this large of a change in daily flow. For the North Fork 11 of 12 warm weather events exceeded this limit, in the Middle Fork 8 of 12 events had a significant response, and for the South Fork zero of the 12 events led to a 15 % flow increase. The average discharge change for the warm weather events are + 26 % in the North Fork, +19 % in the Middle Fork, and −16 % in the South Fork (Table 4.3). It is apparent that warm weather events increase glacier melt enhancing flow in the North Fork, and in a basin without glacier runoff, South Fork, the hydrologic system consistently experiences reduced discharge. Below the response is illustrated for warm weather events in 2009 and 2010, red ellipses indicate the warm weather events (Figs. 4.8 and 4.9) The North Fork and Middle Fork are responsive and the South Fork is not.

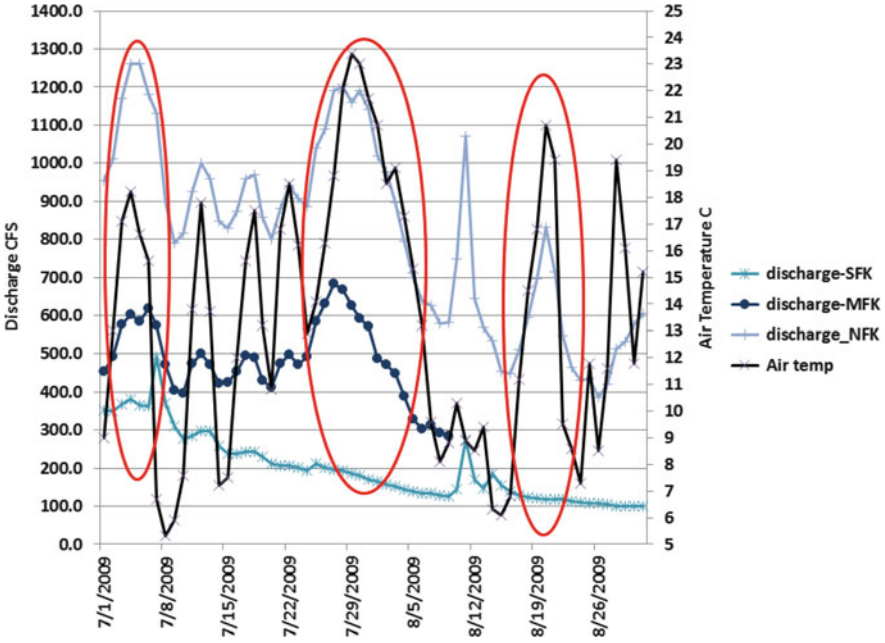

Fig. 4.8 Summer discharge 2009 at the USGS gages in the Middle Fork, North Fork and South Fork Nooksack River compared to daily air temperature at the Middle Fork Nooksack SNOTEL site

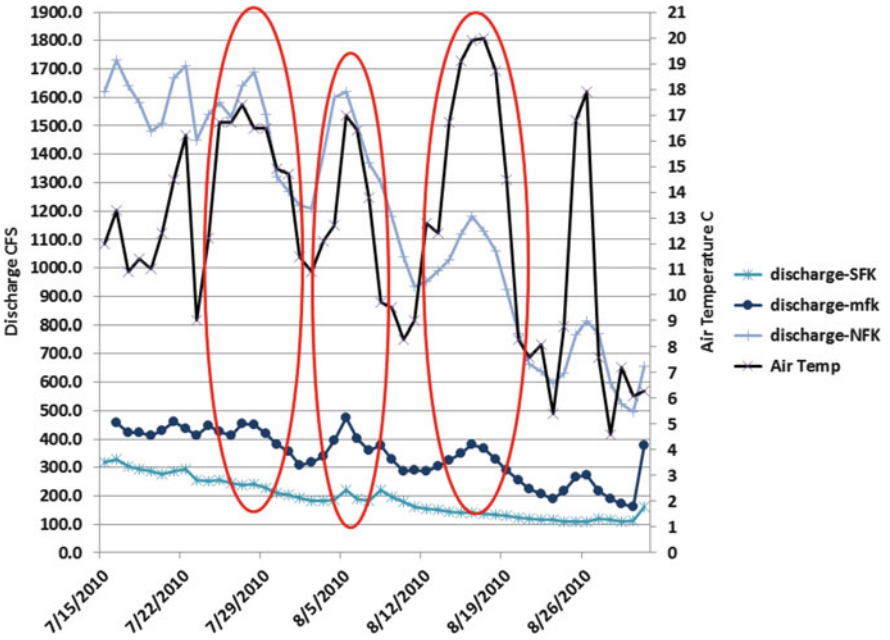

Fig. 4.9 Summer discharge 2010 at the USGS gages in the Middle Fork, North Fork and South Fork Nooksack River compared to daily air temperature at the Middle Fork Nooksack SNOTEL site

References

Bach AJ (2002) Snowshed contributions to the Nooksack River watershed, North Cascades range, Washington. Geogr Rev 92(2):192–212

Caissie D (2006) The thermal regime of rivers: a review. Freshwat Biol 51:1389–1406

Dery S, Stahl K, Moore R, Whitfield W, Menounos B, Burford JE (2009) Detection of runoff timing changes in pluvial, nival and glacial rivers of western Canada. Water Res Res 45. doi:1029/2008WR006975

Dyurgerov M (1996) Substitution of long term mass balance data by measurements of one summer. Gletscherk Glazialgeol 32:177–184

Ebbesmeyer CC, Cayan DR, McLain FH, Nichols DH, Peterson DH, Redmond KT (1991) 1976 step in the pacific climate: forty environmental changes between 1968–1975 and 1976–1984. In: Betancourt JL and Tharp VL (eds) Proceedings on the 7th annual Pacific climate workshop, pp 129–141

Fleming SW, Clarke GKC (2003) Glacial control of water resource and related environmental responses to climatic warming: empirical analysis using historical streamflow data from northwestern Canada. Can Water Res J 28:69–86

Fountain A, Tangborn W (1985) The effect of glaciers on streamflow variations. Water Resour Res 21:579–586

Fritze H, Stewart IT, Pebesma EJ (2011) Shifts in western north American snowmelt runoff regimes for the recent warm decades. J Hydrometall 12:989–1006. doi:10.1175/2011JHM1360.1

Grah O, Beaulieu J (2013) The effect of climate change on glacier ablation and baseflow support in the Nooksack River basin and implications on Pacific salmonid species protection and recovery. Clim Change 120:657–670. doi:10.1007/s10584-013-0747-y

Granshaw F, Fountain A (2006) Glacier change (1958–1998) in the North Cascades National Park Complex, Washington, USA. J Glaciol 52(177):251–256

Harper JT (1993) Glacier terminus fluctuations on Mt. Baker, Washington, USA, 1940–1980, and climate variations. Arct Alp Res 25:332–340

Isaak DJ, Wollrab S, Horan D, Chandler G (2012) Climate change effects on stream and river temperatures across the northwest U.S. from 1980–2009 and implications for salmonid fishes. Climate Chang 113:499–524. doi:10.1007/s10584-011-0326-z

Luce C, Holden Z (2009) Declining annual streamflow distributions in the Pacific Northwest United States. Geophys Res Lett 36:L16401. doi:10.1029/2009GL039407

Luce C, Staab B, Kramer M, Wenger S, Isaak D, McConnell C (2014) Sensitivity of summer stream temperatures to climate variability in the Pacific Northwest. Water Resour Res 50:3428–3443. doi:10.1002/2013WR014329

Nolin AW, Phillippe J, Jefferson A, Lewis SL (2010) Present-day and future contributions of glacier runoff to summertime flows in a Pacific Northwest watershed: implications for water resources. Water Resour Res 46(12):W12509

Pelto MS (2008) Impact of climate change on North Cascade alpine glaciers and alpine runoff. Northwest Sci 82(1):65–75

Pelto MS (2011) Skykomish River, Washington: impact of ongoing glacier retreat on streamflow. Hydrol Process 25(21):3267–3371

Pelto MS, Brown C (2012) Mass balance loss of Mount Baker, Washington glaciers 1990–2010. Hydrol Proc 26(17):2601–2607

Pelto MS, Hedlund C (2001) The terminus behavior and response time of North Cascade glaciers. J Glaciol 47:497–506

Rasmussen LA, Tangborn WV (1976) Hydrology of the North Cascade Region, Washington 1. Runoff, precipitation, and storage characteristics. Water Resour Res 12(2):187–202

Stahl K, Moore RD (2006) Influence of watershed glacier coverage on summer streamflow in British Columbia, Canada. Water Resour Res 42. doi:10.1029/2006WR005022

Stewart I, Cayan DR, Dettinger MD (2005) Changes toward earlier streamflow timing across western North America. J Climate 18:1136–1155

Tennant DL (1976) Instream flow regimens for fish, wildlife, recreation, and related environmental resources. In: Osborn J, Allman C (eds) Instream flow needs, vol 2. American Fisheries Society, Western Division, Bethesda, pp 359–373

Chapter 5
Glacier Runoff Observations at Sholes Glacier

5.1 Glacier Runoff Measurement

To more specifically ascertain the volume of glacier runoff contribution to streamflow in the North Fork and Middle Fork Nooksack River we installed and calibrated a water level recorder below Sholes Glacier. Concurrent to ablation measurements made on the Sholes Glacier, discharge from the glacier has been measured in the summers of 2013 and 2014. The stretch of the outlet stream where the study is conducted offers nearly ideal conditions for assessment (Fig. 5.1). The width of the stream in the study stretch has a small range (10 %) and does not vary significantly for the range of typical water depths (<20 %). The stream bed sediment is relatively uniform. Glacier fed streams in the North Cascades, typically have a heavy sediment load and steep gradient which causes considerable stream bed alterations for most streams. The streambed below the Sholes Glacier is a braided stream channel for the first 75 m and then develops into a straight low slope channel, bounded by columnar basalt banks, where velocity is measured (Figs. 5.2 and 5.3). The study stretch is 100 m beyond the terminus of the Sholes Glacier. This width and depth section of stream has been consistent from year to year. The result of comparatively similar characteristics is that velocity has low variability in the study stretch at a given time, which reduces the error in discharge assessment.

The Sholes Glacier main outlet watershed area is mapped with GPS by directly observing the region where surface streams on the glacier are directed into the basin. This is possible during low snowpack years such as in 2013 and 2014. GPS measurements of this boundary provide the location for 2013 (Fig. 5.4). The watershed is more than 90 % glacier covered, and 95 % snowcovered. Portions of the watershed are on the upper Sholes Glacier, which is not part of our mass balance assessment on the Lower Sholes Glacier.

Discharge was measured directly during 14 occasions between Aug. 3 and 8, 2013 below Sholes Glacier and on three occasions in mid-September to generate a

M. Pelto, *Climate Driven Retreat of Mount Baker Glaciers and Changing Water Resources*, SpringerBriefs in Climate Studies,
DOI 10.1007/978-3-319-22605-7_5

Fig. 5.1 Location of the stream level gage installed by Jezra Beaulieu and Oliver Grah. Note the uniform velocity, depth and width character. Also note turbidity of the stream

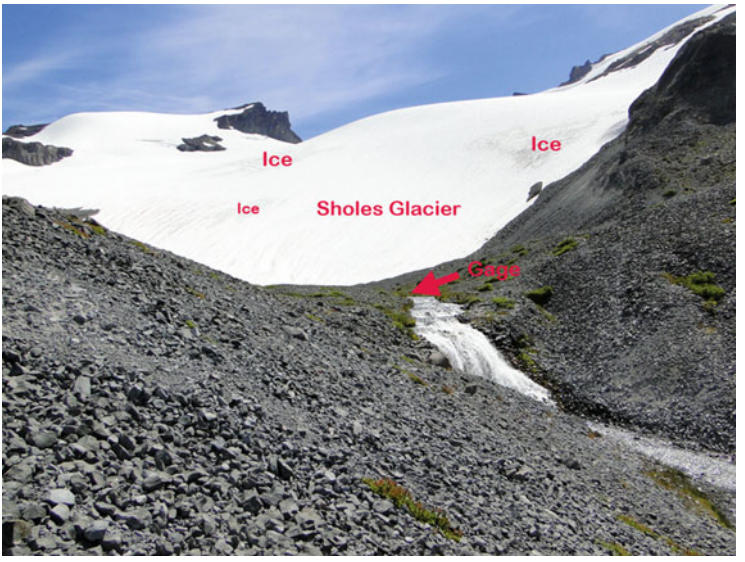

Fig. 5.2 View of the Sholes Glacier draining into the outlet on August 6th, 2013

Fig. 5.3 Study reach on Sholes Glacier Outlet, the section of the stream after it narrows to a relatively uniform width, depth and velocity.

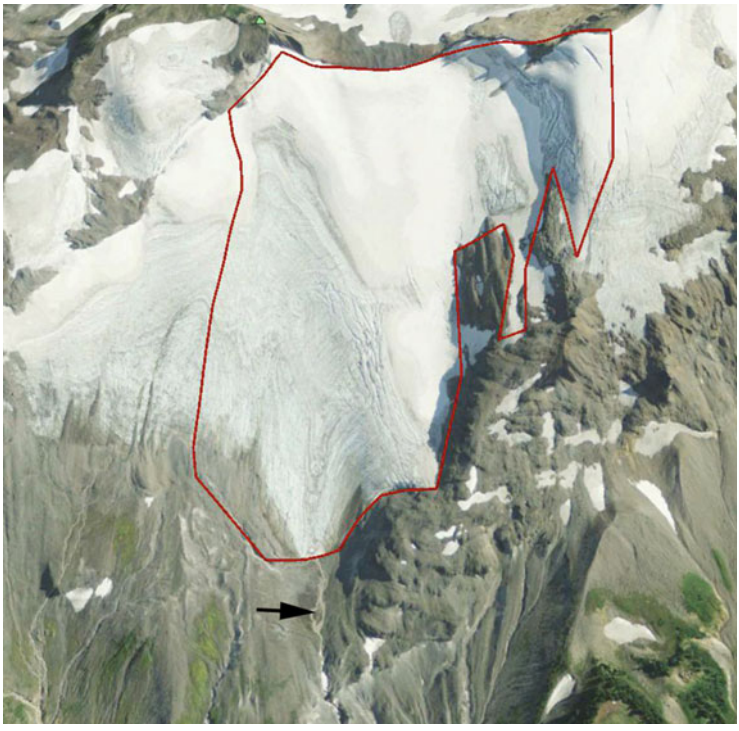

Fig. 5.4 Drainage area of the Sholes Glacier and its outlet

rating curve for the stage level recorder (Table 5.1). The rating curve developed for the study reach is based on direct flow measurements. The statistical fit is not as high for stage reading as for stream depth measured during discharge assessment, because of a minor aggradation issue (Fig. 5.5). Hence, the water level record station was installed in the section of the stream where the bed is columnar basalt in 2014.

The mean discharge from daytime observations only was 0.40 m^3s and from snow melt over the 24 h period 0.35 m^3s. This indicates a 15–20 % decline in nighttime runoff, an amount that can be corroborated by the water level records. This is further supported by the diurnal range in discharge of about 30 %, not large for a small glacier system, during the Aug. 3–8th period. This is likely due to the night time minimum temperature remaining high (8–14 C) at the nearby Middle Fork Nooksack SNOTEL station. Discharge became notably more turbid after 13:00 local, peaking in turbidity around 17:00 local.

Table 5.1 Discharge data observations completed on the Sholes Glacier outlet stream

Date	Time	Width	Depth	Velocity	Length	Stage	Discharge
8/4/2013	10:30	11.50	0.53	1.90	40.00	0.8	11.58
8/4/2013	13:00	11.60	0.54	2.00	40.00	0.82	12.53
8/4/2013	16:00	11.80	0.65	2.10	40.00	0.9	16.11
8/5/2013	10:00	11.80	0.56	2.10	40.00	0.85	13.88
8/5/2013	13:00	11.80	0.59	2.10	40.00	0.87	14.62
8/5/2013	15:30	11.90	0.62	2.10	40.00	0.85	15.49
8/5/2013	17:00	11.90	0.64	2.20	40.00	0.9	16.76
8/6/2013	11:00	11.60	0.52	2.00	40.00	0.8	12.06
8/6/2013	16:00	11.80	0.54	2.10	40.00	0.82	13.38
8/7/2013	9:30	11.50	0.56	1.95	40.00	0.85	12.56
8/7/2013	13:00	11.80	0.60	2.00	40.00	0.88	14.16
8/7/2013	16:30	11.80	0.68	2.20	40.00	0.92	17.65
8/8/2013	13:00	11.80	0.64	2.10	40.00	0.9	15.86
8/8/2013	16:00	11.70	0.61	2.10	40.00	0.9	14.99
9/16/2013	10:00	11.60	0.48	2.00	40.00	0.85	11.14
9/16/2013	16:00	11.60	0.51	2.50	40.00	0.92	14.79
9/17/2013	8:00	11.50	0.43	1.80	40.00	0.80	8.90

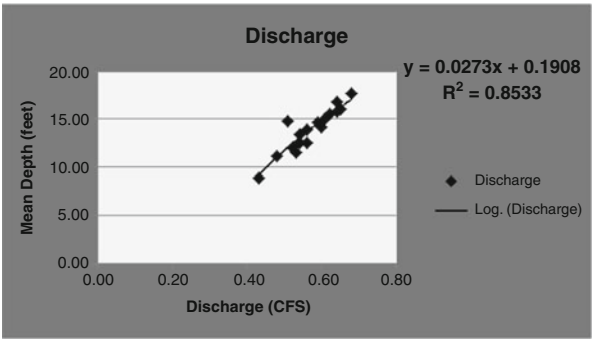

Fig. 5.5 Rating curve for discharge versus mean depth of Sholes Outlet

5.2 Glacier Runoff Ablation Comparison

The 2013 direct streamflow measurements, which recorded flow every 15 min, during the Aug. 3rd–9th period indicate a mean discharge equivalent to a loss of 5.5 cm w.e.d^{-1} of snow and ice melt in the watershed. Average ablation at 12 stakes during the week was 8.8 cm d^{-1} of snowpack or 5.3 cm w.e.d^{-1} of water equivalent. Measured discharge was 5 % greater than amount determined directly from ablation. Runoff from August 9th–20th at the Sholes Glacier outlet averaged 4.6 cm w.e.d^{-1}. From August 9th to the 20th assessment of the same stakes on Aug. 20th indicates mean ablation of 7.8 cm d^{-1}, 4.7 cm w.e.d^{-1}. This also is within 5 % of the discharge determined directly from ablation, an encouraging result.

5.3 Glacier Runoff Observations Sholes Glacier 2014

Discharge was measured directly on 13 occasions between Aug. 6th and Sept. 15th below Sholes Glacier: on nine occasions by the NCGCP and on four occasions by the Nooksack Indian Tribe. We did probe snowpack in this region as well to assess subsequent melt. The rating curve developed for the study reach is based on direct flow measurements. The stream gage was emplaced on August 6th, 2014 and removed on Sept. 15th by Oliver Grah and Jezra Beaulieu. The rating curve is used to convert observed water level to discharge (Fig. 5.6) for the entire period of record. Water level was recorded every 15 min allowing discharge to be determined at the same interval.

5.4 Runoff Ablation Comparison 2014

A comparison of runoff and ablation is examined for specific time periods. We measured ablation during the August 5–11 period at a series of stakes on the Sholes Glacier. Average ablation during the week was 8.0 cm d^{-1} of snowpack or 4.9 cm w.e.d^{-}1. There was no rainfall during this period. Average discharge indicates 5.2 cm w.e.d^{-1}. Ablation measurement from Aug. 20 to Aug. 29 averaged 5.3 cm w.e.d^{-1}. Runoff during this same period that was rain free averaged 5.7 cm w.e.d^{-1}. In each case runoff exceeded measured ablation by 5–10 %, a good validation (Table 5.2).

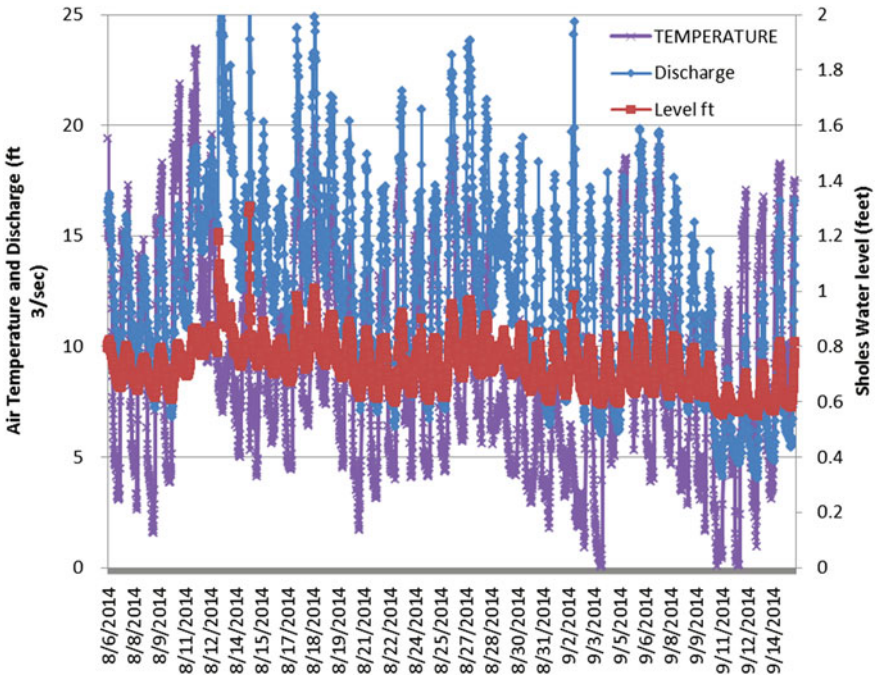

Fig. 5.6 Sholes Glacier outlet discharge, air temperature and water level data. This shows the diurnal range in each

Table 5.2 Ablation during specific periods and the resultant discharge that would be generated

Date	Ablation (cm/day)	SWE (m)	Area	Daily discharge m^3	Discharge (CFS)
3-Aug	9.8	0.0588	580,000	34,104	13.9
4-Aug	9.6	0.0576	580,000	33,408	13.7
5-Aug	8.8	0.0528	575,000	30,360	12.4
6-Aug	8.2	0.0492	570,000	28,044	11.5
7-Aug	7.8	0.0468	570,000	26,676	10.9
8-Aug	8.5	0.051	570,000	29,070	11.9
8/4–8/20	7.8	0.05226	560,000	29,265	12.0
8/6–9/1	7.5	0.0525	550,000	28,875	11.8
8/4–9/12	7.4	0.05328	550,000	29,304	12.0

5.5 Ablation Modelling

From 1990 to 2014, daily ablation measurements on the Sholes and Easton Glaciers provide a direct measure of ablation. The observed ablation is compared to daily mean temperature at the Elbow Lake and Middle Fork Nooksack Snotel stations, to

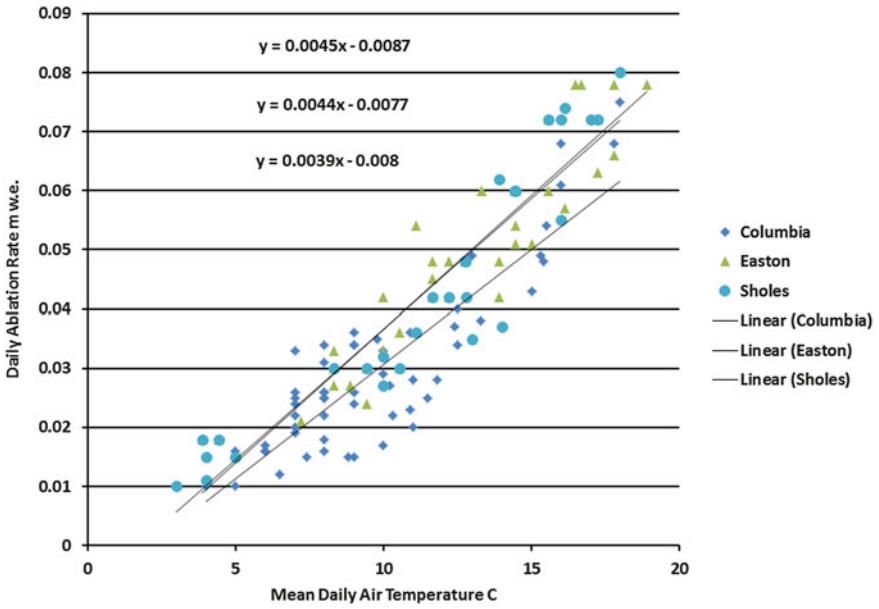

Fig. 5.7 Relationship between Middle Fork Nooksack air temperature and daily ablation observation on Columbia, Sholes and Easton Glacier

generate a degree day function for ablation. This model is based on 109 days of observations (Fig. 5.7). The correlation coefficient between observed ablation and daily temperature is 0.91. The degree day function is the most common means for calculating ablation from weather records for glaciers (Hock 2005). This provides a daily value for ablation that is multiplied by the area of glacier cover to yield the amount of runoff from Sholes Glacier and the North Fork Nooksack River Basin. The cumulative ablation from the model for July 1–Sept. 30 is 3.67 m. Ablation peaked on Aug. 12th the day after our extensive measurements on Sholes Glacier (Fig. 5.8).

5.6 Heliotrope Glacier Observations

In 2014 we installed a gage on an outlet of the Heliotrope Glacier, which is NW of and adjacent to the Coleman Glacier on the NW flank of Mount Baker. The site proved difficult for generating an accurate rating curve and the glacier above the site was too crevassed to allow for adequate ablation assessment and drainage area determination (Fig. 5.9). This gage was installed on August 8th and removed on Sept. 22nd. The actual discharge cannot be adequately determined, nor can the volume of glacier ablation. However, the record has proved valuable in demonstrating the comparability in air temperature and water with the Sholes Glacier site (Figs. 5.10 and 5.11). The correlation coefficient for air temperature between the two sites

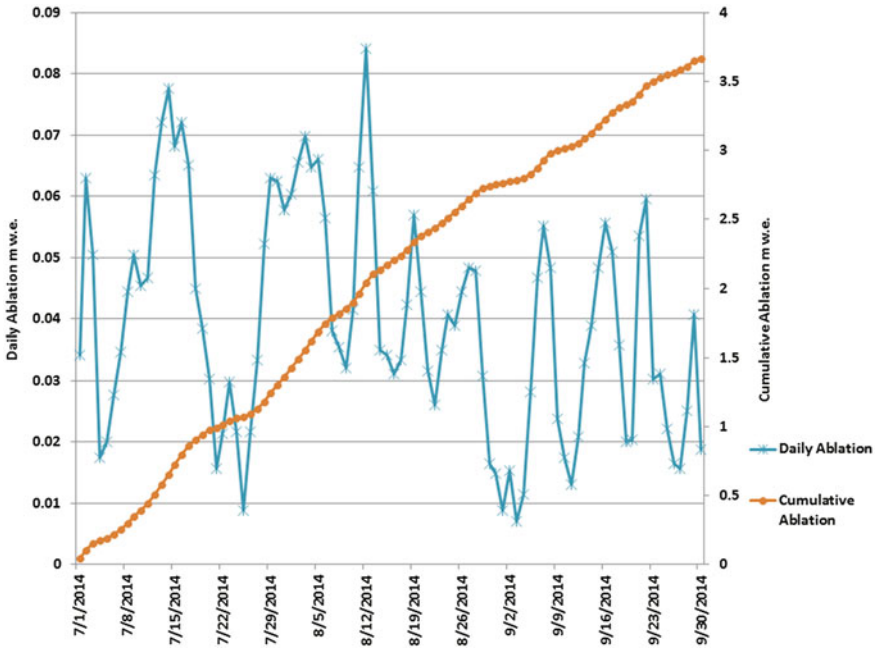

Fig. 5.8 Daily and cumulative ablation from July 1 to Sept. 30, 2014 determined from a degree day function calibrated with direct daily ablation and stream discharge measurements

Fig. 5.9 Study reach on Heliotrope Glacier, basin boundaries could not be accurately defined

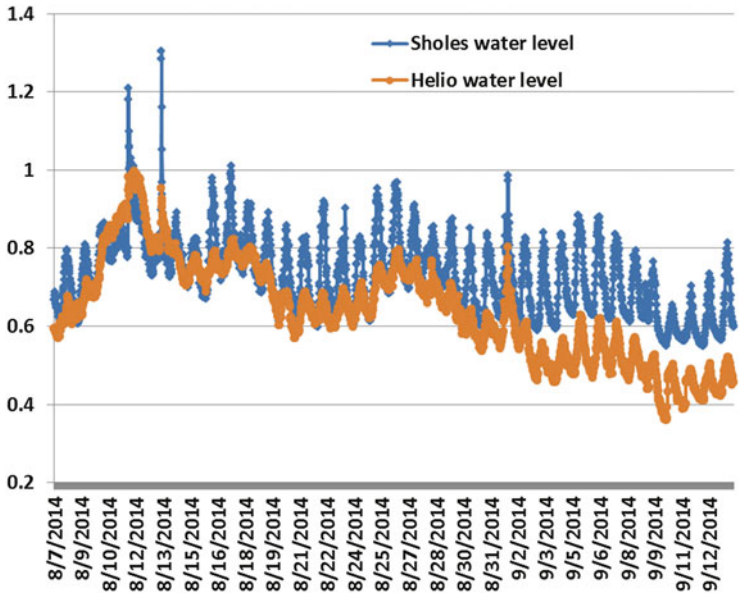

Fig. 5.10 Comparison of Sholes and Heliotrope water level, correlation coefficient 0.8 when the two largest rain events are excluded, 0.76 without removing these events

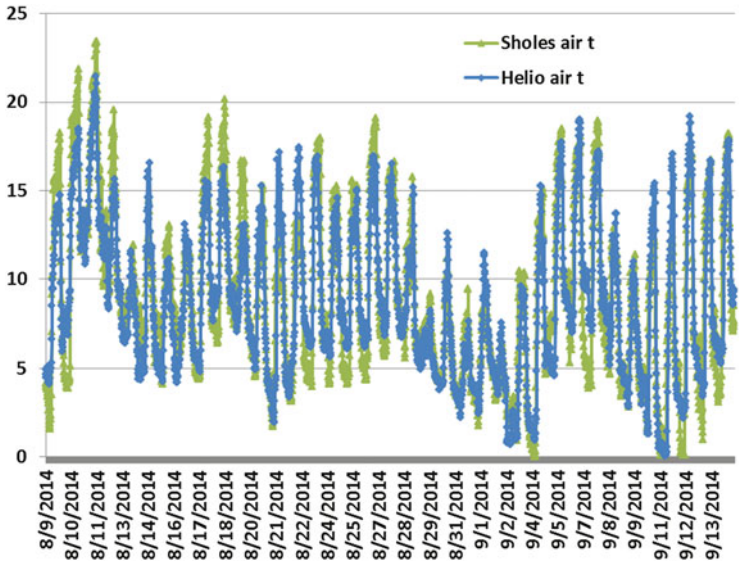

Fig. 5.11 Comparison of Sholes and Heliotrope air temperature, correlation coefficient 0.91

was 0.91 and for stream level (when the two largest rainstorms of the summer are removed) was 0.80. The relationship was run from August 9th to Sept. 14th. The close relationship of the air temperature record indicates that the degree day function for a glacier does not have to be tied to a specific air temperature record measured at the glacier site. This has been noted to be the case in many other instances. For example the USGS uses the Diablo Dam station for generating a degree day function for South Cascade Glacier (Rasmussen 2009). The relationship in stream level for the two sites immediately below their respective glaciers are responding to the same forcing factors, whether it is melt or rainfall, indicating that Sholes Glacier is a good reference site.

5.7 Glacier Runoff Contribution to North Fork Discharge

This record of discharge is compared to the glacier runoff calculated from the degree day function and glacier area. This comparison of measured and modelled glacier runoff yields a correlation coefficient of 0.80 for Sholes Glacier. This correlation is based on the days with less than 0.025 cm w.e., which is the majority of days (Fig. 5.12). Because the degree day function record has already been validated with field observations of ablation, the modelled runoff is an independent validation of the discharge record.

The degree day function ablation record is upscaled to the entire basin. The product of the validated degree day function and glacier area in the North Fork Nooksack watershed above the USGS gage provides daily discharge from glacier runoff. This is compared to the observed discharge at the USGS station on the North Fork Nooksack to determine the percent of runoff generated by glaciers in 2014. The

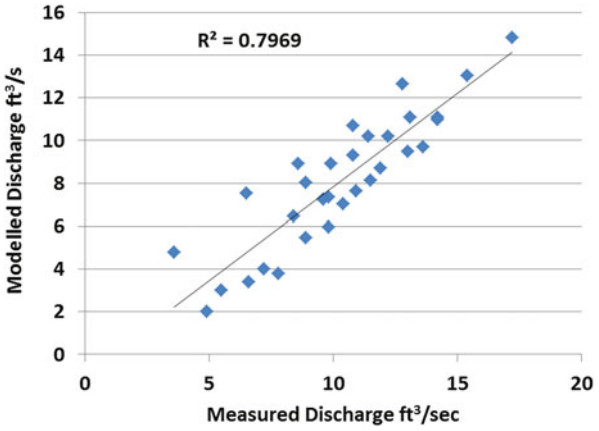

Fig. 5.12 Relationship between modelled discharge from daily ablation calculation and measured discharge at Sholes Glacier

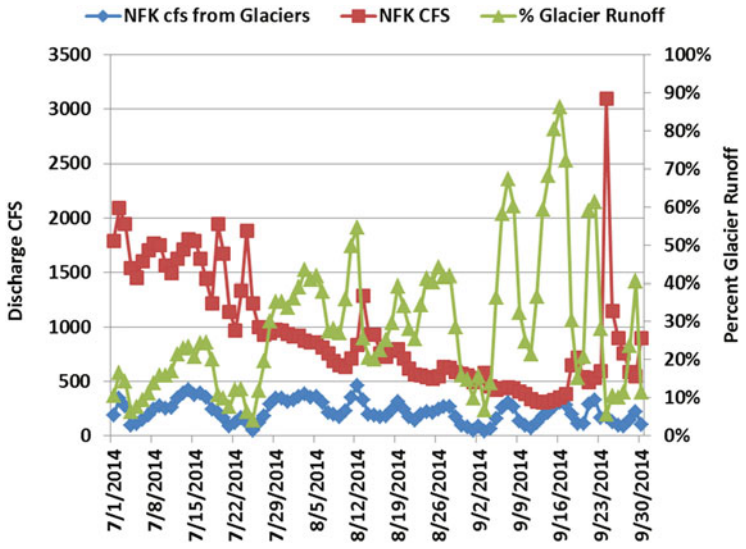

Fig. 5.13 Amount of glacier runoff in the North Fork Nooksack River at the USGS gage, determined from the direct discharge measurements below glaciers and ablation measurements on the glaciers

percent glacier contribution peaked on Sept 15th and 16th at over 80 % of total stream discharge (Fig. 5.13). In 2014 there was minimal non-glacier snowpack remaining on Sept. 15th and there had not been significant precipitation in the previous 14 days. From Aug. 1 to the end of the melt season there were 21 days with glacier runoff providing 40 % or more of the total runoff. There were no days in July where this occurred, indicating that non-glacier snow melt was still important. This is an illustration of the growing seasonal importance of glacier runoff to streamflow after August 1 (Pelto 2008). The model for ablation can be enhanced with further field observations. This year we also had local air temperature measured at the gage sites. In time this local air temperature may provide additional comparative relationships that offer greater accuracy in ablation determination.

The most important finding is that the large local data set used in model construction and for model validation, allowed the production of a model that is both more accurate and more tightly constrained by actual field data than most models.

5.8 Glacier Runoff Conclusions

Warm weather events are a focus, because it is low discharge and high temperatures that are stressful for salmon. There is a marked pattern of reduced temperature sensitivity and of enhanced discharge in basins with higher percentages of glacier cover during warm weather events. The result of continued glacier volume loss and

glacier retreat will be a reduction in the enhanced discharge, leading to reduced flow during warm-dry low flow events. There will also be a greater sensitivity of the water temperature to warm weather events. In the North Fork between August 1st and October 1st, glaciers provided more than 30 % of runoff for a majority of the days, and more than 40 % of the runoff on 21 days.

5.9 Nooksack Salmon

The observed importance of glaciers to both discharge and stream temperature in the North Fork Nooksack and Middle Fork Nooksack has been the focus of the previous section. Both are critical to providing suitable salmon habitat. As anthropogenic climate change progresses aquatic communities in rivers will be forced to shift behavior, if possible, to find thermally suitable habitat (Heino et al. 2009). Some cold-water trout and salmon species are already constrained by unsuitably warm temperatures and additional warming would result in net loss of habitat (Rieman et al. 2007; Isaak et al. 2012).

Nooksack River salmon begin and end their life cycle in the Nooksack River, but mature in the Salish Sea. The Salish Sea supports all seven species of Pacific salmon: chinook, chum, coho, cutthroat, pink, sockeye and steelhead. Population declines have prompted initiation of the Salish Sea Marine Survival Project (2014). This project reports that: chinook, coho, and steelhead have experienced tenfold declines in survival during the marine phase of their lifecycle, with total abundance remaining well below levels of 30 years ago (Zimmerman et al. 2015). The conditions in the Salish Sea have changed and salmon survival has been declining, Zimmerman et al. (2015) observed the primary pattern within the Salish Sea is declining smolt survival from 1977 to 2010.

Isaak et al. (2012) found that air temperature was the dominant factor explaining long-term stream temperature trends, 82–94 %, and inter-annual variability, 48–86 % of stream temperature. In summer, discharge accounted for approximately half, 52 %, of the inter-annual variation in stream temperatures. In spring no temperature increase was observed, the rate of warming was highest during the summer 0.17–0.22 °C/decade (Isaak et al. 2012).

In the Baker River and Nooksack River basins, stream thermal budgets are altered by human activities that have increased solar input through removal of riparian vegetation and flow regulation (Moore et al. 2005, 2006; Beechie et al. 2012; Grah and Beaulieu 2013). Additionally in the Baker River, diversion of water out of streams (Meier et al. 2003), and storage of water in reservoirs (Olden and Naiman 2009) increases the thermal impacts. Moore (2006) observed that in British Columbia the greater the snow and glacier cover the lower the stream temperature. The increased variability in summer streamflow that has been observed in the Fraser River as well is a stress on salmon populations (Padilla et al. 2014). A key issue identified for the bull trout in Flathead River, Montana is that future climate warming will result in a substantial decrease in thermally suitable habitat (Jones et al. 2013). Cowie et al. (2014)

examined gradient, temperature and forest characteristics on streams in the Pacific Northwest including several from Mount Baker. The model results suggest that the loss of ice from the glaciated basins would lead to a maximum weekly temperature 4.5–5.0 °C higher than present. This would in turn reduce the thermally suitable habitat.

That this is an issue for salmon is the observed negative correlation between salmon size and the multivariable El Niño Southern Oscillation Index (ENSO). Smaller fish are observed during El Niño events, which tend to be warmer and dryer, and are associated with decreased snow pack, decreased stream flow and below average salmon survival (Beamish et al. 2012).

The Washington Department of Fish and Wildlife (WDFW 2014) SalmonScape project maps the distribution of salmon in the Nooksack River basin. Each population is mapped separately for spawning, rearing and presence. In each Nooksack Fork the mapped extent is quite similar for each salmon species. Chinook, coho and chum salmon in the North Fork can migrate up to the base of Nooksack Falls 40 km upstream of the North Fork-Nooksack Junction. In the Middle Fork of the Nooksack River salmon populations extend up river just beyond Falls Creek 12.5 km upstream of the junction with the North Fork. The South Fork has the most extensive network of salmon streams with the presence of salmon extending 52 km upstream of the junction with the Nooksack River (Fig. 5.14).

Salmon surveys in the Nooksack River are conducted annually by the WDFW. In the North Fork Nooksack chinook spawn mainly in a 30 km stretch from Mosquito Lake Road to Wells Creek at the base of Nooksack Falls (WDFW 2014). In the North Fork Nooksack the number of returning chinook is divided into natural and

Fig. 5.14 From the WDFW SalmonScape, this indicates the extent of chinook salmon in the Nooskack (*N*) and Baker River (*BR*) watersheds. *MF* Middle Fork, *NF* North Fork, *SF* South Fork. *Red* documented spawning, *Blue* Documented presence, *Green* Documented rearing, *Yellow* Modelled presence, *Purple* Blocked

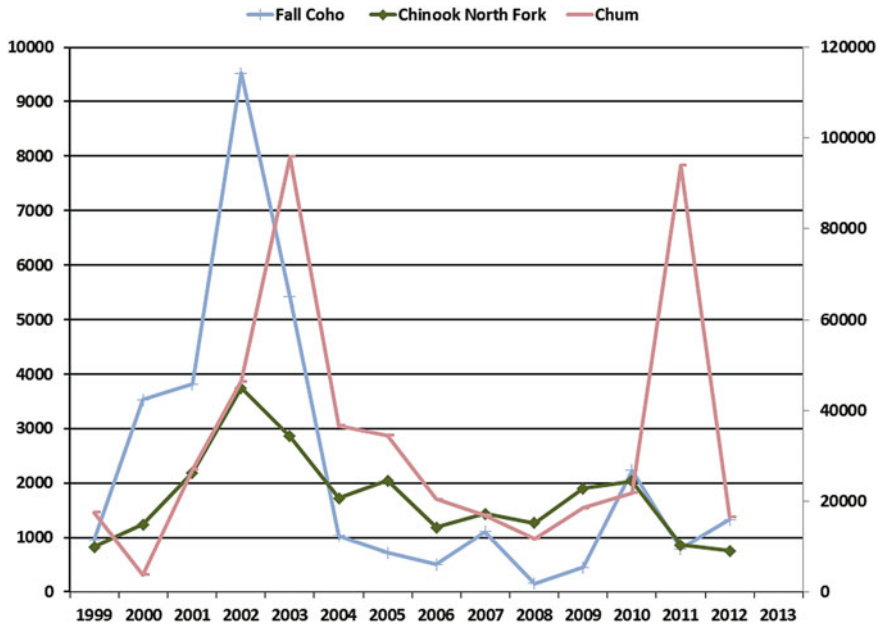

Fig. 5.15 Salmon survey 1999–2013 data from the WDFW for: Chinook salmon in the North Fork and Middle Fork Nooksack. Coho and chum salmon in the Nooksack River

hatchery spawned salmon. The chum and coho salmon data are for the Nooksack River. During the 1999–2013 interval there are two salmon population peaks for each species. The early peak is within a year of 2002 and the second peak is within a year of 2010 (Fig. 5.15) (WDFW 2014).

In the North Fork Nooksack River (which includes the Middle Fork in this survey), the WDFW (2014) report that 88 % of recent spawning chinook salmon are from the Kendall Creek Hatchery. From 2000 to 2011 the number of chinook released in the Middle Fork and North Fork Nooksack watershed averaged 1,036,000 sub-yearling fish (WDFW 2012). The average number of spawning adults is approximately 1,800. This hatchery is at the junction of Kendall Creek and the North Fork Nooksack River. The hatchery chinook spawning numbers have risen as a result of a chinook stock re-building program started at Kendall Creek Hatchery in 1980. Overall populations and escapements have increased as a result, but natural-origin spawning chinooks have not increased and are still doing poorly (WFDW 2014). In 2009 for chinook Kendall Creek hatchery produced 1.1 million juveniles. The number of adults that survive is determined to be the sum of those that return to the hatchery, spawning grounds, and that are harvested, this was a total of 3,950 for that same brood year returning (WDFW 2014).

The Nooksack Salmon Enhancement Association (NSEA) surveyed salmon populations annually during September-January from 1999 to 2013 in specific stream survey areas in the South Fork and main stem Nooksack River reaches. Part of their

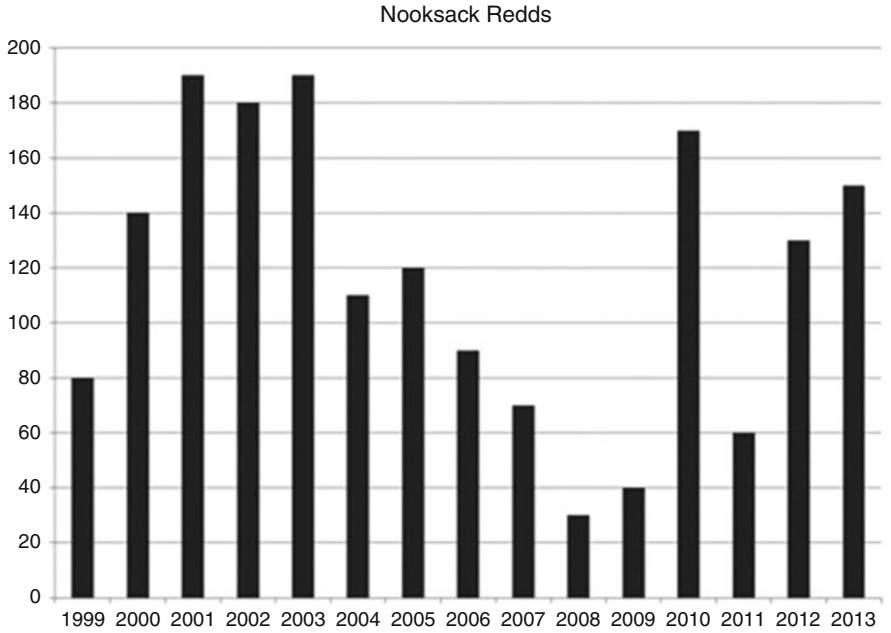

Fig. 5.16 The number of redd's identified for coho salmon in the Nooksack River by the annual Nooksack Salmon Enhancement Association

survey focuses on the number of redd's (salmon spawning nests) (Fig. 5.16). For coho salmon, which is the most populous species, redd counts ranged from a high of 190 to a low of 30 (NSEA 2014). The early peak period was during the 2001–2004 and again in 2010 matching the population peaks observed in the North Fork for salmon population.

Zimmerman et al. (2015) focus more on the marine environment in the Salish Sea, which the Nooksack salmon migrate into. They found an overall pattern of declining salmon smolt survival trend over the 1977–2010 period. Both the riverine and marine environments are experiencing physical changes due to climate change as well as more direct human influence on the aquatic habitat that are placing a stress on the salmon (Zimmerman et al. 2015; Luce et al. 2014).

5.10 Conclusion

It is evident that glaciers play a critical role in the Nooksack River in moderating fluctuations in both discharge and temperature, which reduces stress for salmon in a system fed by glaciers (Bach 2002). The continued loss of glaciers will lead to a functional reduction in this moderating ability. The change in glacier area is the key component to overall glacier runoff, and hence to quantifying the declines in glacier

runoff (Jost et al. 2012). The Skykomish River and South Fork Nooksack River exemplify what will occur to stream discharge as glacier area is lost in the North Fork and Middle Fork basins. Warmer temperatures and lower discharge during the summer will be more prevalent. This will lead to greater stress on salmon populations in the North Fork and Middle Fork Nooksack (Grah and Beaulieu 2013). Despite efforts of the Kendall Creek hatchery, Nooksack habitat restoration by federal, state and tribal governments and citizen efforts the threatened North Fork salmon are not gaining ground on the recovery target. Changes in the rivers impact the beginning and end of their life cycle. Changes in the marine environment impact the maturing portion of their life cycle. Glaciers are just one aspect that can impact success.

References

Bach AJ (2002) Snowshed contributions to the Nooksack River watershed, North Cascades range, Washington. Geogr Rev 92(2):192–212

Beamish R, Neville C, Sweeting R, Lange K (2012) The synchronous failure of juvenile Pacific salmon and herring production in the Strait of Georgia in 2007 and the poor return of sockeye salmon to the Fraser River in 2009. Mar Coast Fish 4:403–414

Beechie T, Imaki H, Greene J, Wade A, Wu H, Pess G, Roni P, Kimball J, Stanford J, Kiffney P, Mantua N (2012) Restoring salmon habitat for a changing climate. River Res Appl 4:403–414. doi:10.1002/rra.2590

Cowie N, Moore RD, Hassan MA (2014) Effects of glacial retreat on proglacial streams and riparian zones in the Coast and North Cascade mountains. Earth Surf Process Landforms 39(3):351–365

Dery S, Stahl K, Moore R, Whitfield W, Menounos B, Burford JE (2009) Detection of runoff timing changes in pluvial, nival and glacial rivers of western Canada. Water Resour Res. doi:10.1029/2008WR006975

Grah O, Beaulieu J (2013) The effect of climate change on glacier ablation and baseflow support in the Nooksack River basin and implications on Pacific salmonid species protection and recovery. Clim Chang 120:667–670. doi:10.1007/s10584-013-0747-y

Heino J, Virkkala R, Toivonen H (2009) Climate change and freshwater biodiversity: detected patterns, future trends and adaptations in northern regions. Biol Rev 84:39–54

Hock R (2005) Glacier melt: a review of processes and their modelling. Prog Phys Geogr 29:362–391

Hock R, Koostra D, Reijmeer C (2007) Deriving glacier mass balance from accumulation area ratio on Storglaciären, Sweden. In: Glacier mass balance changes and meltwater discharge, vol 318. IAHS, pp 163–170

Isaak DJ, Wollrab S, Horan D, Chandler G (2012) Climate change effects on stream and river temperatures across the northwest U.S. from 1980–2009 and implications for salmonid fishes. Clim Change. doi:10.1007/s10584-011-0326-z

Jones LA, Muhlfeld CC, Marshall LA, McGlynn BL, Kershner JL (2013) Estimating thermal regimes of bull trout and assessing the potential effects of climate warming on critical habitats. River Res Appl 30:204–216. doi:10.1002/rra.2638

Jost G, Moore RD, Menounos B, Wheate R (2012) Quantifying the contribution of glacier runoff to streamflow in the upper Columbia River Basin, Canada. Hydrol Earth Syst Sci 16:849–860

Luce C, Staab B, Kramer M, Wenger S, Isaak D, McConnell C (2014) Sensitivity of summer stream temperatures to climate variability in the Pacific Northwest. Water Res Res 50:3428–3443. doi:10.1002/2013WR014329

Meier W, Bonjour C, Wüest A, Reichert P (2003) Modeling the effect of water diversion on the temperature of mountain streams. J Environ Eng 129:755–764

Moore RD (2006) Stream temperature patterns in British Columbia, Canada, based on routine spot measurements. Can Water Res J 31:41–56

Moore RD, Sutherland P, Gomi T, Dhakal A (2005) Thermal regime of a headwater stream within a clear-cut, coastal British Columbia, Canada. Hydrol Process 19:2591–2608

NSEA (2014) Nooksack Salmon Enhancement Association Monitoring Program. http://www.n-sea.org/salmon-info-1/monitoring. Accessed Feb 2014

Olden JD, Naiman RJ (2009) Incorporating thermal regimes into environmental assessments: modifying dam operations to restore freshwater ecosystem integrity. Freshw Biol 55:86–107. doi:10.1111/j.1365-2427.2009.02179.x

Padilla A, Rasouli K, Dery S (2014) Impacts of variability and trends in runoff and water temperature on salmon migration in the Fraser River Basin, Canada. Hydrol Sci J 60(3):523–533

Pelto MS (2008) Impact of climate change on North Cascade alpine glaciers and alpine runoff. Northwest Sci 82(1):65–75

Rasmussen LA (2009) South Cascade Glacier mass balance, 1935–2006. Ann Glaciol 50:215–220

Rieman BE, Isaak D, Adams S, Horan D, Nagel D, Luce C, Myers D (2007) Anticipated climate warming effects on bull trout habitats and populations across the interior Columbia River basin. Trans Am Fish Soc 136:1552–1565. doi:10.1577/T07-028.1

Salish Sea Marine Survival Project (2014) Why focus on the Salish Sea. http://marinesurvivalproject.com/the-project/why/. Accessed May 2015

Tennant DL (1976) Instream flow regimens for fish, wildlife, recreation, and related environmental resources. In: Osborn J, Allman C (eds) Instream flow needs, vol 2. American Fisheries Society, Western Division, Bethesda, pp 359–373

Washington Department of Fish and Wildlife (2012) Fishbooks hatchery database. Hatcheries Data Unit, Washington Department of Fish and Wildlife, Olympia

Washington Department of Fish and Wildlife (2014) SalmonScape. http://apps.wdfw.wa.gov/salmonscape/map.html. Accessed Feb 2015

Washington Department of Fish and Wildlife (2014) Salmon score. https://fortress.wa.gov/dfw/score/. Accessed Feb 2015

Zimmerman MS, Irvine JR, O'Neill M, Anderson JH, Greene CM, Weinheimer J, Trudel M, Rawson K (2015) Spatial and temporal patterns in smolt survival of wild and hatchery Coho Salmon in the Salish Sea. Mar Coast Fish Dyn Manag Ecosyst Sci 7:116–134. doi:10.1080/19425120.2015.1012246

Chapter 6
Individual Glacier Behavior

6.1 Rainbow Glacier

Rainbow Glacier, on the northeast side of Mount Baker, descends from 2200 to 1340 m. This is the lowest starting elevation of any valley glacier on the slopes of Mount Baker. The glacier divide with the Mazama Glacier is a saddle at 1975 m. This saddle area is in the accumulation zone and has retained snowpack each year of observation, 1984–2014. The glacier is the headwaters of Rainbow Creek which drains into Baker Lake. The glacier has a fairly uniform slope of 0.29 from 1350 to 1800 m, a steeper icefall than leads up to the saddle where the glacier has only a minor slope (Fig. 6.1). Above the saddle there is limited inflow from slopes on the south side above the saddle. Most of this slope below and adjacent to the north ridge of Mount Baker drains into the Park or Mazama Glaciers. In 1979 the glacier was advancing, building a terminal advance moraine and had a crevassed terminus. In 1984 at the time of the first field survey of the glacier terminus, the glacier was still in contact with the advance moraine at 1175 m. The terminus was still actively crevassed and convex. By 1997 the terminus had retreated 225 m, no crevassing was evident in the terminus region and the profile in the lower several hundred meters of the glacier was concave. A period of rapid retreat ensued until 2006. A comparison of Digital Globe images from 1993 to 2006 indicate the retreat during this period (Figs. 6.2 and 6.3). From 2006–2012 the terminus was typically covered by avalanche debris even late in the summer, slowing retreat, while the glacier above the terminus reach continues to thin. In 2013 and 2014 exceptional summer melt exposed the terminus leading to further retreat (Fig. 6.4). Total retreat from 1984 to 2014 is 490 m. In 2014 the lower 300 m of the glacier has a concave profile and is uncrevassed indicating limited glacier movement, which will allow continued retreat in the near future. The overall glacier velocity has declined as evidenced by the reduction in crevassing. In 1984 the glacier received significant contribution from the slope below Landes Cleaver on the west side of the glacier, by 2006 there

M. Pelto, *Climate Driven Retreat of Mount Baker Glaciers and Changing Water Resources*, SpringerBriefs in Climate Studies,
DOI 10.1007/978-3-319-22605-7_6

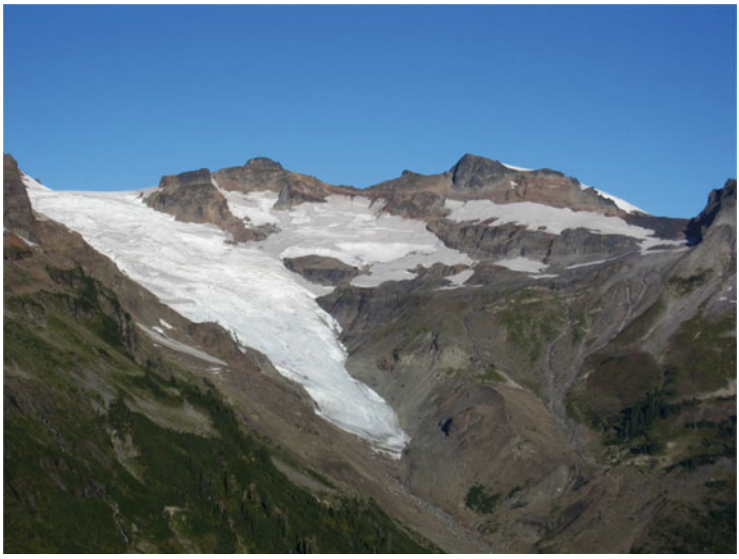

Fig. 6.1 Rainbow Glacier from Rainbow Ridge in Sept. 2014. The saddle with Mazama Glacier is on skyline (Tom Hammond)

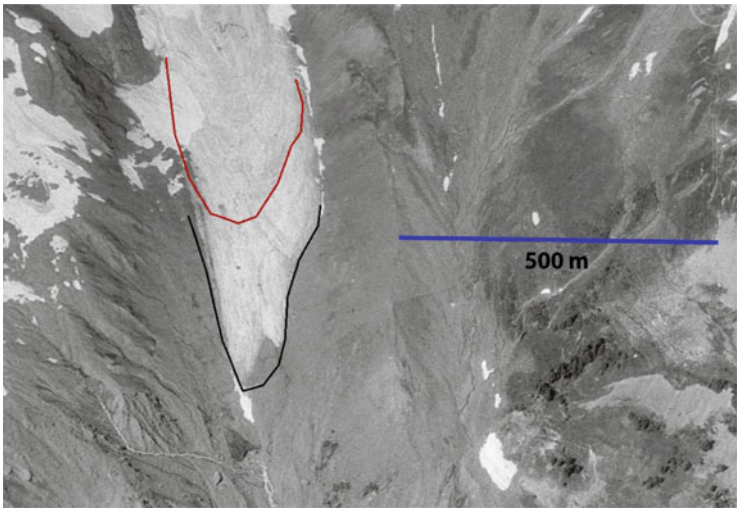

Fig. 6.2 Digital Globe view of the terminus of Rainbow Glacier in 1993, with the 1993 terminus in *black* and the 2006 terminus in *red*

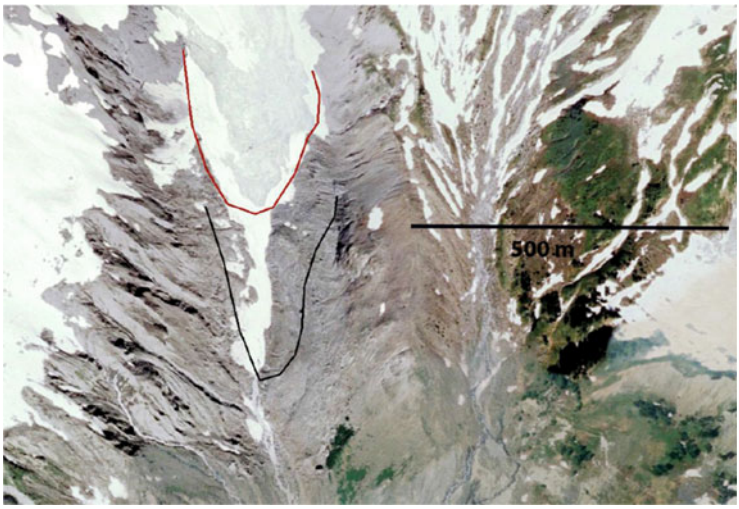

Fig. 6.3 Digital Globe view of the terminus of Rainbow Glacier in 2006, with the 1993 terminus in *black* and the 2006 terminus in *red*

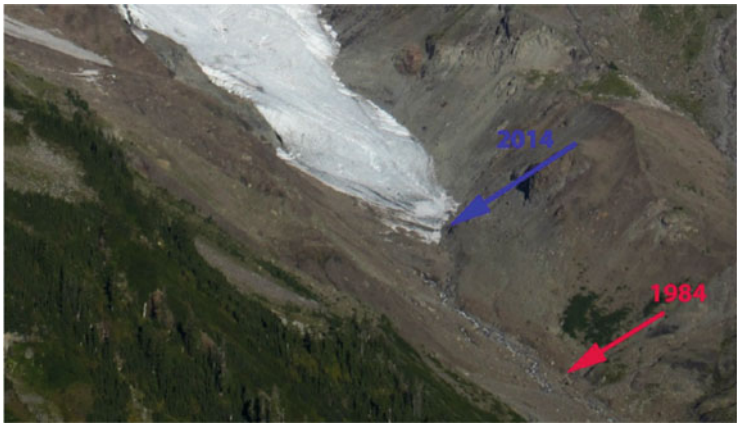

Fig. 6.4 Rainbow Glacier terminus in 2014 from Rainbow Ridge, indicates 1984 terminus position as well (Tom Hammond)

was negligible inflow, and a large rock area now separates most of this slope from the Rainbow Glacier. On the lower east side of the glacier a large rock knob has been exposed since 1984, creating a secondary upper terminus for the glacier. From 1984 to 2014 the mean annual balance has been –0.34 ma^{-1}, this is a cumulative loss of −10.55 m, 12 m of glacier thickness.

6.2 Sholes Glacier

Sholes Glacier is a wide slope glacier below the Portals and Landes Cleaver, these are subsidiary peaks beyond the end of the north ridge of Mount Baker. The glacier has a northern orientation and is separated into an upper and lower section. At present the upper Sholes Glacier does not significantly feed the lower Sholes Glacier. The focus here is on the terminus change and mass balance of the lower Sholes Glacier. The glacier is a slope glacier with a broad lower margin. The main terminus is on the west side of the glacier. In 1984 the terminus was located at the edge of a small proglacial lake, which has since filled in completely with sediment and is simply an outwash plain. Since 1984 the glacier has retreated 95 m, with most of the retreat occurring since 2003 (Fig. 6.5). The annual mass balance (Ba) of the glacier has been measured since 1990. The mean Ba has been −0.52 ma^{-1}, this is a net loss of 13 m w.e., or 14.5 m in ice thickness, which is 25–30 % of the total glacier thickness. Below this glacier we installed a stream level recorder to measure glacier runoff in 2013 and 2014 (Fig. 6.6). Simultaneously on the glacier we observed ablation of the snowpack, note the change in 2013 from early August to early September. In recent years the snow covered extent has been limited by the end of the melt season, this indicates a continuation of extensive thinning and retreat.

Fig. 6.5 Sholes Glacier overview in 2004

Fig. 6.6 Sholes Glacier from the main outlet stream on August 11th, 2014

6.3 Mazama Glacier

Mazama Glacier is on the north side of Mount Baker sharing a divide with Rainbow Glacier at a 1975 m saddle and extending up to a flow divide with Park Glacier near the north ridge. In 1984 at the time of our initial terminus visit, a narrow 350 m long mostly debris covered terminus tongue extended to an elevation of 1250 m. By 1993 the debris cover had expanded across the entire width of the lower glacier, retreat was 50 m from the early 1980s advance moraine (Fig. 6.7). By 2009 the glacier terminus had retreated 700 m to an elevation of 1370 m (Fig. 6.8). In 2014 the terminus had retreated 800 m from the early 1980s advance moraine (Fig. 6.9). There is still some buried ice cored moraine on the west side of the valley below the terminus. The more rapid retreat of this glacier in recent years is likely in part due to the reduced rate of retreat due to debris cover during the first half of the twentieth century. The glacier terminus remains thin and uncrevassed in its lowest 600 m, this section of the glacier is not in a steep avalanche valley and retreat will remain rapid.

6.4 Roosevelt Glacier

Roosevelt Glacier drains the northwest side of Mount Baker and is joined with the Coleman Glacier in its accumulation zone. The glacier retreated 3200 m from a joint terminus with the Coleman Glacier at its LIAM until 1949, LIAM dated to 1823 by Heikkinnen (1984). Harper (1993) noted the glacier advanced 350–400 m from 1949 to 1970. In 1984 the glacier was nearly in contact with its advance moraine at 1400 m, which was ice cored and quite prominent (Fig. 6.10). By 1993 the glacier had retreated 140 m. From 1993 to 2014 the glacier retreated above two

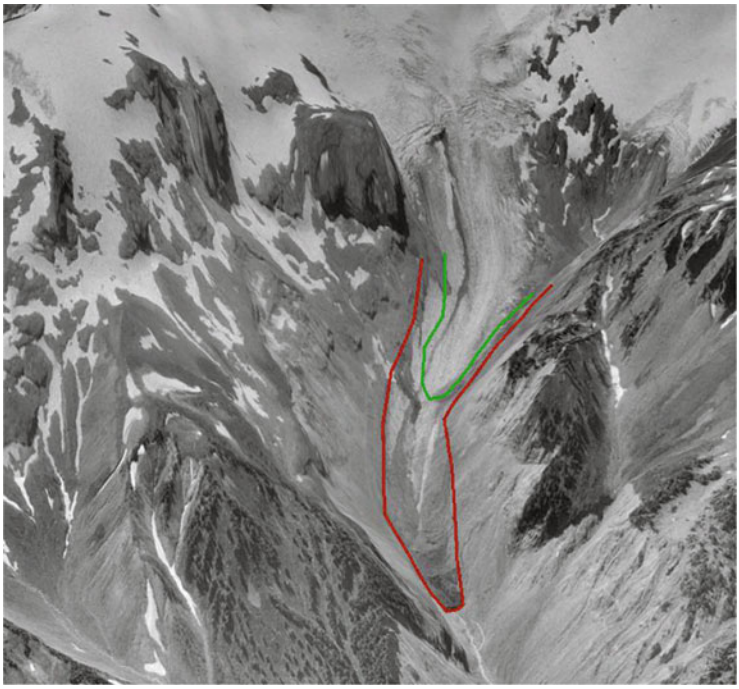

Fig. 6.7 Mazama Glacier in 1993, terminus is outlined in *red*, 2009 terminus in *green* on this Google Earth image

lava flow bands and in 2014 terminated at 1560 m (Fig. 6.11). The retreat from 1984 to 2014 is 400 m, with the terminus now back to the 1949 terminus position (Figs. 6.12, 6.13, and 6.14). The glacier is fed by three principal accumulation zones: (1) A glacier tongue that descends from the summit plateau at 3200 m, (2) an avalanche fed and direct snowfall region beneath the north ridge, at 2200 m (3) an avalanche and direct snowfall fed region beneath the northwest face, at 2400 m. The annual snowline has averaged 2150 m on Roosevelt Glacier from 1984 to 2010. The lower portion of the glacier is thin indicating retreat will continue.

6.5 Coleman Glacier

Coleman Glacier drains the northwest side of Mount Baker and is joined with the Roosevelt Glacier in its accumulation zone. The glacier drains the largest area of the volcano above 3000 m, which combined with its steep slope leads to a higher velocity and more crevassing than on other glaciers. The glacier retreated 2600 m from a joint terminus with the Coleman Glacier at its LIAM, dated to 1823 by Heikkinnen

Fig. 6.8 Mazama Glacier in 2009, terminus is outlined in *green*, 1993 terminus in *red* on this Google Earth image

Fig. 6.9 Mazama Glacier in 2010 looking towards terminus

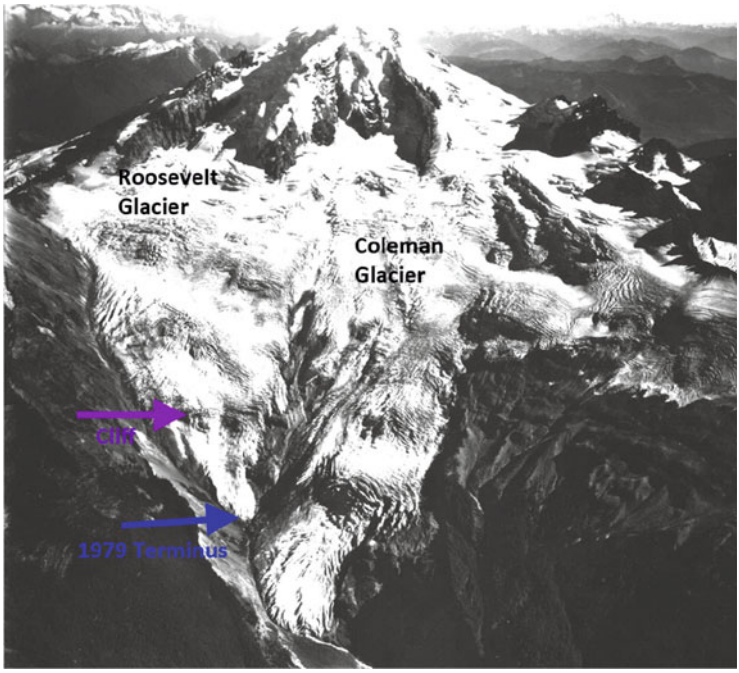

Fig. 6.10 Roosevelt Glacier in 1979 (Austin Post, NCGCP Archive)

(1984) until 1949. The glacier separated from the Roosevelt Glacier in the 1930s. By 1949 the glacier had reached a minimum position (Bengston 1956), before advancing 350 m by 1979 (Harrison 1960; Harper 1993) (Fig. 6.15). The advance terminated in the bottom of the Glacier Creek valley. From 1979 to 2014 the glacier has retreated up the west side of the valley wall, 480 m (Figs. 6.16, 6.17, and 6.18). The most rapid period of retreat was from 1979 to 1998. The snowline has averaged 2100 m during the 1990–2010 period, which is too high to maintain the current terminus position. The current terminus descends over a steep lava flow and has active crevassing indicating slow retreat in the near future. This glacier is currently the most active in the terminus region. The extensive melting in 2013–2015 may change this.

6.6 Deming Glacier

Deming Glacier is the headwaters of the Middle Fork Nooksack River. The glacier descends the southwest flank of Mount Baker beneath the Black Buttes. The glacier has the most spectacular icefall in the North Cascades from 2100 to 1700 m, The LIAM maximum moraine is at 970 m. Long (1953) noted that this glacier retreated

Fig. 6.11 Roosevelt Glacier terminus from Heliotrope Ridge, just reaching over the edge of the cliff in 2014. Coleman Glacier is in the foreground

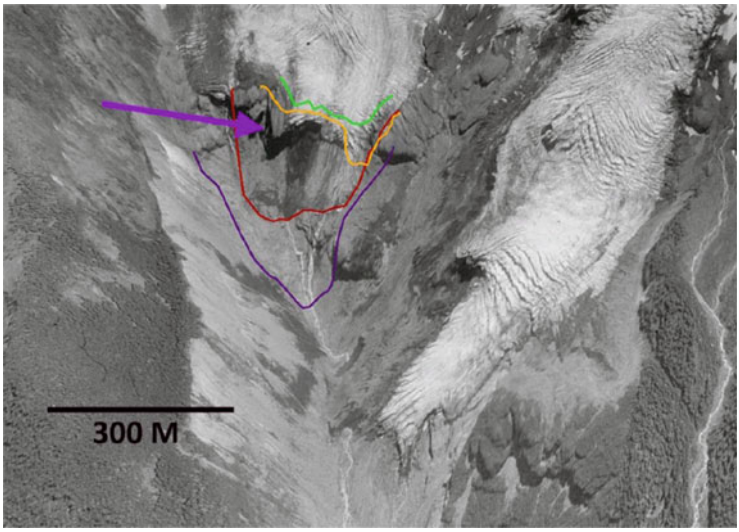

Fig. 6.12 1993 Google Earth Image of Roosevelt Glacier terminus with the *purple line* marking the 1979 terminus, *red line* the 1993 terminus, *yellow line* the 2003 terminus and *green line* the 2009 terminus

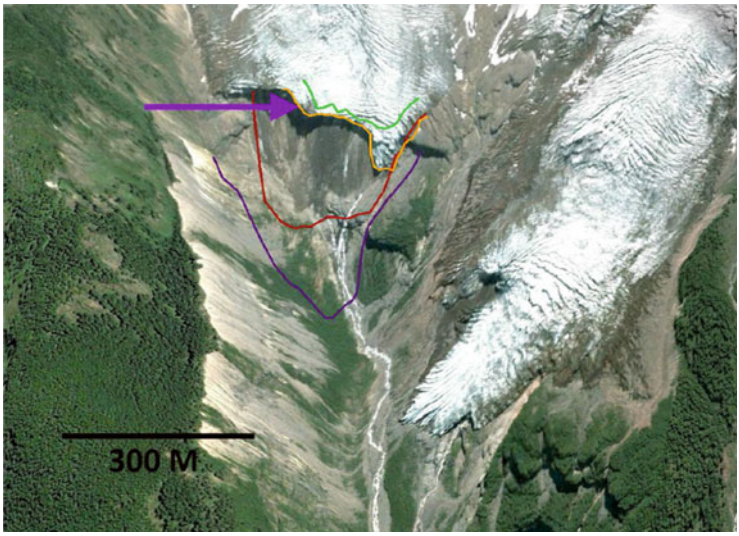

Fig. 6.13 A 2003 Google Earth image of Roosevelt Glacier terminus with the *purple line* marking the 1979 terminus, *red line* the 1993 terminus, *yellow line* the 2003 terminus and *green line* the 2009 terminus

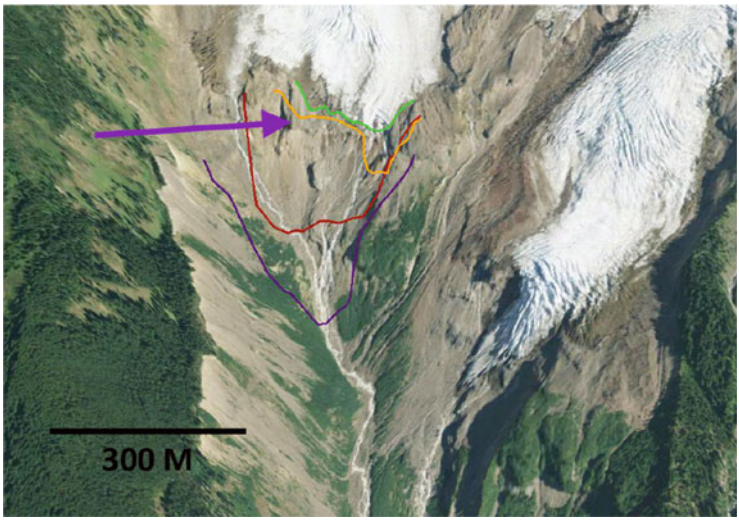

Fig. 6.14 A 2009 Google Earth image of Roosevelt Glacier terminus with the *purple line* marking the 1979 terminus, *red line* the 1993 terminus, *yellow line* the 2003 terminus and *green line* the 2009 terminus

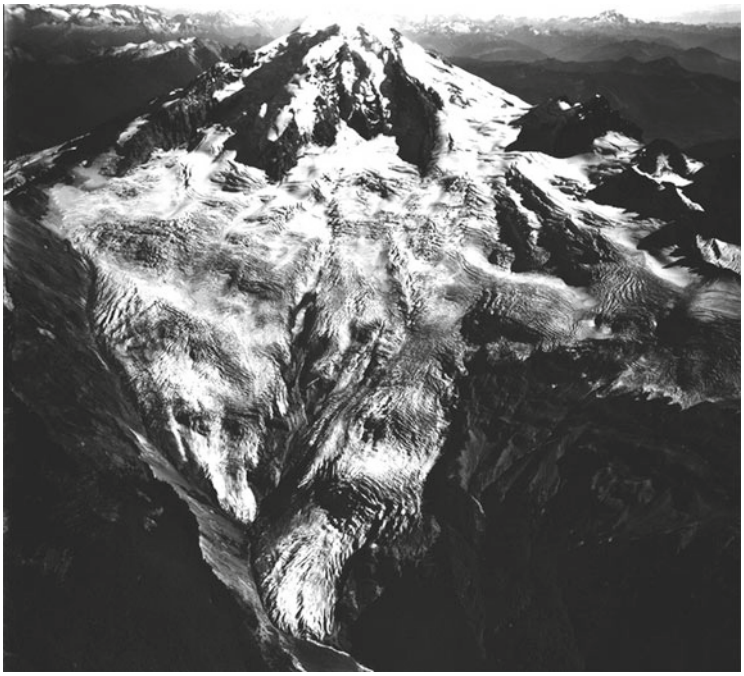

Fig. 6.15 Coleman Glacier descending to the main valley of Glacier Creek in 1979 (Austin Post, NCGCP Archive)

Fig. 6.16 Coleman Glacier terminus area in 2005 with evident low slope and thin ice

Fig. 6.17 Coleman Glacier from Glacier Creek Road in 1984 still reaching the Glacier Creek Valley bottom

Fig. 6.18 Coleman Glacier *right* and Roosevelt Glacier *left* in 2014 from Glacier Creek Road. The Glacier Creek valley bottom that Coleman Glacier reached in 1979 is evident in the *middle* foreground

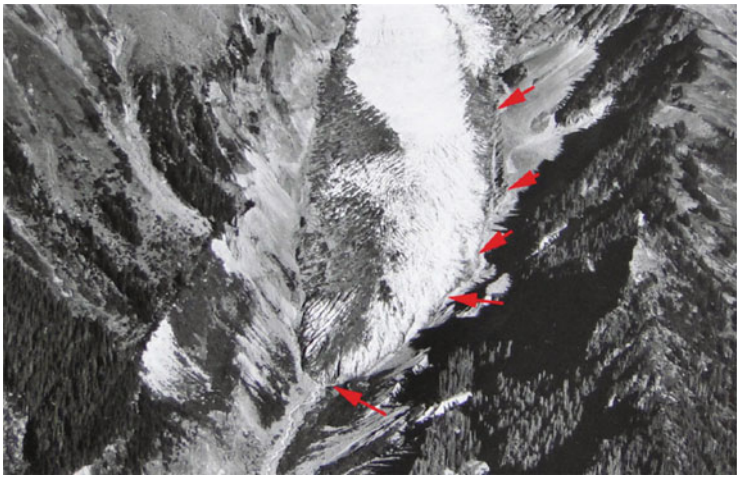

Fig. 6.19 Deming Glacier in 1979, with *red arrows* indicating the location of a moraine that is developing (Austin Post, NCGCP Archive)

1360 m from 1907 to 1947 a total retreat of 2700 m from the LIAM. The glacier then experienced a period of advance. The glacier was still in contact with its 1970s advance moraine in 1985 during our first visit to the terminus (Fig. 6.19). From 1979 to 2014 the glacier retreated 615 m, it is now close to the 1947 minimum position at 1250 m. A key change in the terminus section has been the expansion of the debris cover across the width of the glacier from 2003 to 2014. The lower 800 m of the glacier has a low slope and limited crevassing, suggesting this section will be lost to retreat with current climate. The reduction in width and crevassing in the Deming Glacier Icefall indicates a reduced flow into the terminus reach of the Deming Glacier.

Each year since 1990 we have been able to observe the terminus of the Deming Glacier from our survey point, but as recent landslides indicate, visiting the terminus is too dangerous. We have only visited the terminus three times in more than 30 years of the study: 1985, 1996 and 2002. The latter proved hazardous enough to discourage further attempts. The first set of images include a 1979 Austin Post USGS image and the rest are from the Google Earth showing in order the 1984 map position (blue), 1994 terminus (magenta), 2006 terminus (green) and 2011 terminus (yellow) (Figs. 6.20, 6.21, and 6.22). Note similarity of blue line and 1979 terminus. The glacier retreated 160 m from 1984 to 1994, 16 m/year. From 1994 to 2006 the glacier retreated 240 m, 20 ma^{-1}. From 2006 to 2011 the glacier retreated 120 m, a rate of 24 ma^{-1}. The rate is still on the increase.

The sequence of images from our survey point begins with a view from 2003 showing the end of the glacier (Fig. 6.23). The front was still steep at the time and the width of the debris near the terminus limited, clean ice width is 200 m. By 2008 the terminus is not as steep and most of the glacier width is debris covered (Fig. 6.24).

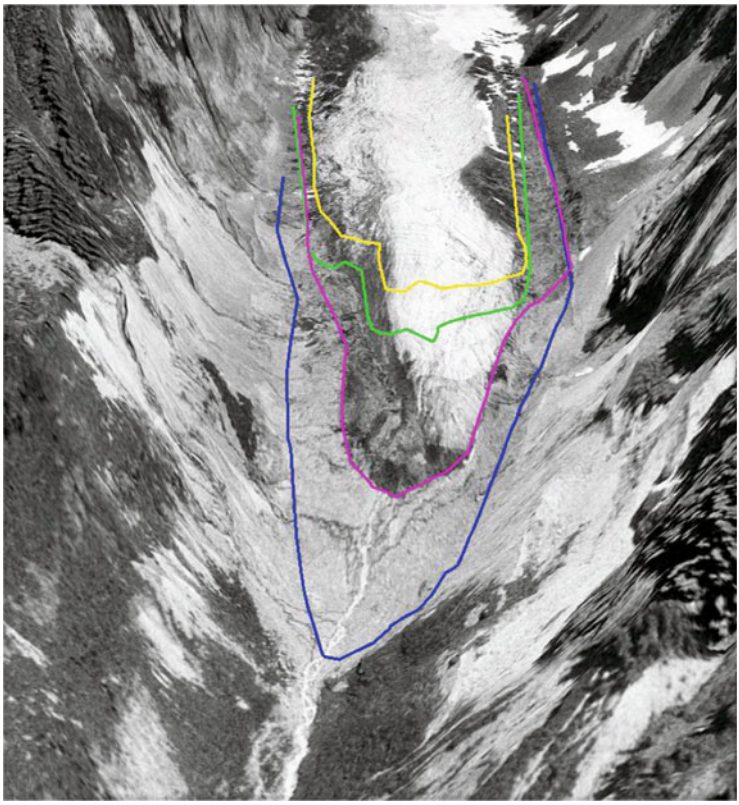

Fig. 6.20 Deming Glacier in a 1994 Google Earth image indicating the terminus location of 1984 = *blue line*, 1994 = *magenta line*, 2006 = *green line*, 2011 *yellow line*

The red arrows indicate the lateral and terminal moraines emplaced in the 1970s, with which the glacier remained in contact until the 1980s. The last image is from 2014 indicating the debris free ice section is 40 m wide (Fig. 6.25). What is causing the narrowing of the debris free ice is the reduction in velocity, the increased thinning of the clean ice in the center compared to the insulated debris covered ice at the edges. As the elevation difference increases debris slides off the side of the developing debris covered ridge (Pelto and Hedlund 2001). We also observed annually the icefall and have seen reduction in its width.

6.7 Easton Glacier

Easton Glacier flows down the south side of Mount Baker. The glacier terminates in a valley confined by lateral moraines that were built during the Little Ice Age, Railroad Grade to the west and Metcalf Moraine to the east. Easton Glacier extends

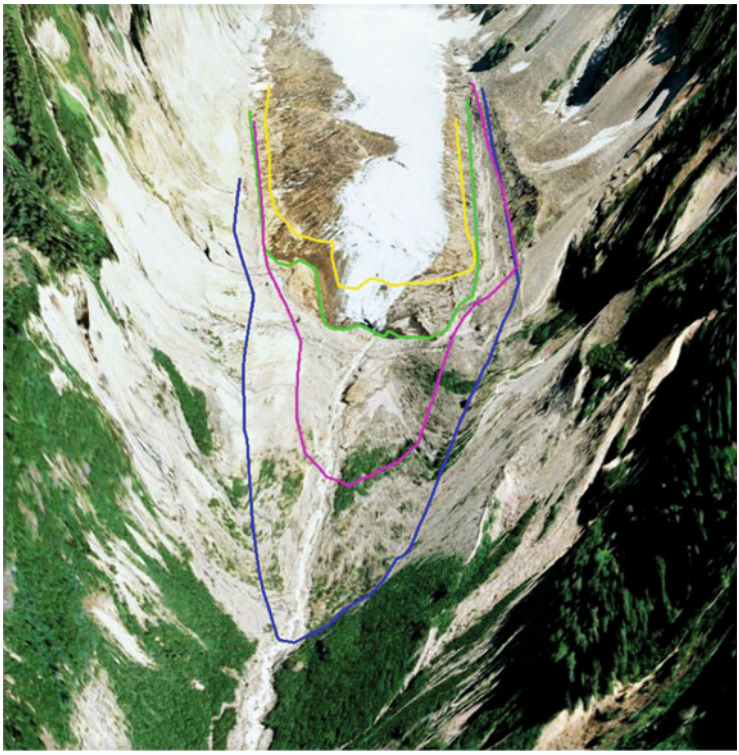

Fig. 6.21 Deming Glacier in a 2006 Google Earth image indicating the terminus location of 1984=*blue line*, 1994=*magenta line*, 2006=*green line*, 2011 *yellow line*

from the slopes near Sherman Crater at 2950 m to the terminus at 1700 m. Each summer since 1990 NCGCP has measured the mass balance of this glacier. Snowpack typically increases from the terminus to 2500 m and then remains comparatively constant. In 1907 the glacier ended at 1250 m, by 1947 the glacier had retreated 2100 m (Long 1953). Changes from 1911 to 2011 indicate the large change in ice thickness and extent at the terminus and limited change in the upper reach (Figs. 6.26 and 6.27). The Easton Glacier has a lower slope than the other largest glaciers on Mount Baker leading to a slower response to climate change (Pelto and Hedlund 2001). The glacier started advancing after 1954, the last of the large Mount Baker glaciers to advance. The glacier advanced 500–600 m by 1979. The glacier was in contact with the moraine emplaced by this advance until 1990 (Fig. 6.28). The retreat was the last to begin of the large Mount Baker glaciers, due to the slower response time (Pelto and Hedlund 2001). By 2014 the glacier had retreated 320–340 m from the advance moraine, 15 ma^{-1} (Figs. 6.29, 6.30, and 6.31). During this same period the glacier has had a mean annual mass balance of −0.51 ma^{-1}, a cumulative loss of −12.7 m. This is equivalent to a losing a 14 m of thickness. Given a thickness in 1990 between 60 and 75 m, this is about 20 % of the total glacier volume (Harper 1993). The lowest 350 m of the glacier has limited crevassing and

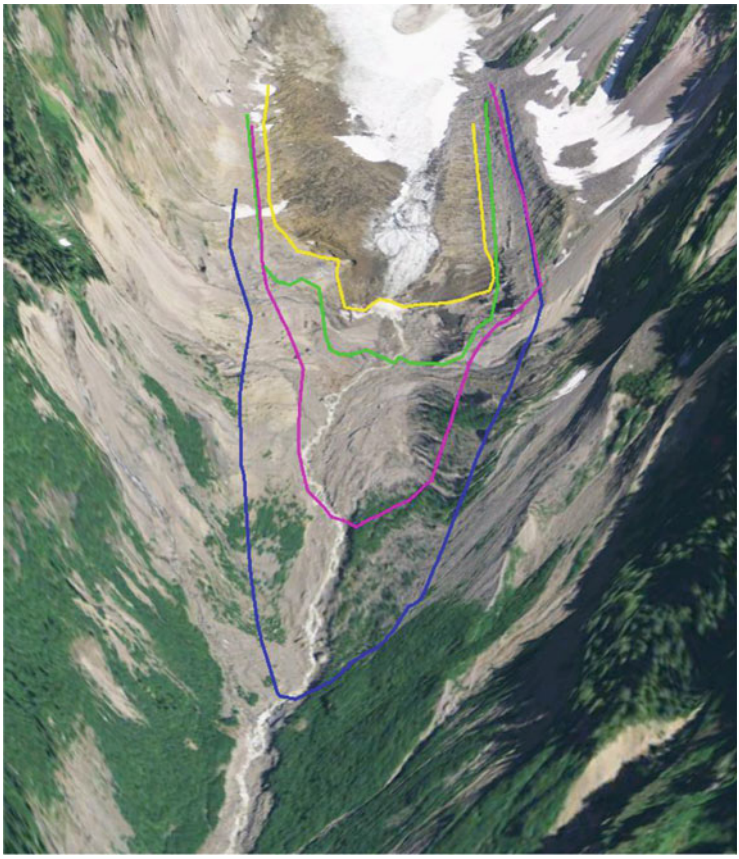

Fig. 6.22 Deming Glacier in a 2011 Google Earth image indicating the terminus location of 1984=*blue line*, 1994=*magenta line*, 2006=*green line*, 2011 *yellow line*

movement indicating retreat will continue. The glacier has developed a separate terminus on the east side at 1800 m. Each summer we complete a profile across the glacier at 1950 m, the glacier has thinned 16 m across this profile since 1984 (Fig. 6.32).

6.8 Squak Glacier

Squak Glacier shares a western margin with Easton Glacier draining the southeast flank of Mount Baker. The glacier retreated 2500 m from its LIAM maximum to 1950 (Pelto and Hedlund 2001). The glacier was advancing by 1952 and advanced 300 m by 1979. By 1990 the glacier had retreated from the advance moraine (Pelto

Fig. 6.23 Deming Glacier from the survey Point in 2003, indicating the 1985 terminus position

Fig. 6.24 Deming Glacier terminus in 2008 from survey point. *Red arrows* indicate moraines noted in the 1979 image. The *yellow arrow* indicates debris cover spreading

Fig. 6.25 Terminus in 2014 from survey point indicating expansion of debris cover across terminus

Fig. 6.26 Easton Glacier in 1911 from Park Butte, *purple arrow* is main terminus, *yellow arrow* rock knob amidst upper glacier, *red arrow* is a glacier tongue on the west side of the main glacier, and the *blue arrow* a glacier tongue east of the main glacier (From William Long, NCGCP Archive)

Fig. 6.27 Easton Glacier in 2011 from Park Butte, *purple arrow* is main terminus, *yellow arrow* rock knob amidst upper glacier has not changed in size much, *red arrow* is where there was a glacier tongue on the west side of the main glacier, and the *blue arrow* where there had been a glacier tongue east of the main glacier

Fig. 6.28 Terminus of Easton Glacier from base camp in 1990. The advance moraine is the center of the image

Fig. 6.29 Easton Glacier in 1998 from base camp. Terminal moraine is the ridge on the right foreground

Fig. 6.30 Easton Glacier terminus in 2003 from the basecamp, with 1985 terminus indicated

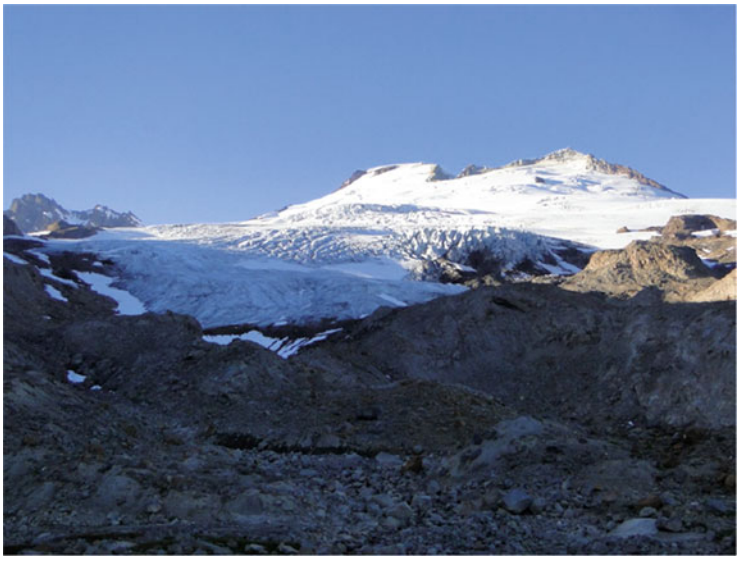

Fig. 6.31 Easton Glacier from base camp in 2014

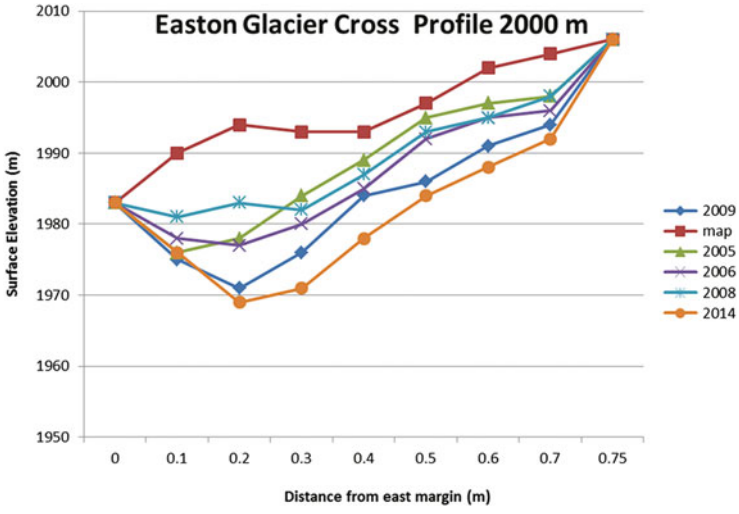

Fig. 6.32 Change in surface elevation along a fixed profile across the glacier at approximately 2000 m. The map is based on a 1984 surface elevation

Fig. 6.33 Squak Glacier in 1990 from the Sulphur Ridge west of the glacier

1993) (Fig. 6.33). In 2013 the glacier had retreated 300–350 m from the advance moraine. The main terminus is currently at 1730 m. The terminus in 2005 retained a convex shape and some crevassing indicating thicker ice and a slower retreat rate than other Mount Baker glaciers (Figs. 6.34 and 6.35).

6.9 Talum Glacier

Talum Glacier begins beneath Sherman Peak on the southwest side of Mount Baker. The glacier has the highest terminus elevation of the large glaciers on the mountain at 1850 m. The glacier has a limited accumulation area above 2300 m which leads to a smaller ablation zone and higher terminus elevation. The glacier's main terminus, northern side, during the LIAM was at 1000 m. By 1950 the terminus had retreated 1970 m (Pelto and Hedlund 2001). The glacier was advancing by 1952 (Hubley 1956), with a total advance of 270 m by 1979. By 1990 the glacier had retreated 60 m from the advance moraines. In 2013 the glacier retreat was 320 m for the north terminus and 440 m for the south terminus. In 2009, 2013 and 2014 Landsat imagery indicates an accumulation area ratio of less than 0.20. A ratio of at least 0.60 is required for equilibrium. A limited accumulation zone, crevassing and ice thickness is limited in the lower reach of this glacier indicating rapid retreat will occur.

Fig. 6.34 Squak Glacier from Sulphur Ridge in 2005

Fig. 6.35 Terminus of Squak Glacier in 2005

6.10 Boulder Glacier

Boulder Glacier is the most prominent east side glacier on Mount Baker. This steep glacier responds quickly to climate change and after retreating more than 2 km from its LIAM, it began to advance in the 1950s as observed by William Long (1955, 1956). The glacier advance had ceased by 1979. From 1988 to 2008 we visited this glacier every 5 years recording its changes. In 1988 the glacier had retreated only 25 m from its furthest advance of the 1950–1979 period. By 1993 the glacier had retreated 100 m from this position. At this time the lower 500 m of the glacier was stagnant. By 2003 the glacier had retreated an additional 300 m (Figs. 6.35, 6.36, and 6.37). In 2008 the glacier had retreated 490 m from its 1980 advance position, a rate of 16 ma^{-1} (Fig. 6.38). The glacier as seen in 2008, despite the steep slope, has few crevasses in the debris covered lower 400 m of the glacier. This indicates this section of the glacier is stagnant and will continue to melt away. The transition to active ice is at the base of the icefall on the right-north side of the glacier. This glacier after 25 years of retreat is still not approaching equilibrium and will continue to retreat. This is a reflection of continued negative mass balance as measured on the adjacent Easton Glacier. It does respond fast to climate change, and the climate has not been good for this glacier. The glacier does have a consistent accumulation zone and can survive current climate. Boulder Glacier in 1908 viewed across the glacier 1 km below the current terminus location during a Mountaineers trip taken by Asahel Curtis (Fig. 6.39). A satellite image from 2009 (green = 2009, brown = 2006, purple = 1993 yellow = 1984), shows additional retreat now at 515 m from 1984 to 2009, 20 m per year (Fig. 6.40).

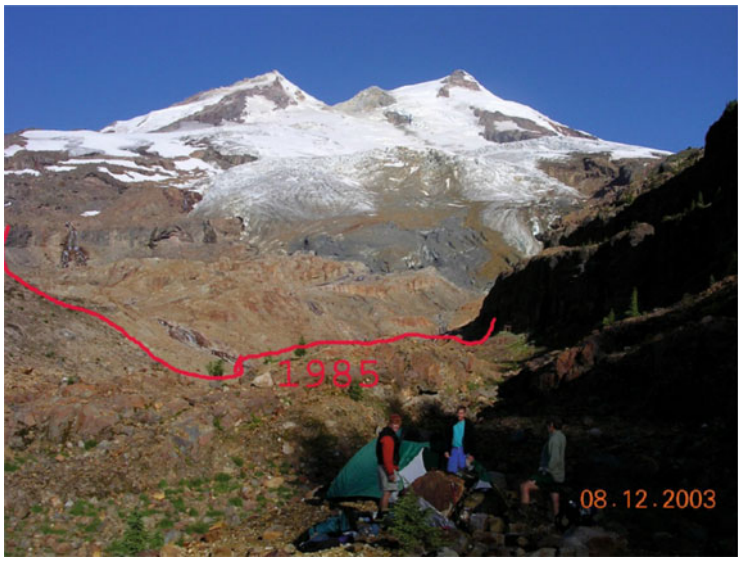

Fig. 6.36 Boulder Glacier in 2003 indicating the 1985 terminus position of an earlier survey

Fig. 6.37 On the Boulder Glacier terminus in 2003, the view beyond the margin indicates the recent retreat to the trimline of vegetation

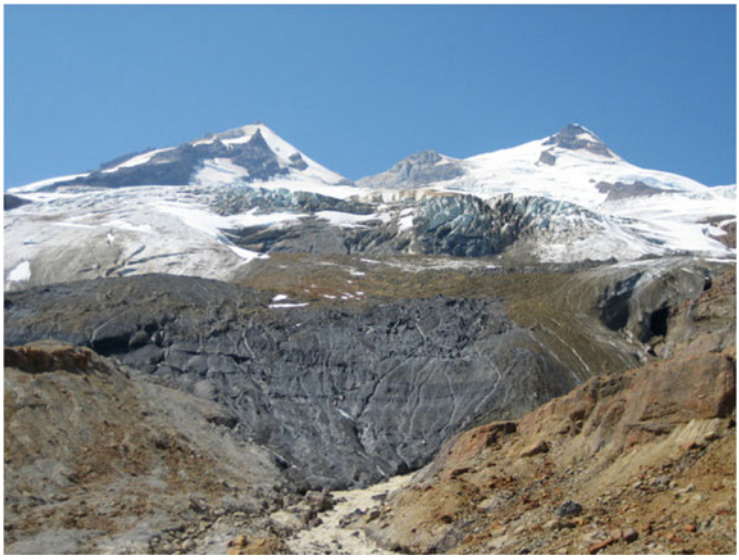

Fig. 6.38 Boulder Glacier terminus in 2008 with considerable debris cover and low slope and limited crevassing. This indicates a stagnant retreating tongue

Fig. 6.39 Boulder Glacier in 1908 looking across the glacier from an elevation of 1300 m. Note the considerable crevassing (Asahel Curtis, NCGCP Archive)

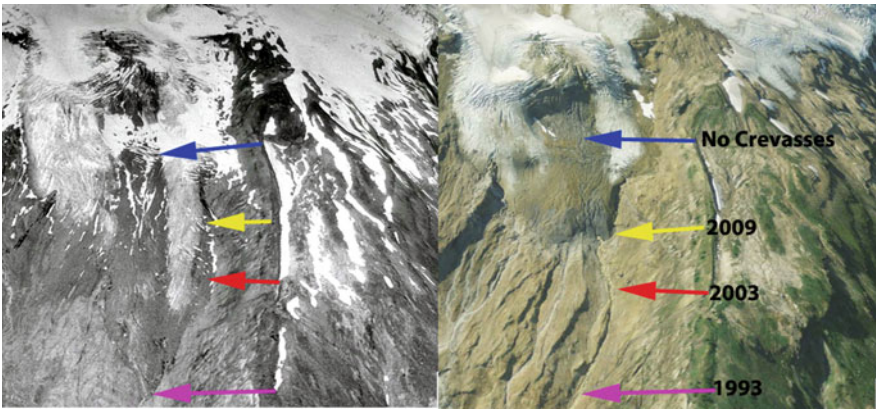

Fig. 6.40 Boulder Glacier in Google Earth image from 1993 to 2009 indicating the retreat

6.11 Park Glacier

Park Glacier is on the east side of Mount Baker draining directly from the summit ice cap. A portion of this glacier reaches an ice cliff and avalanches off of this onto the valley section of the glacier that also flows around the end of this cliff (Fig. 6.41). The terminus of this glacier is the most difficult to reach on Mount Baker. We have not visited the terminus of this glacier. The glacier was observed to be advancing by 1955 (Hubley 1956). By 1985 our first observation of the glacier, from the ridge between Boulder Glacier and Park Glacier indicated that retreat had begun. In 1979 the glacier was in contact with an advance moraine (Figs. 6.42 and 6.43). Examination of the terminus in 1998 and 2013 Google Earth images indicates a 180 m retreat during this interval and a 350 m retreat since 1979 (Fig. 6.44). The glacier has pulled back from the cliffs and is not avalanching frequently; this reduced contribution to the lower glacier will lead to continued retreat.

Fig. 6.41 Park Glacier ice cliffs in 2003

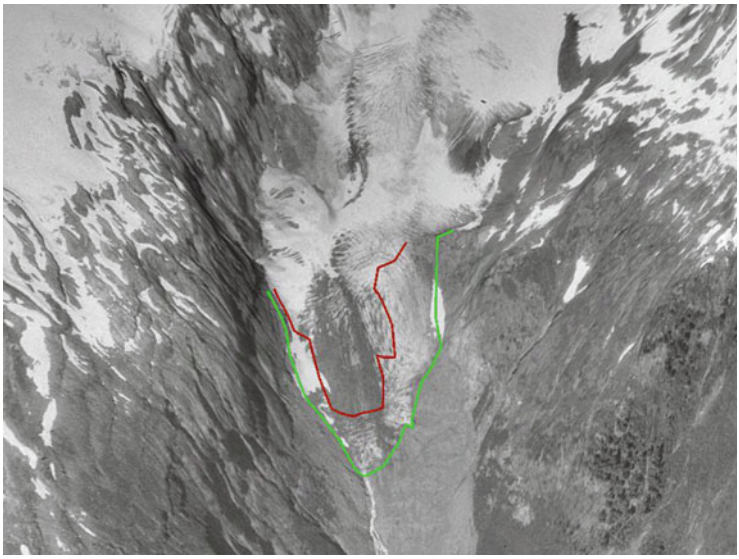

Fig. 6.42 Park Glacier Google Earth image from 1993, the *green line* is the terminus in 1993, *red line* the 2009 terminus

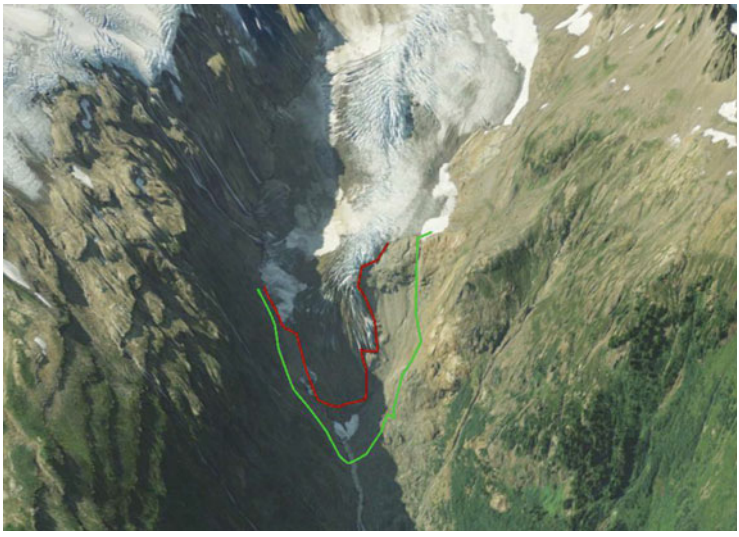

Fig. 6.43 Park Glacier Google Earth image from 2009, the *green line* is the terminus in 1993, *red line* the 2009 terminus

Fig. 6.44 Park Glacier (2013) is on the skyline. The ice cliffs have pulled back from the steeper bedrock slopes and do not avalanche as frequently during the summer (Tom Hammond)

References

Bengston K (1956) Activity of the Coleman Glacier, Mt. Baker, Washington, USA., 1949–1955. J Glaciol 2:708–713

Harper JT (1993) Glacier terminus fluctuations on Mt. Baker, Washington, USA, 1940–1980, and climate variations. Arctic Alp Res 25:332–340

Harrison AE (1960) Exploring glaciers- with a camera. Sierra Club, San Francisco

Heikkinnen A (1984) Dendrochronological evidence of variation of Coleman Glacier, Mt. Baker, Washington. Arctic Alp Res 16:53–54

Hubley RC (1956) Glaciers of Washington's cascades and Olympic mountains: their present activity and its relation to local climatic trends. J Glaciol 2(19):669–674

Long WA (1953) Recession of Easton and Deming Glacier. Sci Mon 76:241–247

Long WA (1955) What's happening to our glaciers. Sci Mon 81:57–64

Long WA (1956) Present growth and advance of Boulder Glacier, Mt. Baker. Sci Mon 83:1–2

Pelto MS (1993) Current behavior of glaciers in the North Cascades and effect on regional water supplies. Wash Geol 21(2):3–10

Pelto MS, Hedlund C (2001) Terminus behavior and response time of North Cascade glaciers. Wash USA J Glaciol 47:497–506